Chapter 1
Introduction and Overview

1.1 Industrial Innovation

A model for the dynamics of industrial innovation is described in the book, *Mastering the Dynamics of Innovation* [1]. In brief, the model states that product design innovation dominates at first. After the dominant product design, holding the largest market share is established, production process innovation follows. Today, LWRs are the dominant product design of nuclear power plants. Their design is characterized mainly by a reactor pressure vessel, control rods, a containment vessel, steam turbines, feedwater pumps, an emergency core cooling system, etc. These design features were established in the 1950s and 1960s. LWRs have reached the era of production process innovation. Standardization is one type of production process innovation.

The modular construction of the Kashiwazaki–Kariwa ABWR is shown in Fig. 1.1. Modules of base mat, control room, containment shell, etc. are prefabricated either at their factories or at the construction site. They are erected and put in place at the construction site. This is another type of production process innovation and it shortened the construction period.

In the 1980s, computer aided design (CAD) of nuclear power plants was extensively developed in Japan. It replaced handwritten drawings and the scaled plastic models of the plants. Handling and modification of the drawings became much easier than before. Connection of piping and maintenance spaces for equipment could be easily checked on the computer. Presently, design information in the computer is used not only for construction but also for maintenance of the plants. This is a third type of production process innovation.

1.2 Evolution of Boilers

Evolution of boilers is shown in Fig. 1.2. Boilers have evolved from primitive boilers to circular boilers and once-through boilers. Primitive boilers are like a large tea kettle. They have a transfer surface at the bottom. The coolant can be circulated

Y. Oka et al., *Super Light Water Reactors and Super Fast Reactors*,
DOI 10.1007/978-1-4419-6035-1_1,

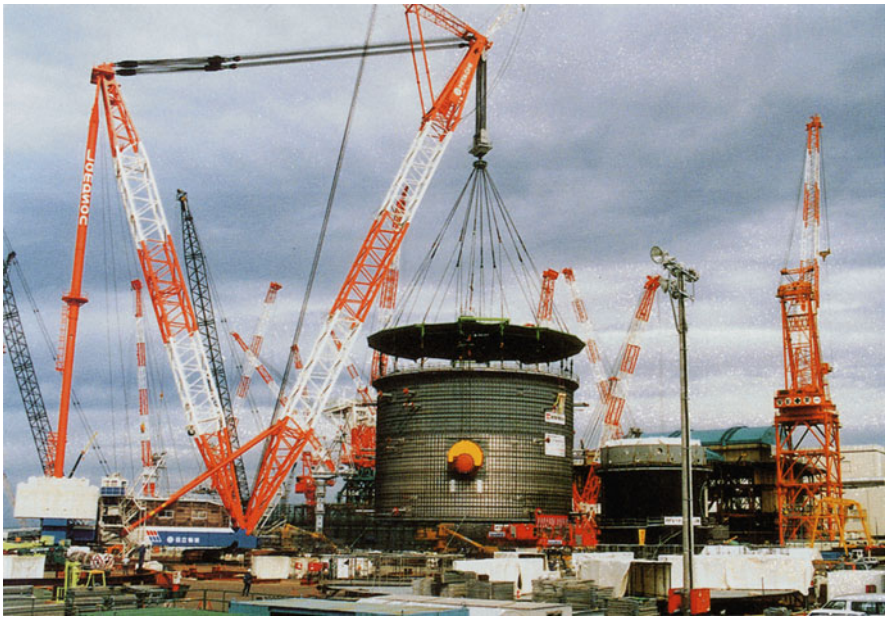

Fig. 1.1 Modular construction of the Kashiwazaki–Kariwa ABWR (courtesy of Tokyo Electric Power Co.)

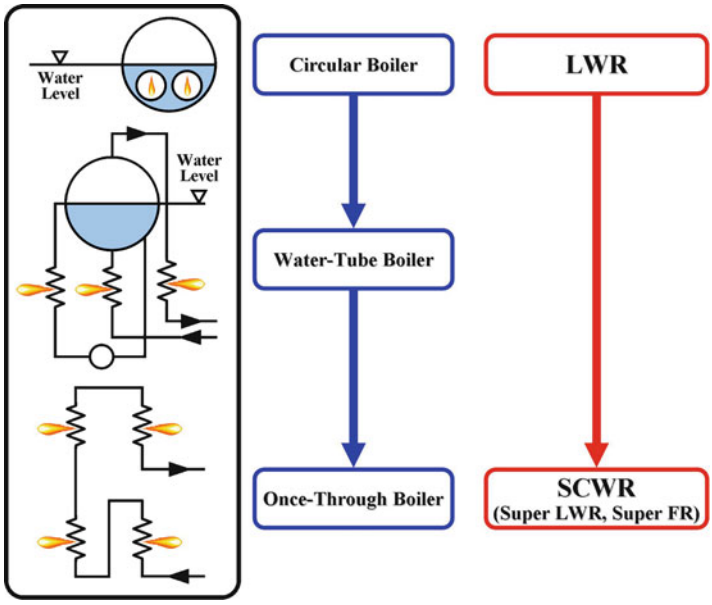

Fig. 1.2 Evolution of boilers

naturally in the boilers. Primitive boilers operate at atmospheric pressure. They take a long time to start up when their capacity is large. A primitive boiler was adopted as Newcomen's thermal engine in 1715. Circular boilers have an inside heat transfer surface. This heat transfer surface was increased in water tube boilers. Coolant circulation has been enhanced with its evolution from boilers without circulation to those with natural circulation and forced circulation. The capacity was increased with the evolution. Once-through boilers are considered as the newest type of boilers. They operate at supercritical pressure where the boiling phenomenon does not exist. The water level disappears. All the feedwater is converted to steam. BWRs are a type of circular boiler that adopts an immersion principle of the heat transfer surface. PWRs are a type of circular boiler with forced circulation. Judging the boilers from the history of evolution, the once-through supercritical pressure light water cooled reactors will be the natural evolution of current LWRs.

The milestone parameters of the supercritical fossil-fuel fired power plants (FPPs) in the USA and in Japan are shown in Table 1.1. The plants were developed in the USA in the late 1940s and 1950s. The first plant Philo No.6 started operation in 1957 and the second, Eddystone No.1, in 1959. Both plants used higher pressures and steam temperatures than today's plants. But Breed No. 1, also started in 1959, used 24.1 MPa and 566°C for operating pressure and steam temperature; later plants also used similar pressure and temperature. Due to the low fossil fuel prices in the USA and constantly increasing power demands, it was not economically attractive to pursue high thermal efficiency and use of expensive austenitic steels with large thermal expansion coefficients for the boiler units. The steam conditions of supercritical pressure FPPs in the USA stayed the same as those of Breed No.1 for a long time.

In Japan, the first supercritical FPP, Anegasaki No.1 started operation in 1967 with a rated power of 600 MWe. The supercritical FPP technologies have been improved constantly in Japan because of the high fossil fuel prices. Since fuel cost is the major part of the power generation cost in FPPs, improvement of the thermal efficiency would reduce the power cost. The sliding pressure plant Hirono No. 1 was deployed in 1980. It operates at subcritical pressure at partial load. Japanese

Table 1.1 Supercritical fossil-fuel fired power plants in USA and Japan

USA; Developed in 1950s
Philo #6 (125 MWe, 31 MPa, 621°C, 1957)
Eddystone #1 (325 MWe, 34.5 MPa, 649°C, 1959)
Breed #1 (450 MWe, 24.1 Mpa, 566°C, 1959)
Largest unit operated: 1,300 MWe
Japan; Deployed in 1960s and constantly improved
Anegasak I #1(600 MWe, 24.1 MPa, 538°C, 1967)
Hirono #1 (600 MWe, Sliding-pressure, 1980)
Kawagoe #2 (700 MWe, 31.0 MPa, 566°C, 1989)
Hekinan #3 (700 MWe, 24.1 MPa, 593°C, 1993)
Tachibanawan #1 (1,050 MWe, 25 MPa, 610°C, 2001)
28 units (600–1,050 MWe) started operation in 1990–2000

FPPs need to be operated in the daily load-follow mode. Frequent startups and shutdowns are necessary. Sliding pressure plants meet these needs.

Since sliding pressure plants are operated at subcritical pressure at partial load, they achieve higher thermal efficiency than constant pressure operation at supercritical pressure. To improve the thermal efficiency at rated power, the high pressure plant, Kawagoe No. 2 started operation with conditions of 31 MPa and 566°C in 1989. This was followed by the high temperature plant, Tachibanawan No. 1, with conditions of 25 MPa and 610°C.

The technology of supercritical steam turbines has also been improved. Compact 700 MWe turbines without an intermediate pressure turbine were used for Kawagoe No. 2. The design and development of supercritical FPPs is described in Appendix A.

Supercritical boilers and power plants were also developed in Russia and Western Europe. The number of FPPs worldwide is larger than that of LWRs.

The research and development of ultra high temperature and high pressure plants was started in Japan, Europe, and the USA to achieve higher thermal efficiency and reduce greenhouse gas emissions. Examples for goals of steam temperatures and pressure are (650°C/30 MPa), (650°C/35.4 MPa), (700°C/37.5 MPa), and (760°C/38 MPa).

The steam conditions of FPPs and nuclear power plants are shown in Fig. 1.3. The steam condition of current LWRs has remained low. The superheat test reactors that were studied in the USA in the 1960s tried to increase the coolant temperature at subcritical pressure.

Competition among uses of thermal engines has been strong as shown in Table 1.2. Steam engines are used for central power stations, internal combustion

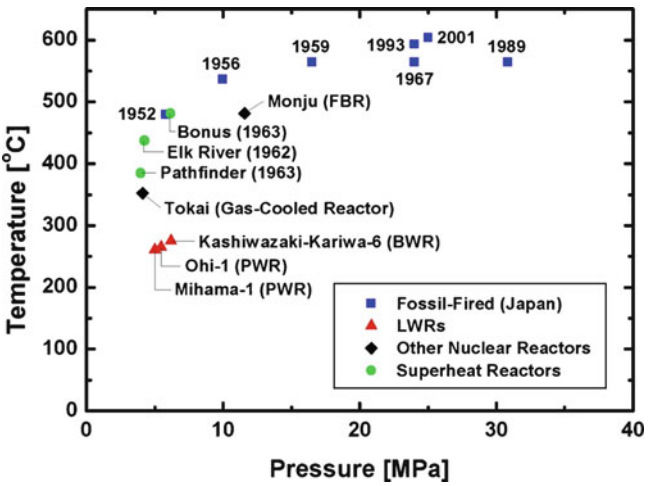

Fig. 1.3 Steam conditions of nuclear and fossil-fuel fired power plants

Table 1.2 Competition among uses of thermal engines

Present
Steam engines (steam turbines): large central power plants
Internal combustion engines: automobiles, ships etc.
Jet engines (gas turbines): aircraft and modular power plants
Rocket engines: rockets
Past steam engine applications
Nineteenth century: automobiles
Before 1960: ships
Before 1970: locomotives
Jet engines entered use in central power plants as natural gas combined cycle gas turbine power plants from the 1980s.

engines for automobiles and ships, jet engines for aircraft, and rocket engines for rockets. Steam power was used for automobiles in the nineteenth century, ships before 1960, and locomotives before 1970. Use of jet engines in central power plants was introduced into combined cycle gas turbine power plants in the 1980s. These plants consist of one or more gas turbine generators equipped with heat recovery steam generators to capture heat from the gas turbine exhaust. Steam produced in the heat recovery steam generators powers a steam turbine generator to produce additional electric power. Use of the otherwise exhausted wasted heat in the turbine exhaust gas results in high thermal efficiency compared to other combustion-based technologies. These plants use natural gas as the fuel. The power rating of gas turbines is not as large as that of steam turbines of nuclear power plants. But modules of the combined cycle power plants are used for large central power stations.

Nuclear power plants are expected to play an important role for meeting the challenges of protecting the global environment, reducing greenhouse gas emissions, and securing stable energy supplies. When total power cost is considered, nuclear power generation has advantages over fossil-fuel fired power in its lower fraction of production cost. The production cost consists of the costs of fuel and plant operation. The cost of nuclear fuel including fabrication and enrichment is approximately 15–20% of the total power generation cost, while it is 60–70% for FPPs. The capital cost of nuclear power plants is very high; while it is low for FPPs, in particular combined cycle power plants. The construction of a nuclear power plant requires a large investment. Reducing investment volume and financial risk is important in a deregulated market economy. Capital cost reduction of nuclear power plants through innovative technologies is a very important goal; increasing thermal efficiency is effective in reducing capital cost and the volume of spent fuel and radioactive waste per generated watt of electricity.

Pursuing innovation of nuclear power plant technologies in making plants more compact and raising their thermal efficiency is important for the competitiveness of nuclear power plants in the twenty-first century.

1.3 Overview of the Super LWR and Super FR

1.3.1 Concept and Features

The critical pressure of water is 22.1 MPa. The changes in specific heat and water density at 25 MPa are depicted in Fig. 1.4. Supercritical water does not exhibit a change of phase. The water density decreases continuously with temperature. The concept of boiling does not exist. The specific heat exhibits a peak at the pseudo-critical temperature. This corresponds to the boiling point at the subcritical water cooling. No abrupt change of coolant density, however, is observed at supercritical water cooling. The heat is efficiently removed at the pseudo-critical temperature, which is approximately 385°C at 25 MPa. The low density fluid above this temperature is often called "steam" and high density fluid below it is called "water." The enthalpy difference between water and steam is so large that much heat can be removed with low coolant flow rates.

The design concept of a light water cooled reactor operating at supercritical pressure was devised by one of this book's authors, Y. Oka [2, 3]. The reactor concept has been actively developed within his research group at the University of Tokyo [4–8]. It adopts a once-though coolant cycle without recirculation and a reactor pressure vessel (RPV) as shown in Fig. 1.5.

The water coolant is pressurized to the supercritical pressure by the main coolant pumps. They drive the coolant through the core to the turbines. A comparison of plant systems of BWRs, PWRs, and supercritical FPPs is made in Fig. 1.6. The coolant cycle of the Super Light Water Reactor (Super LWR) and Super Fast Reactor (Super FR) is a once-through direct cycle as the supercritical FPPs. The steam-water separators, dryers, and recirculation system of BWRs and the

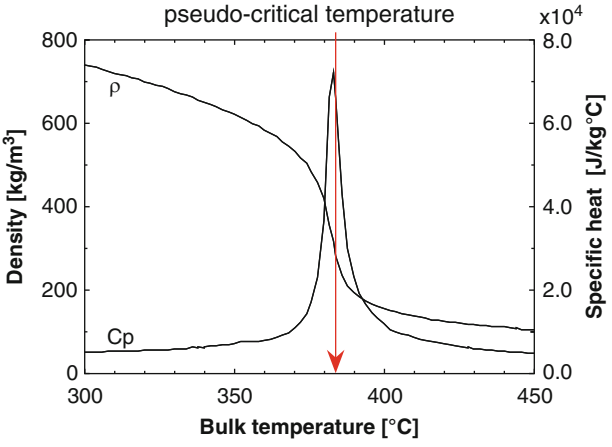

Fig. 1.4 Changes in specific heat and density of water at 25 MPa

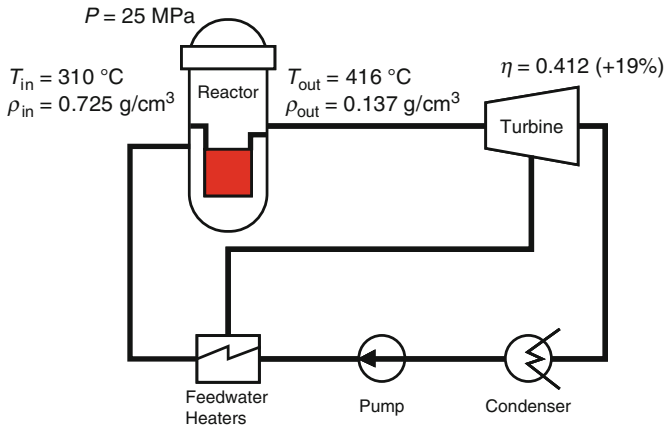

Fig. 1.5 Once-through coolant cycle reactor plant system (original plant parameters)

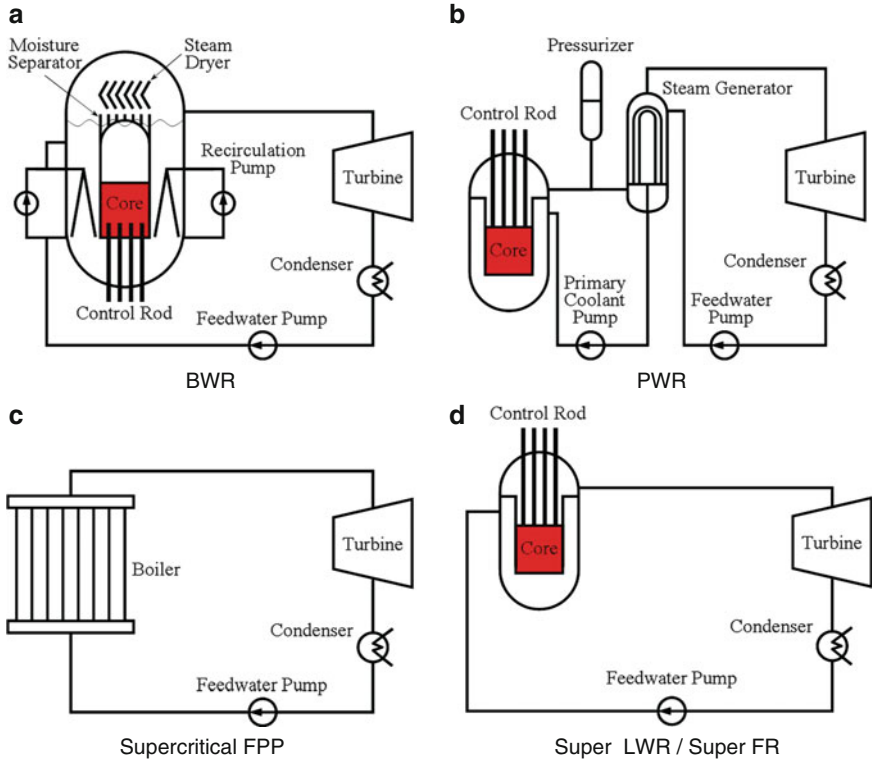

Fig. 1.6 Comparison of plant systems of BWR, PWR, supercritical fossil-fuel fired power plants and the Super LWR and Super FR

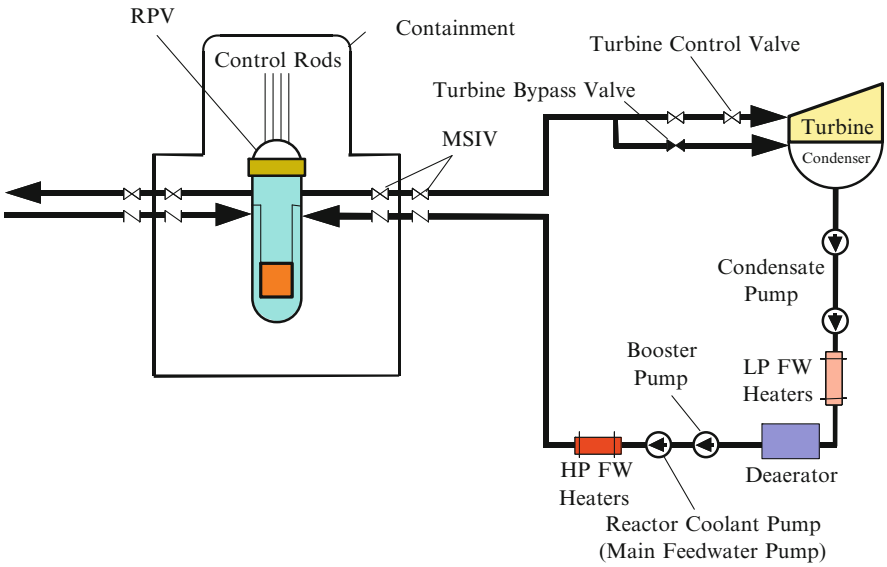

Fig. 1.7 Plant system of the Super LWR and Super FR

pressurizer, steam generators, and primary coolant loops of PWRs are not necessary. The control rod drives are mounted on the top of the RPV.

Some more details of the plant system of the Super LWR and Super FR are shown in Fig. 1.7. The RPV and control rods are similar to those of PWRs, the containment and safety systems are similar to those of BWRs and the balance of plant (BOP) is like that of supercritical FPPs. All RPV walls are cooled by inlet coolant as in PWRs. The operating temperatures of major components such as the RPV, control rods, steam turbines, pipings and pumps are within the experiences of those of LWRs and supercritical FPPs.

There are several advantages to the plant system of the Super LWR and Super FR. The first two advantages are the compactness of the plant system due to the high specific enthalpy of supercritical water and the simplicity of the plant system without the recirculation system and dryers of BWRs and steam generators of PWRs.

The RPV is as small as that of PWRs. The enthalpy difference in the core is so large that much heat is removed with low coolant flow rates. The rates are from one-fifth to one-tenth of BWRs and PWRs. The number of main coolant pipings is two for a 1,000 MWe reactor.

The control rod drives are mounted on the top of the RPV since there is no need for the steam-water separators and dryers. The position of the RPV in the containment vessel (CV) is lowered due to the top-mounted control rod drives. No space below RPV is necessary for the withdrawal and maintenance of the control blades.

Adopting the RPV rather than pressure tubes simplifies the plant system by eliminating not only many pressure tubes but calandria tanks and the auxiliary systems of pressure tube reactors.

The coolant enthalpy inside the primary coolant loops and the RPV in the CV is substantially smaller than that of LWRs. This makes the CV more compact and lower in height. The construction period will be shortened due to the decrease in the number of reactor building floors.

The third advantage is the high temperature of the coolant. Boiling phenomenon does not exist at supercritical pressure. The temperature of the coolant can be raised without the limit of boiling point. The high thermal efficiency is good not only for producing electricity but also for reducing the amount of spent fuel per generated watt of electricity.

The fourth advantage is the good compatibility of the once-through plant with a tight fuel lattice fast reactor core. The plant system configuration can be identical for both fast and thermal reactors. The water-cooled fast reactor needs to adopt a tight fuel lattice. But increases in the core pressure drop and pumping power due to the tight lattice are not problems as they are in LWRs. The reactor coolant flow rates are substantially lower than those of BWRs and PWRs. The slight increase in the core pressure drop does not impose a problem for required power of the feedwater pump that drives coolant up to 25 MPa.

Both thermal and fast reactors have been studied. Here, they are called the Super LWR and Super FR. Early designs carried different names such as SCLWR and SCLWR-H for the thermal reactors and SCFBR, SCFBR-H, SCFR-H, and SWFR for fast reactors.

LWRs were developed 50 years ago. Their successful implementation was based in part on experiences with subcritical fossil-fuel fired power technologies at that time. The number of supercritical FPPs worldwide is larger than that of nuclear power plants. Considering the evolutionary history of boilers and the abundant experiences with supercritical FPP technologies, the supercritical pressure light water cooled reactor is the natural evolution of LWRs.

The guidelines of the Super LWR and Super FR concept development are the following:

1. Utilize supercritical FPP and LWR technologies as much as possible.
2. Minimize large-scale development of major components.
3. Pursue simplicity in design.

The maximum temperature of the major components such as turbines, RPV, main steam piping, reactor coolant pumps, and control rod drives has been kept within the experiences of supercritical FPPs and LWRs. The concept development started from the simplest design. If a design did not meet a goal, for example, a reactor outlet temperature of 500°C, then an alternative design was studied.

It should be pointed out that the advantages of the Super LWR and Super FR remain valid even if the outlet temperature is 400°C. The general corrosion of fuel cladding at the high temperature will be reduced substantially than that of the

reactor of 500°C outlet coolant temperature. Starting from the low temperature test reactor will be the one way of the development.

1.3.2 Improvement of Thermal Design Criterion

The plant parameters of the original supercritical pressure light water cooled reactors were shown in Fig. 1.5. The outlet coolant temperature is low, 416°C. In the early designs before 1996, the core was designed to satisfy the limits of the critical heat flux that was determined from the empirical correlation proposed by Yamagata et al. [9] to avoid deteriorated heat transfer which occurs at high heat flux and low flow conditions at supercritical pressure. The criterion was called the minimum deteriorated heat flux ratio (MDHFR) criterion. But the critical heat flux increases greatly with coolant mass flux by reducing the fuel pitch to diameter ratio. The heat transfer deterioration is milder than the dryout and cladding temperature does not increase sharply even if the deterioration does occur as shown in Fig. 1.8.

The mechanisms of heat transfer deterioration were not clearly understood by experiments. But the numerical simulation based on the k–ε model by Jones–Lander successfully explained them [10]. Heat transfer deterioration occurs via two mechanisms depending on the flow rate. When the flow rate is high, viscosity increases locally near the wall by heating. This makes the viscous sublayer thicker and the Prandtl number smaller. Both effects reduce the heat transfer. When the flow rate is low, buoyancy force accelerates the flow velocity distribution, flattening it, and generation of turbulence energy is reduced. This heat transfer deterioration mechanism appears at the boundary between forced and natural convection. The heat transfer coefficient and deterioration heat flux that was calculated by the numerical simulation [10] agreed with the experimental data obtained by Yamagata et al. [9].

Taking critical heat flux as the core design criterion is not necessary at the supercritical pressure where no dryout and burnout phenomena occur. Supercritical water is a single-phase fluid. No critical heat flux criterion is used for the design of gas cooled reactors and liquid metal cooled fast reactors. The maximum cladding surface temperature (MCST) is taken as the design criterion and it is limited accordingly so that the fuel cladding integrity is maintained at abnormal transients.

To evaluate the cladding temperatures directly during abnormal transients, it was necessary to develop a database of heat transfer coefficients at various conditions of heat flux, flow rate, and coolant enthalpy. The database of heat transfer coefficients was prepared by numerical simulations that successfully analyzed the deterioration phenomenon itself. The database, Oka–Koshizuka correlation, has been used for safety analysis.

The concept for refining the transient criteria, without using the MDHFR criterion, was reported in 1997 [11]. Higher temperature cores for thermal reactors and the fast reactor SCFR-H were designed using the new transient criterion of the

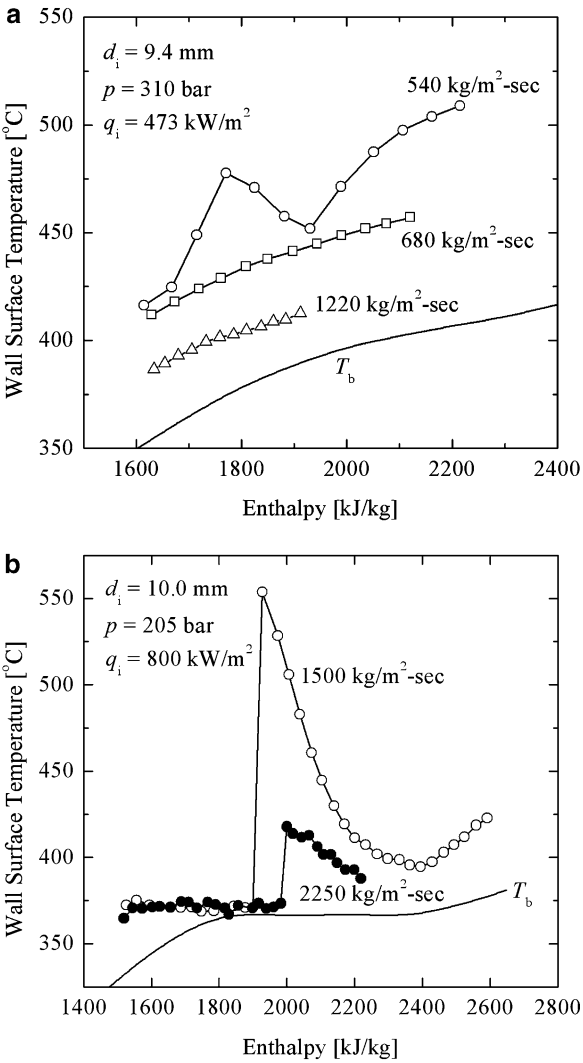

Fig. 1.8 Comparison of heat transfer deterioration at supercritical pressure and dryout at subcritical pressure

MCST [12, 13]. For high temperature reactors, the coolant enthalpy rise in the core is high and coolant flow rate is inevitably low. The gap between fuel rods is kept small to increase the coolant velocity in the core.

Removing the critical heat flux criterion (i.e., the MDHFR) from the core design and taking the MCST criterion makes it possible to raise the outlet coolant temperature of the Super LWR and Super FR to that of the supercritical FPP. The high enthalpy rise and low coolant flow rate are advantages of the once-through coolant cycle.

1.3.3 Core Design Criteria

The core design criteria are summarized in Table 1.3. The maximum linear heat generation rate (MLHGR) at rated power is 39 kW/m. It is slightly lower than those of PWRs (42.6 kW/m) and BWRs (44 kW/m) due to the high average coolant temperature. The fuel centerline temperature stays nearly the same as that of LWRs. The fission gas release rate from the fuel pellets is similar to that of LWRs. The fuel design of the Super LWR follows that of LWRs.

The maximum cladding temperature criterion is determined considering the strength of cladding material. Stainless steel is used for the design of the Super LWR and Super FR. Nickel-base alloys are an alternative. Cladding material development is an important R&D issue and requires extensive experiments and testing. Both general corrosion at high temperatures and stress cracking corrosion at low temperatures need to be considered. Supercritical water shows "gas-like" properties above the pseudo-critical temperature. General corrosion by oxidation occurs at high temperature and it is primarily reduced by lowering oxygen content in the coolant. Stress corrosion cracking must be avoided during the service life of the fuel cladding. Joint R&D into material science and water chemistry is necessary.

The MCST is taken as another criterion. The surface temperature is taken from the viewpoint of corrosion, but the cladding centerline temperature is taken from the viewpoint of the cladding material strength. By adding the temperature difference between the surface and the centerline of the cladding, which is approximately 12°C for austenitic stainless steel cladding, the MCST can be used as the criterion for the strength of fuel cladding of Super LWR and Super FR.

All the reactor coolant is purified after condensation in the once-through coolant cycle of the Super LWR and Super FR. This differs from BWRs and PWRs in which reactor coolant is circulated in a closed loop as recirculating coolant and primary loop coolant, respectively. The purity of reactor coolant is therefore different from that of LWRs.

The moderator temperature in the water rods should be below the pseudo-critical temperature to keep the moderator density high. Thin layer of zirconia (ZrO_2) is used for thermal insulation on the water rods. The thermal insulation also reduces the stress of stainless steel plates of water rods below allowable stress level.

Table 1.3 Core design criteria

Thermal design criteria
Maximum linear heat generation rate (MLHGR) at rated power $\leqq$ 39 kW/m
Maximum cladding surface temperature at rated power $\leqq$ 650°C for Stainless Steel cladding
Moderator temperature in water rods $\leqq$ 384°C (pseudo critical temperature at 25 MPa)
Neutronic design criteria
Positive water density reactivity coefficient (negative void reactivity coefficient)
Core shutdown margin $\geqq$ 1.0%Δk/k

The positive reactivity coefficient or negative coolant void reactivity coefficient is necessary for the inherent negative feedback of the Super LWR and Super FR at the loss of coolant accident. The reactor power should decrease automatically at the loss of coolant accident.

The core shutdown margin should be above 1.0%Δk/k with one-rod stuck condition. It is the same criterion as in LWRs.

1.3.4 Improvement of Core Design and Analysis

The first design of the supercritical pressure light water cooled reactor (SCLWR) in 1992 adopted zirconium hydride rods as moderator for flattening axial power distribution [2]. The next core design in 1994 adopted water rods [14]. Heat transfer between core coolant and water rods was considered by single channel models of a fuel rod and a water rod. The core design was carried out in the two-dimensional R-Z model with the cell burn-up calculation [15]. It was used for the designs of early version of the Super LWR and the Super FR. The neutronic–thermal hydraulic coupling was considered in the two-dimensional core calculation [16, 17]. Plant heat balance and thermal efficiency were also analyzed in 1997 [17].

The high temperature core without the critical heat flux criterion (i.e. the MDHFR) was designed in 1998 [12]. The two-dimensional R-Z model of the core cannot accurately predict burn-up of fuel rods. The three-dimensional coupled neutronic–thermal-hydraulic core calculation was developed in 2003 [18]. It is shown in Fig. 1.9. This calculation considered the control rod pattern and fuel loading pattern [19, 20] and was similar to the core calculation for BWRs. But the finite difference code SRAC [21] was used for the three-dimensional neutronic calculation instead of a nodal code. The core design of the Super FR also adopted the three dimensional neutronic and thermal hydraulic coupled core burn-up calculation.

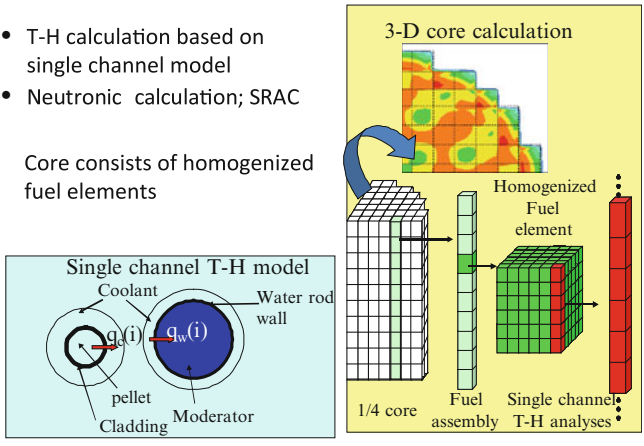

Fig. 1.9 Three-dimensional neutronic and thermal-hydraulic coupled core calculation

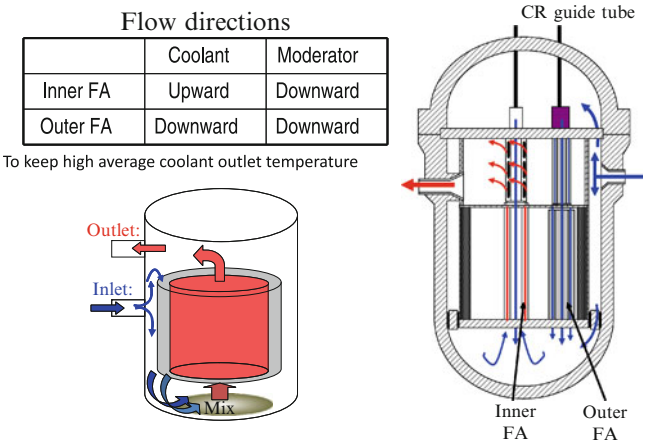

Fig. 1.10 Coolant flow scheme of two-pass core

A new coolant flow scheme was proposed in which the fuel assemblies loaded on the core periphery are cooled by a descending flow. The coolant mixes with the rest of the coolant from the downcomer at the lower plenum and then rises up the fuel channels in the fuel assemblies loaded in the inner region of the core. It is called a two-pass core and shown in Fig. 1.10. The average reactor outlet coolant temperature is increased in this core [22, 23]. The two-pass core is compatible with the low leakage fuel loading pattern (LLLP) that the burnt (third cycle) fuel assemblies are loaded in the core periphery [24]. The average fuel enrichment is decreased using the LLLP. The one-pass core where whole coolant is upward flow needs fresh fuel assemblies in the core periphery not to decrease the outlet coolant temperature. But the fuel enrichment of the out-in fuel loading becomes inevitably higher than that of the LLLP.

The Super FR also adopted the two-pass core where all blanket fuel assemblies and part of seed fuel assemblies are cooled by a descending flow so as to keep average reactor outlet coolant temperature high. By adopting the two-pass core, the conventional concepts of the hot channel factors of PWR and the peaking factors of BWR are not applicable to the Super LWR and the Super FR.

The cladding temperature that was obtained by the three-dimensional coupled core calculation is the average temperature over the assembly. The peak cladding temperature of a fuel rod is necessary for the evaluation of the fuel cladding integrity. The subchannel analysis code of the Super LWR is coupled with the fuel assembly burn-up calculation code for this purpose [25]. Fuel pin-wise power distributions are produced for various burn-ups, coolant densities, and control rod positions. The pin-wise power distributions are combined with the homogenized fuel assembly power distribution to reconstruct the pin-wise power distribution of the core fuel assembly. The power distribution over the fuel assembly is taken into account as shown in Fig. 1.11. The reconstructed pin-wise power distribution is used in the evaluation of peak cladding temperature with the subchannel analysis.

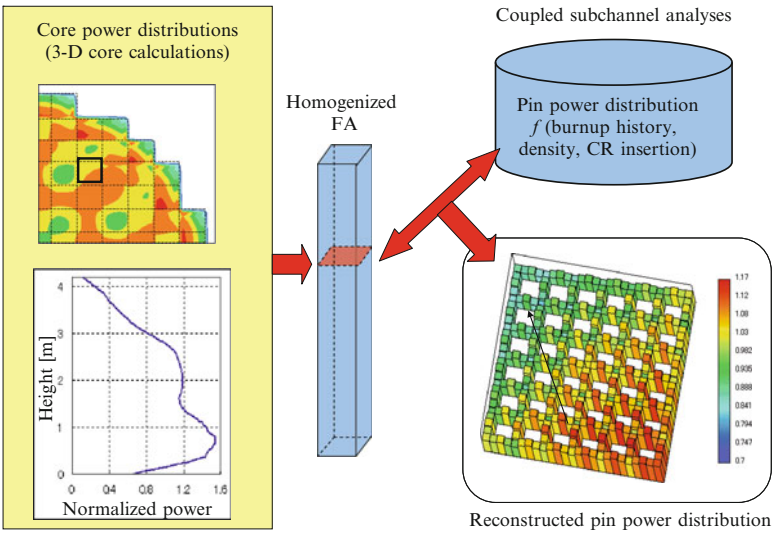

Fig. 1.11 Coupling of subchannel analysis with three-dimensional core calculation (Reconstruction of pin-wise power distribution for the subchannel analysis)

The maximum cladding temperature predicted by the subchannel analysis is higher than that predicted by single channel analysis which is used for the three-dimensional core calculation.

The thermal performance of a nuclear reactor core contains various engineering uncertainties which arise from calculation, measurement, instrumentation, fabrication, and data processing. A statistical method is developed and employed in the thermal design of the Super LWR to compensate for such uncertainties [26, 27].

The evaluation of peak cladding temperature is summarized in Fig. 1.12. The radial and local flux factors are evaluated separately, but further improvement was made. Incorporating subchannel analysis into the three-dimensional core coupled calculation, iterating the subchannel analysis with the core calculation rationalizes the evaluation of radial and local flux factors [28]. The nominal peak steady state temperature decreases 25°C from the value of the separate evaluation of Fig. 1.12.

Increasing the fuel rod spacing decreases the coolant velocity in the fuel channel, but the sensitivity of the maximum cladding temperature to the engineering uncertainties of the spacing decreases. The core with a 2-mm fuel rod spacing was designed for the two-pass core. It was 1 mm in the first two-pass core. The improved core design with the 2-mm fuel rod spacing was studied with rationalization of the core design method. The subchannel analysis was iterated with the three-dimensional core design. The local flux factor effect on cladding temperature was incorporated in the core design. The cladding temperature at the nominal peak steady state condition of the new core with 2-mm fuel rod spacing decreased 12°C, even if the average coolant flow rate in the fuel channel decreased 27%. The core

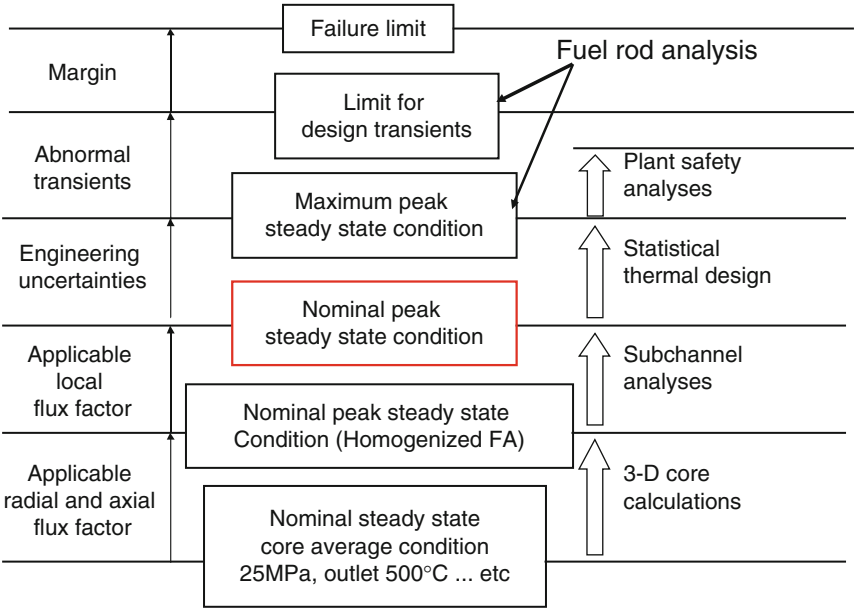

Fig. 1.12 Evaluation of peak cladding temperature

height was increased slightly from 4.2 m to 5 m not to decrease the coolant flow rare in the fuel channel substantially [28].

A correlation of the heat transfer coefficient of supercritical water is needed for the design work. The Oka–Koshizuka correlation was used for the early designs. But it is applicable to upward flow only. Watts–Chou correlation includes both upward flow and downward flow correlations. It was used for the core designs of the Super LWR and Super FR. But present correlations are based on experiments using smooth tubes. These experiments did not include the effect of fuel rod spacers on the heat transfer coefficient. Since supercritical fluid exhibits gas-like properties at high temperatures, nitrogen gas was used as the fluid and the effect of spacers was evaluated by measuring the turbulence due to the grid spacers at Kyushu University. The experiments were analyzed by a computational fluid dynamics (CFD) code. The effect of various geometries of grid spacers on the heat transfer coefficient in the downstream was derived. The cladding temperature was expected to decrease 20–30°C due to the effect of grid spacers [29].

1.3.5 Fuel Design

The fuel design of the Super LWR follows that of LWRs [30]. UO_2 is used for fuel pellets. Stainless steel and Ni-base alloy are the candidate cladding materials.

Its fuel rod design also follows that of LWRs. The failure modes of fuel rods considered are over-heating, pellet cladding mechanical interaction (PCMI), buckling collapse, and creep rupture at both normal and abnormal transients.

The four basic design criteria in the fuel rod design are as follows, for both normal and abnormal transients:

(a) Fuel rod failure by any of the four failure modes does not occur.
(b) Fuel rod centerline melting does not occur.
(c) The stress and pressure difference on the cladding are less than the maximum allowable values defined in the fuel rod failure modes.
(d) Internal pressure of the fuel rod does not exceed the normal operating coolant pressure (25 MPa).

PCMI is the limiting failure mode in LWRs, because the thermal expansion rate coefficient of the Zircaloy cladding is smaller than that of the UO_2 pellets. The criterion in LWRs is that the plastic deformation of the fuel rod is less than 1.0%. This criterion should be applied to the Super LWR fuel too. However, it is not likely to be limiting because the thermal expansion rate coefficients of the candidate cladding materials are likely to be greater than, or close to, that of UO_2 pellets. The MLHGR of 39 kW/m in the core design is determined from the rates of 44 kW/m of BWRs and 43.1 kW/m of PWRs so that the fuel centerline temperature and the fission gas release rate are about the same as in LWRs considering the high average reactor coolant temperature.

In LWRs, buckling collapse and creep rupture are not included in the design failure modes, because experimental verifications have shown that these failure modes are not limiting as long as the plastic deformation of the fuel rod is less than 1.0%. The core pressure and temperature of the Super LWR are much higher than those in LWRs, so these failure modes need to be included in the design failure modes. The evaluations of stresses on the cladding are based on ASME Boiler and Pressure Vessel Code Section III as adopted in BWRs for simplified evaluations.

In BWRs, all stresses (pressure difference, hydraulic vibrations, contact pressure of spacers, etc.) are first evaluated and categorized into primary membrane stress, primary bending stress, and secondary stress. The maximum allowable stresses are set for each of these categorized stresses at both normal and abnormal transients. The maximum allowable stresses in the Super LWR fuel rod design are determined similarly.

For the evaluation of stress rupture, the limiting criterion is to maintain the stress below one half of the tensile strength at abnormal transients. In LWRs, this is the limiting criterion in evaluating the maximum allowable stress on the cladding. In the Super LWR, the buckling collapse or creep rupture of the cladding can also be limiting depending on the cladding materials and its temperature.

The ratio of the gas plenum volume to the pellet volume is roughly the same as that in BWR fuel rods, 01. The gas plenum temperature is determined assuming it is placed at the top of the fuel rod and the temperature is equal to that of the outlet coolant.

The maximum allowable cladding temperature at abnormal transients is determined for the fuel rod design purpose. The relevant material properties of the cladding are used to determine the cladding thickness in the design. Exceeding the maximum cladding temperature does not mean that the cladding fails above the maximum design temperature.

The fuel rods are to be internally pressurized with helium gas as in BWRs and PWRs. The initial internal pressure of the fuel rods should be optimized to minimize the stresses and especially the pressure difference on the cladding. However, the internal pressure should not exceed the normal operating coolant pressure (25 MPa) to prevent any creep deformations that causes the gap between the pellet and cladding to increase. The four basic design criteria were determined to ensure the fuel integrity at all anticipated transients based on simple, but conservative evaluations [30].

However, such conservative criteria severely limited the plant operability during anticipated transients. In order to maximize the economical potential of the Super LWR and Super FR, and minimize the R & D efforts, the criteria were rationalized based on detailed fuel analyses. The FEMAXI-6 code [31] for LWR fuel analyses was used for the study. The principle of rationalization of the criteria for anticipated transients of Super LWR was developed [32, 33]. The design and integrity analysis of the Super LWR fuel rods is summarized in ref. [34].

An example of fuel assembly design of the Super LWR is shown in Fig. 1.13 [35]. An example Super LWR core and fuel characteristics are given in Table 1.4 [24]. The core coolant flow rate of the Super LWR is substantially lower than that of LWRs due to the high enthalpy rise in the core. The gap between fuel

Design requirements →	Solution
Low flow rate per unit power (< 1/8 of LWR) due to large ⊿T of once-through system	Narrow gap between fuel rods to keep high mass flux
Thermal spectrum core	Many/Large water rods
Moderator temperature below pseudo-critical	Insulation of water rod wall
Reduction of thermal stress in water rod wall	
Uniform moderation	Uniform fuel rod arrangement

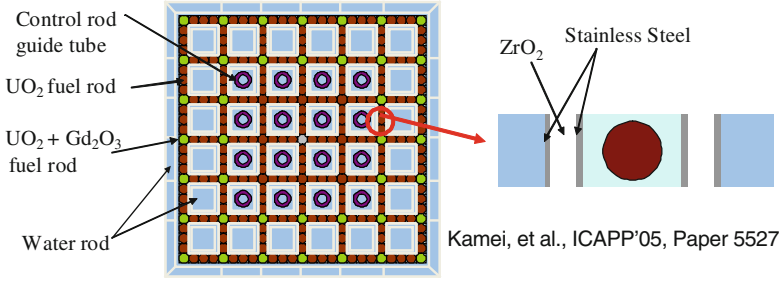

Fig. 1.13 Example of fuel assembly design of Super LWR

Table 1.4 Example of Super LWR core and fuel characteristics

Core pressure (MPa)	25
Thermal/Electrical power (MW)	2,744/1,200
Coolant inlet/outlet temperature (°C)	280/500
Thermal efficiency (%)	43.8
Core flow rate (kg/s)	1,418
Number of all fuel assemblies/fuel assemblies with descending-flow cooling	121/48
Fuel enrichment bottom/top/average (wt%)	6.2/5.9/6.11
Active height/equivalent diameter (m)	4.2/3.73
Fuel assembly average discharge burn-up (GWd/t)	45
MLHGR/ALHGR	38.9/18.0
Average power density (kW/l)	59.9
Fuel rod diameter/Cladding thickness [material] (mm)	10.2/0.63 [Stainless Steel]
Fuel assembly structure thickness [material] (mm)	0.2 [Stainless Steel]
Thermal insulation thickness [material] (mm)	2.0 [ZrO_2]

Taken from ref. [24] and used with permission from Atomic Energy Society of Japan

rods should be small to keep the high mass flux. The coolant density in the upper part of the core is low. Moderation is provided by introducing large square water rods. Single-array fuel rods are surrounded by the water rods for achieving uniform moderation. There are two fuel enrichments, 5.9% and 6.2%. Further flattening of pin power distribution will be possible by increasing the number of enrichments.

A thin thermal insulation of Zirconia is provided between the water rods and fuel coolant channels. Gadolinia is used for compensating burn-up reactivity and axial power flattening. The control rods are the cluster rod type. The control elements are inserted in the guide tubes that are located in the central water rods.

The water rods are supplied with the water from the top dome of the RPV through the control guide tubes. Descending flow in the water rods is employed. The moderator is mixed with the reactor coolant through the downcomer in the lower plenum of the RPV. This design concept is good for keeping the average reactor outlet coolant temperature high and the axial power distribution uniform.

1.3.6 Plant Control

The plant control system has been designed in a similar way to that of BWRs [36–39]. It is shown in Fig. 1.14. The plant transient analysis code SPRAT-DOWN was developed and used in the design work. The node-junction model, shown in Fig. 1.15, contains the RPV, the control rods (CRs), the main feedwater pumps, the turbine control valves, the main feedwater lines, and the main steam lines. The characteristics of the turbine control valves and the changes of the feedwater flow rate according to the core pressure are given in the calculation.

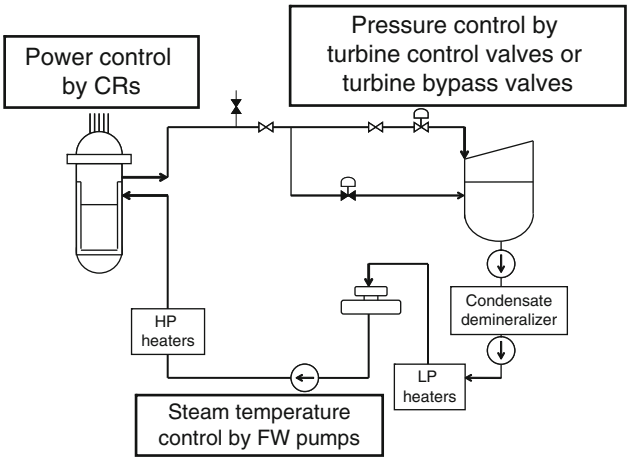

Fig. 1.14 Plant control system of the Super LWR

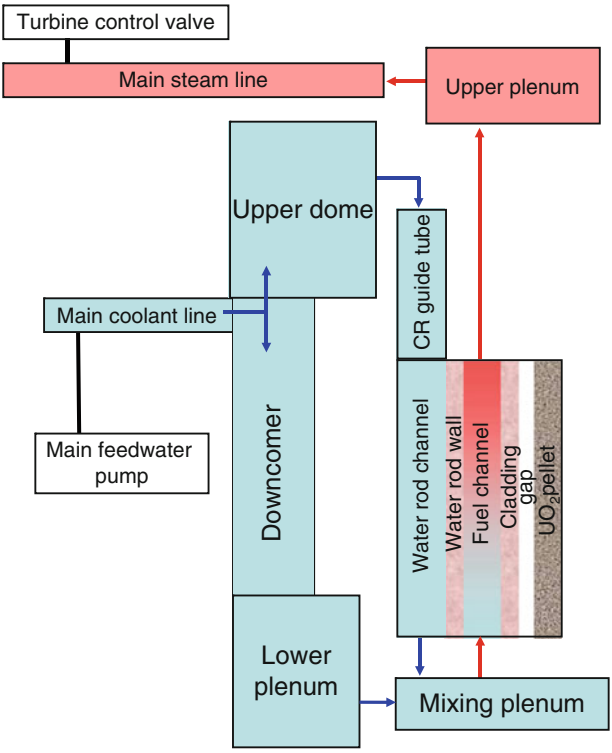

Fig. 1.15 Node junction model of transient analysis code SPRAT-DOWN

First, the step responses without the plant control system are analyzed. The major perturbations are:

1. Increase in the reactivity by \$0.1 resulting from withdrawal of a control rod cluster.
2. Decrease in the feedwater flow rate by 5%.
3. Decrease in the main steam flow rate by 5% resulting from closure of the turbine control valves.

The core power of the Super LWR was found not to be sensitive to the feedwater flow rate due to the existence of many water rods.

According to the calculated step responses, the pressure is sensitive to the turbine control valve opening and the feedwater flow rate. The main steam temperature is sensitive to the control rod position and the feedwater flow rate. Therefore the turbine inlet pressure is controlled by the turbine control valves. The main steam temperature is controlled by the feedwater pumps. The core power is controlled by the control rods.

The plant control system should be designed so that it does not generate divergent or continuous oscillations that exceed the permissible range. The criteria are as follows:

1. Damping ratio is less than 0.25. This is most generally used as the criterion for control quality and is applied to existing FPPs.
2. Over shoot is less than 15%.

The plant control system is designed based on the proportional, integral, and differential (PID) control principle (see Sect. 4.4). The reactor behavior has been analyzed against various perturbations with the designed and optimized plant control system.

BWRs have an inverse response of reactor power to the turbine load. When the electricity demand and the turbine load increase, the turbines consume more steam. This decreases the reactor pressure and increases the average void fraction of the core. The reactor power decreases due to the negative void reactivity effect. Then BWRs are operated as turbine-following-reactor control strategy. PWRs have normal response of reactor power to the turbine load. When the electricity demand and consumption of steam increase in the turbine, more heat is removed in the steam generators. The coolant temperature of the primary loop and the reactor inlet coolant temperature decrease. This increases reactor power due to the negative coolant temperature coefficient. Then PWRs are operated as reactor-following-turbine control. The Super LWR is like BWRs because of the direct cycle and it is operated as the turbine-following-reactor control strategy.

FPPs adopt turbine-boiler-coordination control. The ratio of the boiler (fuel) input and the feedwater flow rate is used for the control parameter of the feedwater pumps. The plant control strategies of BWRs, PWRs, FPPs, and the Super LWR are compared in Table 1.5.

Table 1.5 Comparison of plant control strategies

	Control strategy	Control method		
		Electric power	Steam pressure	Reactor or boiler power
Super LWR	Turbine following reactor	Reactor power	Turbine control valves	Control rods
BWR	Turbine following reactor	Reactor power	Turbine control valves	Control rods, recirculation pumps
PWR	Reactor following turbine	Turbine control valves	Reactor power	Control rods
FPP	Boiler turbine coordinated	Turbine control valves, boiler input		

The turbine-boiler coordination control using the power to feedwater flow rate ratio was studied for the control of the Super FR and good performance was predicted to be obtained [40].

1.3.7 Startup Schemes

There are two types of supercritical FPPs. One is the constant pressure FPP that starts heating and operates at partial load at the supercritical pressure. The other is the sliding pressure FPP that starts heating at a subcritical pressure, and operates at subcritical pressure at partial load. A steam-water separator and a drain tank are needed for the startup of the sliding pressure FPP. The sliding pressure FPP operates with better thermal efficiency at subcritical pressure at partial load than the constant pressure FPP. In Japan, nuclear power plants are used for base load, and the FPPs are used for daily load following. Minimum partial load is 30% for the constant pressure FPP and 25% for the sliding pressure one [41, 42].

Startup schemes of the Super LWR are considered by referring to those of supercritical FPPs [43–45]. The constant pressure startup systems of the Super LWR and a supercritical FPP are shown in Fig. 1.16 [41]. The register tube and flash tank are installed on the bypass line. The supercritical steam is depressurized at the register tube and used for heating up the turbine during the startup (Table 1.6).

The sliding pressure startup systems of the Super LWR and a supercritical FPP are shown in Fig. 1.17 [41]. A steam-water separator is installed on the bypass line for the Super LWR, while it is installed on the main steam line for the supercritical FPP. The Super LWR has an additional heater installed to recover heat from the drain of the steam-water separator. When the enthalpy is low, the drain is dumped into the condenser directly. A boiler circulation pump can be used instead of the additional heater the same as in the sliding pressure FPP.

The thermal criteria for startup of the Super LWR are summarized in Table 1.9. The maximum cladding temperature during the power raising phase is limited below the same value as the rated power. The moisture content of steam sent to

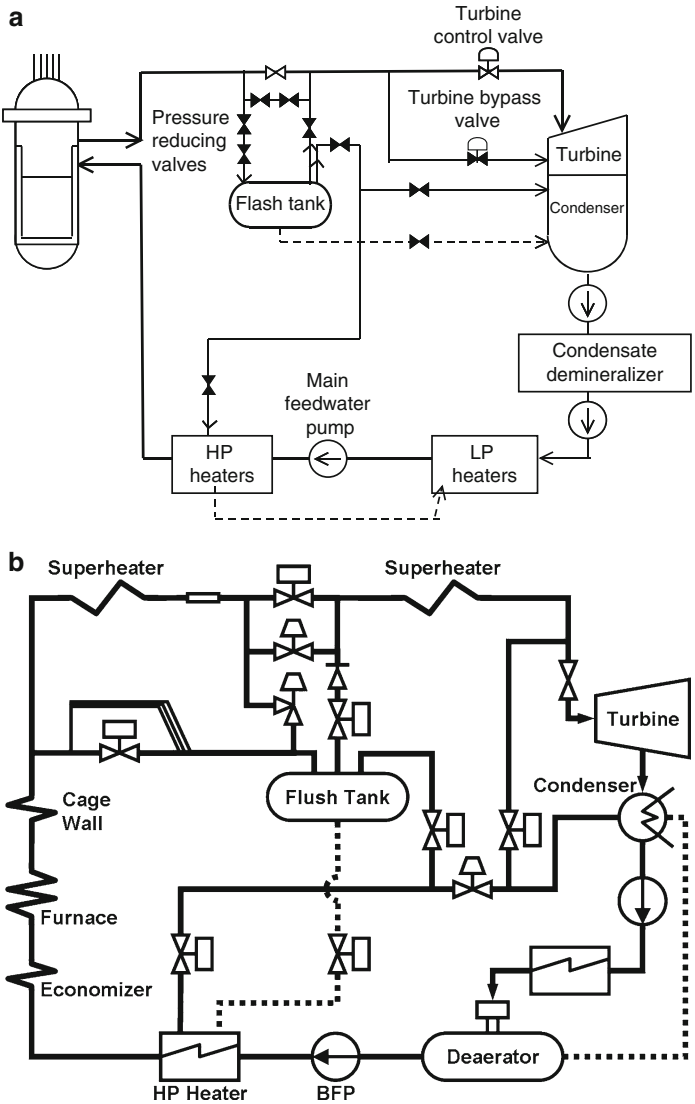

Fig. 1.16 Constant pressure startup systems of the Super LWR and supercritical FPP. (a) Super LWR (b) Supercritical FPP

Table 1.6 Thermal criteria for startup of Super LWR

Maximum cladding surface temperature must be the same as the rated power limit.
Moisture content in the turbine inlet must be less that 0.1% (the same criterion as BWR)
The enthalpy of the core outlet coolant must be high enough to provide the required turbine inlet steam enthalpy.
Boiling (and dryout) must be prevented in the water rods at subcritical pressures (in sliding pressure startup scheme).

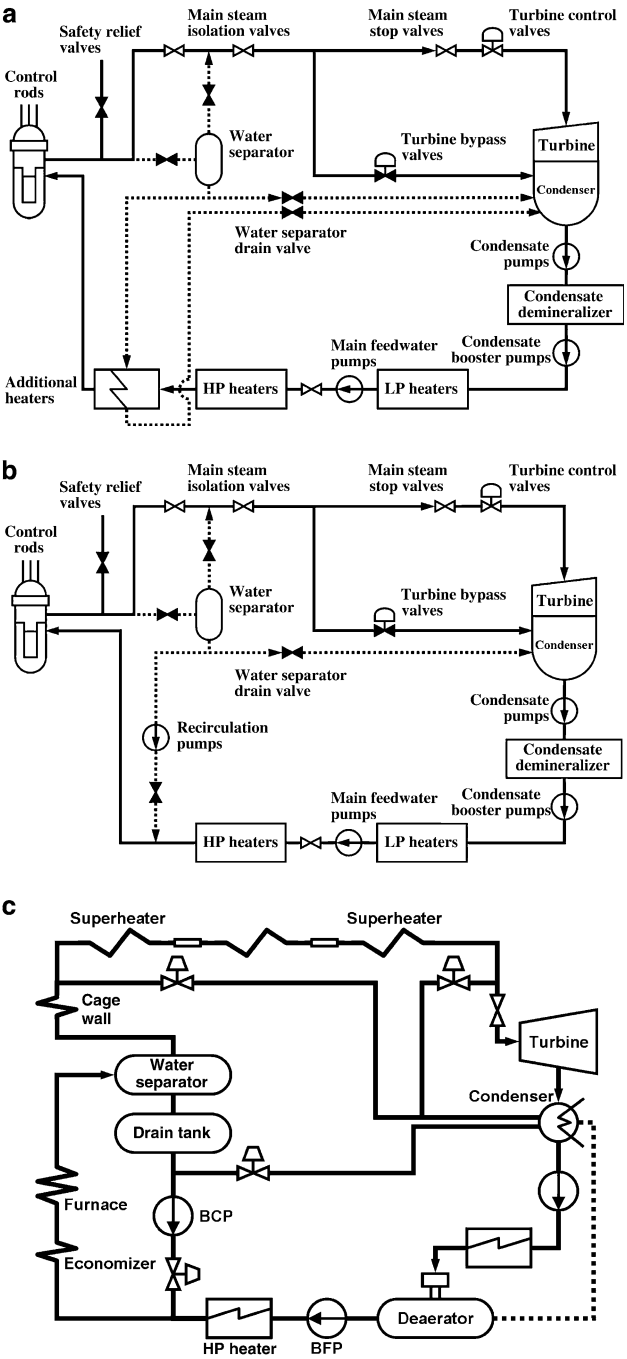

Fig. 1.17 Sliding pressure startup systems of the Super LWR and supercritical FPP. (a) Super LWR with additional heaters [41] (b) Super LWR with recirculation pumps [41]. (c) Supercritical FPP. (Taken from ref. [41] and used with permission from American Nuclear Society)

the turbine should be low enough not to damage the turbine blades at startup. The wetness in steam should be less than 0.1% at turbine startup, which is consistent with that of BWRs.

The third criterion states the enthalpy of the core outlet coolant must be high enough to provide the required turbine inlet steam enthalpy. Boiling must be prevented in the water rods at subcritical pressure of the sliding pressure startup scheme.

The calculation model for sliding pressure startup of the Super LWR is shown in Fig. 1.18 [43]. Examples of the sliding pressure startup curves based on the thermal considerations are shown in Fig. 1.19 [43].

With sliding pressure startup, the reactor starts up at a subcritical pressure and the pressure increases with the load. A steam-water separator and a drain tank are needed for two-phase flow. The heat loss is less than that of the constant pressure operation. At the reactor outlet, coolant evaporation is almost completed. Dryout inevitably occurs in the core at subcritical pressure in the once-through plant. The strategy for protection of furnaces in the once-through boilers is to keep the wall temperature in the post-dryout region below an adequate value by having a sufficient feedwater flow rate. To reduce the volume of the separator, it is also desirable for the core to be pressurized to a supercritical pressure with a low flow rate and a low power. The minimum feedwater flow rate is determined from the viewpoints of stability, core cooling, and pump performance. The cladding temperature can be calculated for a certain feedwater flow rate with various core powers. The reactor is pressurized to supercritical at 35% feedwater flow rate and 20% core power.

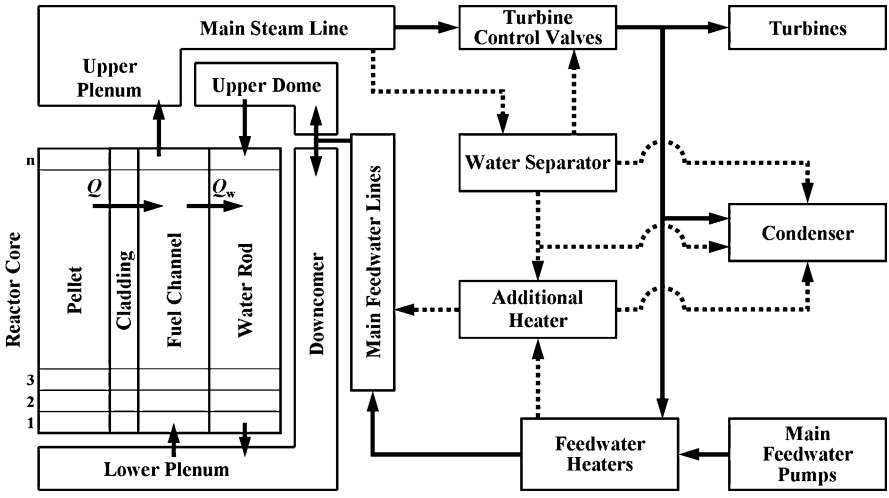

Fig. 1.18 Calculation model for sliding pressure startup scheme. (Taken from ref. [43] and used with permission from Atomic Energy Society of Japan)

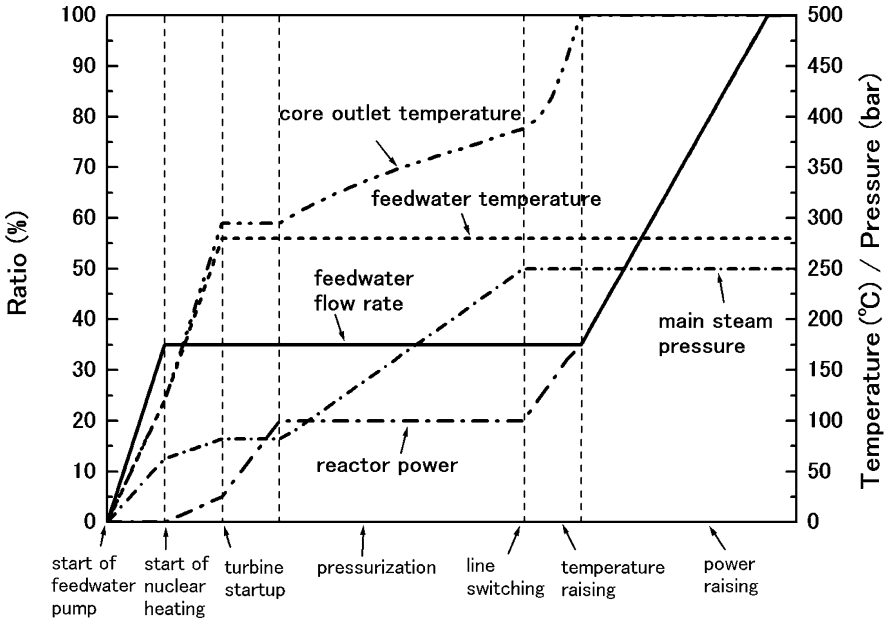

Fig. 1.19 Sliding pressure startup curves based on thermal considerations. (Taken from ref. [43] and used with permission from Atomic Energy Society of Japan)

After setting the feedwater flow rate at 35%, nuclear heating starts at a subcritical pressure. When the pressure of the core reaches an adequate value, saturated steam from the separator flows to the turbines. After startup of the turbines, the core is pressurized to a supercritical pressure with a core power at 20%. Startup operation ends and the plant is switched to the normal operation mode. The reactor power increases with the feedwater flow rate.

The sizes of the components required for the startup schemes are assessed. The sliding pressure startup with a steam separator in a bypass line is the best from the viewpoint of weight of the components. A study of the times needed for the startup schemes remains as future work. There is a limitation on the rate due to thermal stresses on thick-walled components such as the RPV. In BWRs, the temperature rise rate of the RPV wall is limited to below 55°C per hour.

The minimum allowable power and the minimum required power during the pressurization phase in the sliding pressure startup scheme are depicted in Fig. 1.20. The reactor power should be kept within narrow ranges at the pressure range between 20 and 22 MPa where boiling transition occurs. The MCST becomes high in this pressure range due to dryout as shown in Fig. 1.21 [43, 44]. But it is maintained below the limit of the rated value of the cladding temperature.

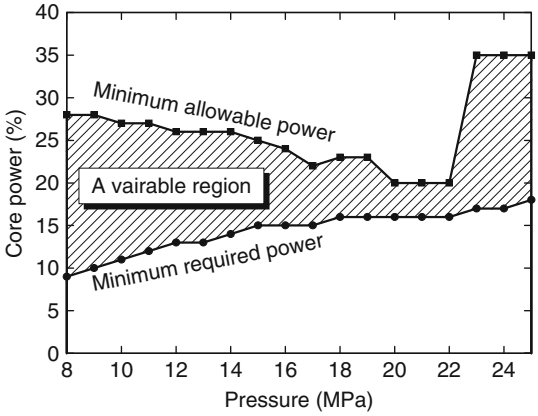

Fig. 1.20 Maximum allowable power and minimum required power during pressurization phase with feedwater flow rate of 35% and feedwater temperature of 280°C

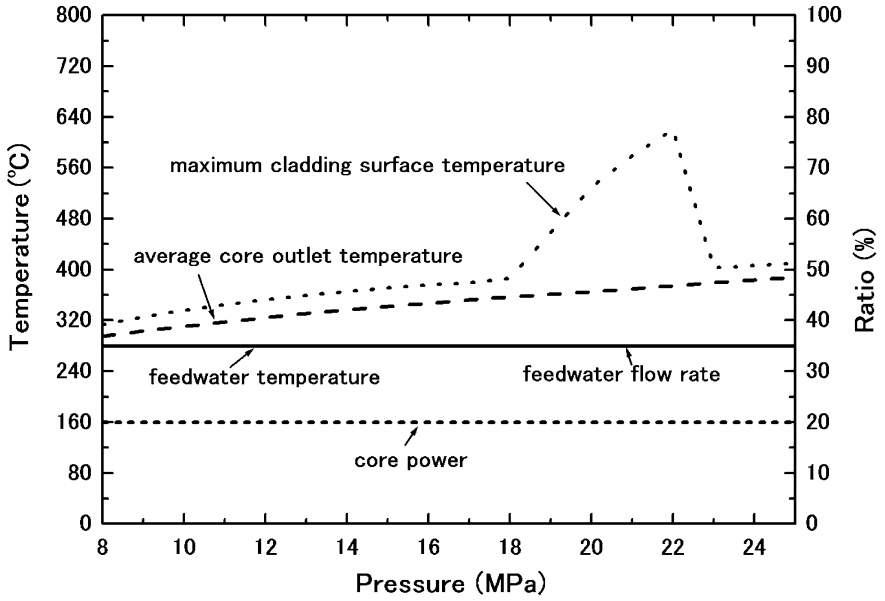

Fig. 1.21 Plant parameters in pressurization phase. (Taken from ref. [43] and used with permission from Atomic Energy Society of Japan)

The present analysis is based on the heat transfer correlations for smooth tubes. When turbulence is promoted, the cladding temperature rise at dryout will be suppressed. The maximum allowable power between 20 and 22 MPa will increase. Ribbed or rifled tubes and spiral tapes are used in supercritical FPPs to suppress the boiling transition during the sliding pressure operation and the sliding pressure

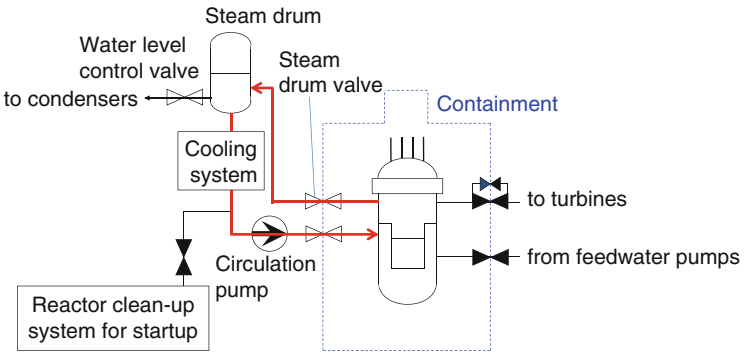

Fig. 1.22 Revised sliding pressure startup system of the Super LWR and the Super FR

startup. The critical heat flux correlations should be improved, including the effect of grid-spacers on the boiling transition.

Further elaboration of the startup considerations was made [46]. The turbines of the Super LWR and the Super FR and their startup will be similar to or the same as for of FPPs where the turbines are warmed and started using subcritical pressure superheated steam generated by superheaters. However, the Super LWR and the Super FR have no superheater and it is difficult to generate superheated steam in the core due to concern about fuel damage by dryout. A startup loop with a pump and a steam drum is used instead of the additional heater. This revised startup system is shown in Fig. 1.22. The Super LWR and Super FR adopt the once-through coolant cycle like FPPs without a circulation loop. Since it is difficult to raise the pressure and temperature in the once-through cycle, however, a circulation loop, just for startup, is added to the Super LWR and the Super FR plant (cf. the FPP shown as Fig. 1.17). Since the Super LWR and Super FR have no pressurizer heater, nuclear heating is chosen for raising the pressure and temperature in the loop. The circulation loop for startup consists of the reactor, the steam drum, the heat exchanger ("cooling system"), the circulation pump, and the piping. The roles of each component are described in Sect. 5.7. Startup of the Super FR is analyzed and the startup curves are shown in Fig. 1.23. The startup curves of the Super LWR will be obtained in the same way as that of the Super FR.

1.3.8 Stability

Instability is a nonlinear phenomenon. However, the dynamic behavior of nuclear reactors can be assumed to be linear for small perturbations around steady-state conditions. This allows the reactor stability to be studied and the threshold of instability in nuclear reactors to be predicted by using a linear model and solving linearized equations. Linear stability analyses in the frequency domain have been

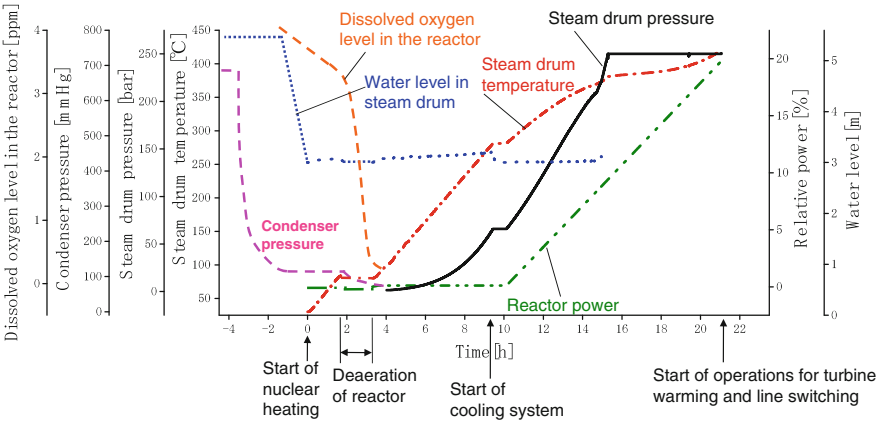

Fig. 1.23 Redesigned curves of sliding pressure startup before the power raising phase

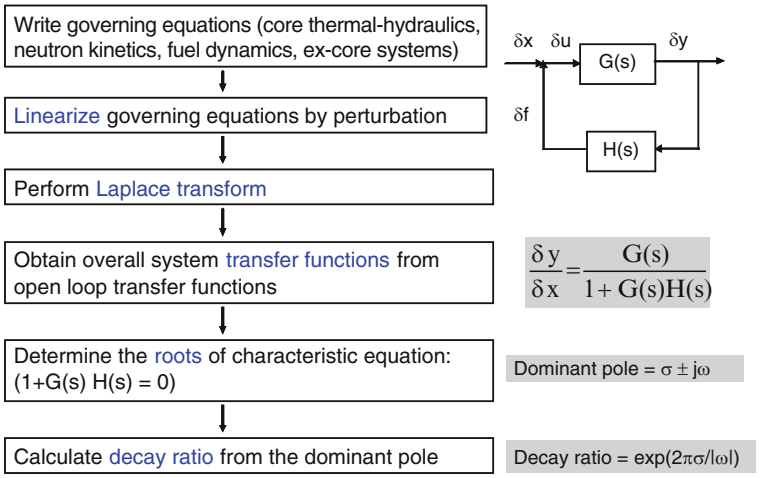

Fig. 1.24 Procedure for frequency domain linear stability analysis

made [44, 47–51]. Thermal-hydraulic stability, coupled neutronic and thermal-hydraulic stability and the stabilities during sliding pressure startup at subcritical pressure of Super LWR were analyzed [44, 47–50]. The thermal-hydraulic stability of the Super FR was also analyzed [51]. The present stability analysis code was developed by using a linearized one-dimensional, single-channel, and single-phase model. It is known from the parallel channel stability analysis of BWRs that the single-channel stability analysis is sufficient if the upper plenum and lower plenum are large [52, 53].

The procedure for the linear stability analysis is shown in Fig. 1.24. In the linear stability analysis, the governing equations are first perturbed around the steady-state

parameters. The perturbed equations are then linearized and Laplace transformed from the time domain to the frequency domain. The resulting equations are used to evaluate various system transfer functions by applying proper boundary conditions. After all the required transfer functions are derived, the individual transfer functions are combined to provide the overall system transfer functions. The frequency response and stability characteristics of the Super LWR are studied with respect to small perturbations in system parameters such as inlet flow velocity, inlet coolant pressure, etc.

The linearized and Laplace-transformed equations of the models are used to evaluate the various system transfer functions as functions of the Laplace variables $s = \sigma + j\omega$, where σ is the real part and ω is the imaginary part of the complex variable s. σ refers to the damping constant (or damped exponential frequency) and ω refers to the resonant oscillation frequency of the system. The forward transfer function and feedback transfer function of the system are represented by $G(s)$ and $H(s)$, respectively. The closed loop transfer function or system transfer function is obtained from $G(s)$ and $H(s)$. The poles of the closed loop transfer function are determined by solving the characteristic equation: $1+ G(s)\, H(s) = 0$. The poles may be real and/or complex conjugate pairs. For systems with more than one pole, the pole which has the slowest response is dominant over other poles after some time. For stable systems, the dominant pole is the pole nearest to the imaginary axis (the pole with the largest value of σ/ω) and it is used to determine the stability of the system. The stability of the system depends on the value of σ. For the system to be stable, all the poles of the closed loop transfer function must have negative real parts ($\sigma < 0$). The system becomes unstable if a pole crosses the imaginary axis and enters into the right half of the s-plane ($\sigma > 0$). The system will be on the margin of stability and will sustain an oscillation without damping if the pole lies on the imaginary axis ($\sigma = 0$).

The system stability is described by the decay ratio, which is defined as the ratio of two consecutive peaks of the impulse response of the oscillating variable as shown as Fig. 1.25. For the complex pole $s = \sigma + j\omega$, the impulse response of the system is represented by $Ke^{\sigma t}(\cos\omega t + j\ \sin\omega t)$ where K is a constant. Hence, if the positions of the complex poles of the closed loop transfer function are known, the decay ratio DR can be calculated by using the following equation:

$$\text{Decay ratio} = \text{DR} = \frac{y_2}{y_1} = \frac{\left|Ke^{\sigma t_2}(\cos\omega t_2 + j\sin\omega t_2)\right|}{\left|Ke^{\sigma t_1}(\cos\omega t_1 + j\sin\omega t_1)\right|} = e^{\sigma(t_2 - t_1)} = e^{2\pi\sigma/\omega} \quad (1.1)$$

The axial mesh size has a significant effect on the decay ratio and the frequency response just as it does for LWR stability analysis. The decay ratio generally increases as the axial mesh size decreases. The decay ratio is determined by extrapolation to zero mesh size using the method of least squares.

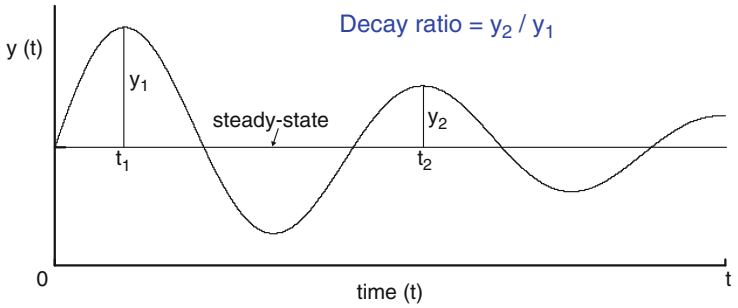

Stability Criteria

	Normal operating conditions	All operating conditions
Thermal-hydraulic stability	Decay ratio ≤ 0.5 (damping ratio ≥ 0.11)	Decay ratio <1.0 (damping ratio > 0)
Coupled neutronic thermal-hydraulic stability	Decay ratio ≤ 0.25 (damping ratio ≥ 0.22)	Decay ratio < 1.0 (damping ratio > 0)

The same stability criteria as BWR

Fig. 1.25 Definitions of the decay ratio and stability criteria

The stability criteria of the decay ratio are taken to be the same as those of BWRs as shown in Fig. 1.25.

(a) The decay ratio of thermal-hydraulic stability should be less than 0.5 for normal operating conditions and that of coupled stability should be less than 0.25.
(b) The decay ratio must be less than 1.0 for all operating conditions.

The decay ratios of the thermal-hydraulic stability of the hottest channel and the average channel are obtained as shown in Fig. 1.26.

The relation between the decay ratios and orifice pressure drop coefficients is shown in Fig. 1.27. The reactor becomes more stable when the orifice pressure drop coefficient increases as is also known for BWRs. It can be seen that the thermal-hydraulic stability criterion is satisfied in the Super LWR at full power normal operation for the average power channel. The maximum power channel can be stabilized by applying a proper orifice pressure drop coefficient. The minimum orifice pressure drop coefficient required for thermal-hydraulic stability at full power operation is found to be 6.18 (a pressure drop of 0.0054 MPa). The total core pressure drop at 100% maximum power operation is 0.133 MPa. The required orifice pressure drop is small compared with the total core pressure drop.

The block diagram used for coupled neutronic and thermal-hydraulic stability of the Super LWR is shown in Fig. 1.28. The neutronic model is used to find the forward transfer function $G(s)$ and the thermal-hydraulic heat transfer and ex-core models are used to determine the backward transfer function $H(s)$. The frequency

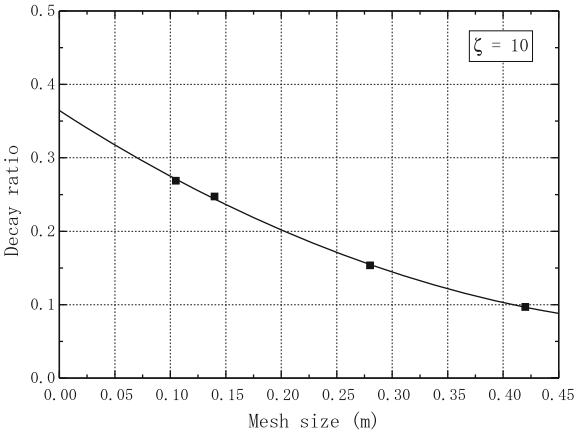

Fig. 1.26 Effect of axial mesh size on decay ratio. (Taken from ref. [49] and used with permission from Atomic Energy Society of Japan)

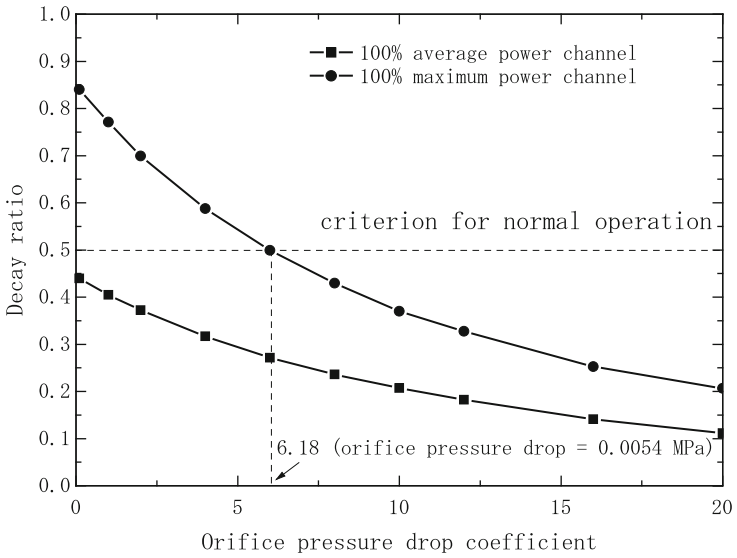

Fig. 1.27 Orifice pressure drop coefficient versus decay ratio of thermal-hydraulic stability at full power operation. (Taken from ref. [49] and used with permission from Atomic Energy Society of Japan)

response of the closed loop transfer function for coupled neutronic and thermal-hydraulic stability of the Super LWR for the 100% average power channel is shown in Figs. 1.29 and 1.30. The presence of water rods clearly increases the resonant peak and the phase lag of the closed loop transfer function due to the destabilizing effects of neutronic feedback.

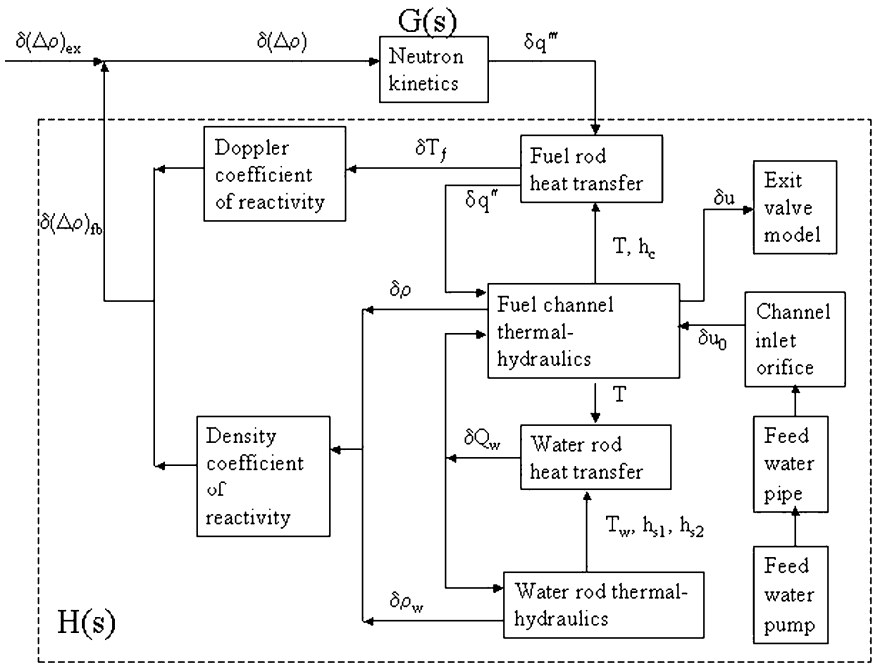

Fig. 1.28 Block diagram for coupled neutronic thermal-hydraulic stability of the Super LWR. (Taken from ref. [50] and used with permission from Atomic Energy Society of Japan)

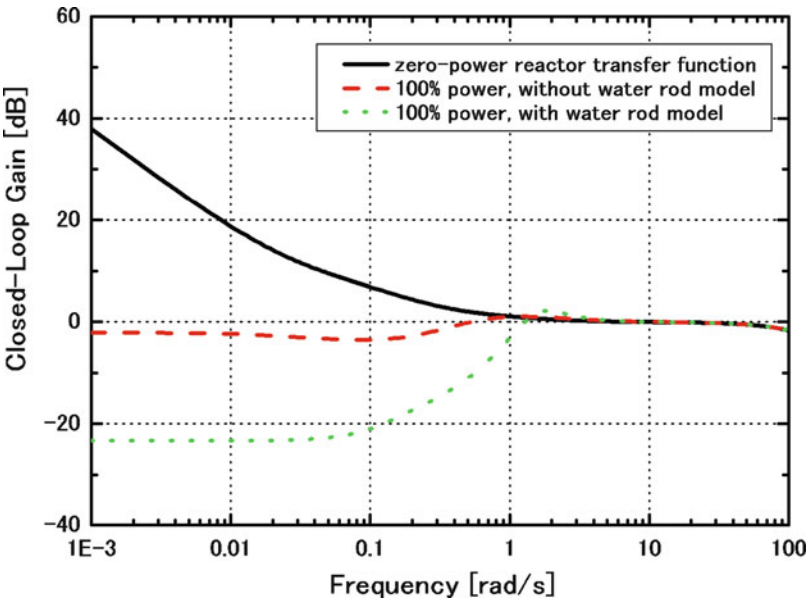

Fig. 1.29 Gain response of closed loop transfer function of coupled neutronic thermal-hydraulic stability

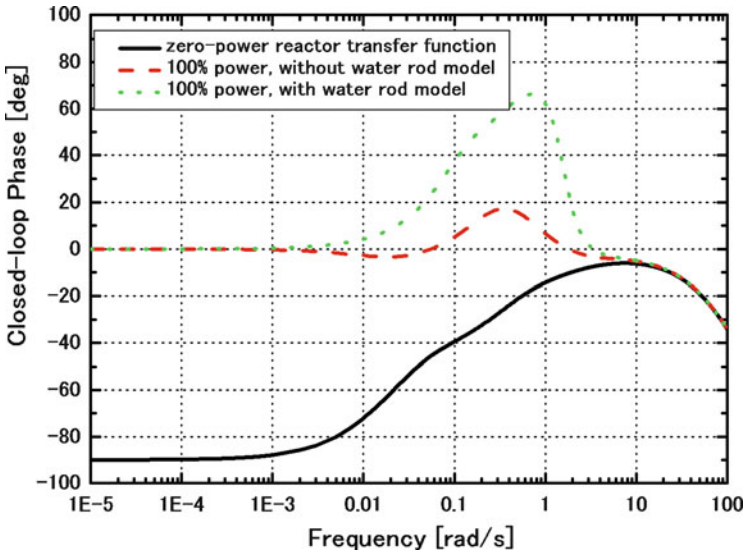

Fig. 1.30 Phase response of closed loop transfer function of coupled neutronic thermal-hydraulic stability

The time delay of the heat transfer to the coolant and moderator water is an important factor in the mechanism of coupled neutronic and thermal-hydraulic instability. The Super LWR is a reactor system with a positive density coefficient of reactivity and a large time delay constant. If there is no time delay, a decrease in density would cause a decrease in power generation, which suppresses any further decrease in density, stabilizing the system. However, if there is a large time delay, it causes a decrease in the gain of the density reactivity transfer function, and reduces the effect of density reactivity feedback, making the system less stable. The time delay of the heat transfer to the water rods is much larger than that to the coolant. Thus the reactor system becomes less stable when the water rod model is included than the case without it.

Figure 1.31 shows the decay ratio contour map for coupled neutronic and thermal-hydraulic stability of the Super LWR. The decay ratio contour line of DR = 1.0 indicates the stability boundary on the power versus flow rate map of the Super LWR. At the high power low flow rate region, the reactor becomes unstable. At low power operation and during startup, it is necessary to take care to satisfy the stability criteria. At the low power low flow rate region, the unstable conditions should be avoided by carefully adjusting the flow rate.

In summary, the following points are obtained regarding stability of the Super LWR.

1. In spite of the low flow rate and large coolant density change, the thermal-hydraulic stability of the Super LWR can be maintained by a sufficient orifice pressure drop coefficient.

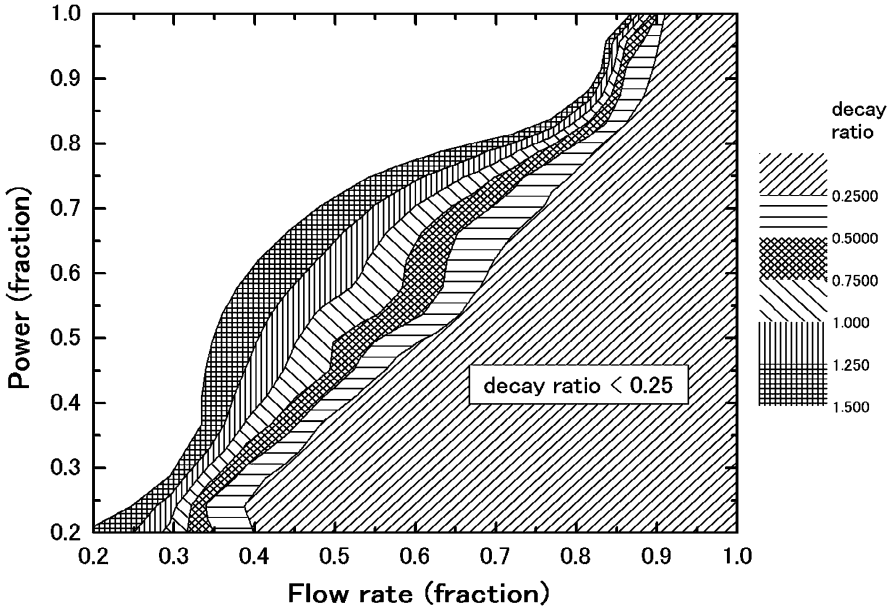

Fig. 1.31 Decay ratio map for coupled neutronic and thermal-hydraulic stability of the Super LWR

2. The presence of water rods reduces the density reactivity feedback effect due to the large time delay in the heat transfer to the water rods, and this affects the coupled neutronic and thermal-hydraulic stability.
3. The coupled neutronic and thermal-hydraulic stability of the Super LWR can be maintained by controlling the power to flow rate ratio.

Stability during sliding pressure startup was analyzed [44]. The changes of decay ratio and flow rate with core power during the power raising phase are shown in Fig. 1.32. A high flow rate is necessary at low core power. Figure 1.33 shows the sliding pressure startup curves with the stability criteria. High flow rate is required after line switching compared with the startup curves without the stability criteria.

In summary, at the subcritical pressure operation during the pressurization phase, thermal criteria are more limiting due to dryout. The startup scheme prior to line switching is mainly determined by thermal criteria. The thermal-hydraulic stability criterion is satisfied by applying a sufficient orifice pressure drop coefficient. The coupled neutronic and thermal-hydraulic stability is also satisfied, since the power to flow rate ratio is low during this phase.

In the power raising phase, the thermal criteria are not as limiting as stability criteria, because the coolant flow is a single phase one at supercritical pressure operation. If only thermal criteria are considered, the power to flow rate ratio in the power raising phase can be kept as one, and the MCST can be maintained so it does not exceed the rated value. However, if stability considerations are also taken into

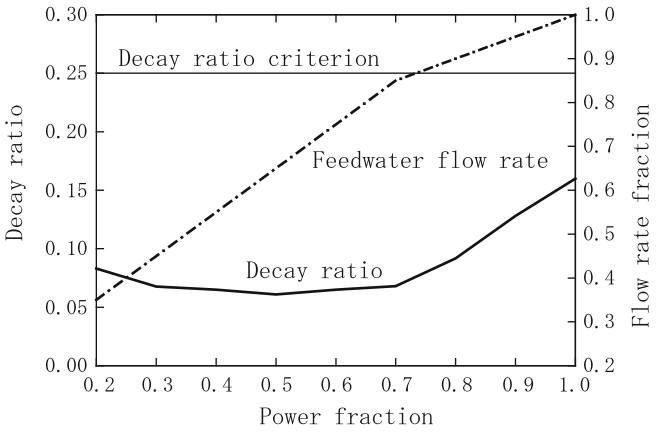

Fig. 1.32 Coupled neutronic thermal-hydraulic stability analysis result at power increase phase

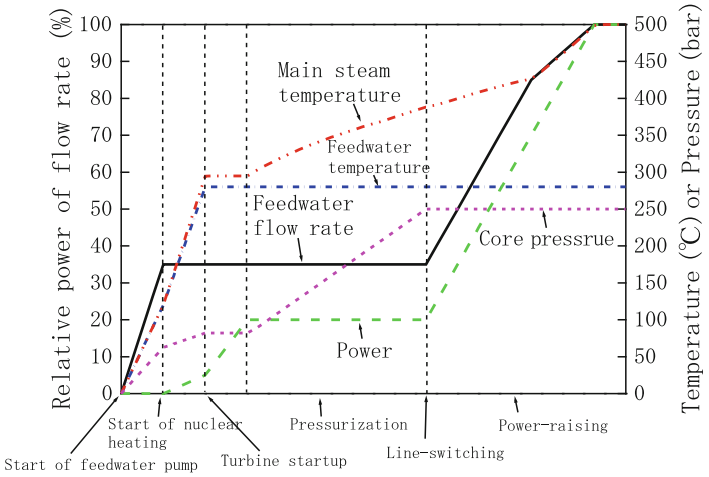

Fig. 1.33 Sliding pressure startup curve with thermal and stability considerations

account, while the thermal-hydraulic stability criterion can be satisfied with an orifice pressure drop coefficient, the power to flow rate ratio needs to be reduced at low-power operations to satisfy the coupled neutronic and thermal-hydraulic stability criterion. The power and flow rate are to be controlled as required during this phase. Thus, the startup procedure after line switching is determined and limited by stability criteria, more than it is by thermal criteria.

Stability is maintained by increasing orifice pressure drop in the design. The pumping power increases with the total pressure drop, but it is not a problem in the once-through cycle reactor. The pump is powerful and pumping power is not excessive because of the small reactor coolant flow rate.

1.3.9 Safety

1.3.9.1 Safety Principle

The unique advantage of the once-through cooling system is that depressurization cools the core effectively [54–56]. The coolant flow during depressurization is shown in Fig. 1.34 [56]. Actuating the automatic depressurization system (ADS) induces core coolant flow. The downward flow water rod system enhances this effect because low temperature water in the top dome and in the water rods flows through the core to the ADS. An example of depressurization behavior is shown in Fig. 1.35 [56]. The core coolant flow rate is maintained during depressurization even though the feedwater flow is lost. Due to the downward-flow water rod system, the coolant flowing to the core during depressurization is not only from the bottom dome and the downcomer but also from the top dome and the water rods. The top dome serves as an "in-vessel accumulator". The core coolant flow rate changes with the ADS flow rate, which oscillates due to the change of the pressure, temperature, and the steam quality. The reactor power increases immediately after the ADS actuation due to the increased flow rate and then decreases due to boiling and the reactor scram. The hottest cladding temperature does not increase from the initial value because the power to flow rate ratio is kept above unity. After the depressurization, the decay heat is removed by the low pressure core injection system (LPCI).

LWRs have a coolant circulation system such as the recirculation system of BWRs and the primary coolant system of PWRs. The fundamental safety requirement for LWRs is keeping the coolant inventory so as to maintain core cooling by

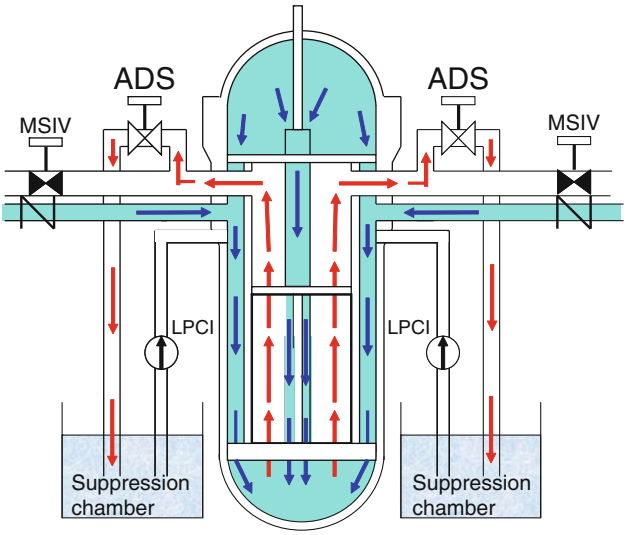

Fig. 1.34 Coolant flow during reactor depressurization. (Taken from ref. [56] and used with permission from Korean Nuclear Society)

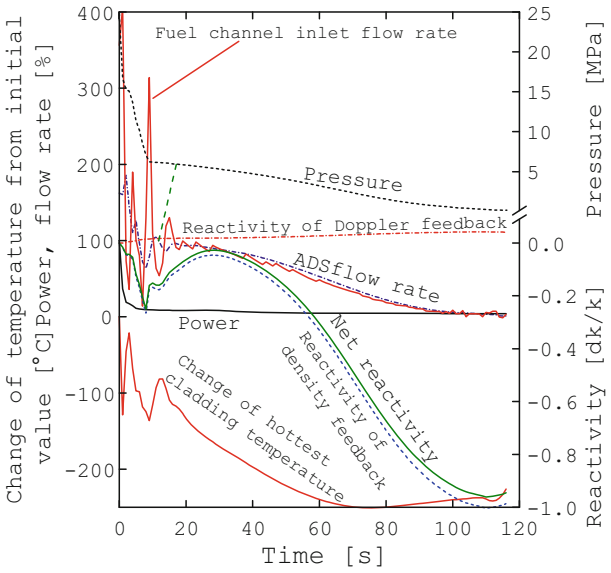

Fig. 1.35 Behavior during reactor depressurization. (Taken from ref. [56] and used with permission from Korean Nuclear Society)

either forced circulation or natural circulation. Coolant inventory is kept by maintaining the water level in the RPV of a BWR and the pressurizer of a PWR. It is monitored and used for the fundamental safety signal of LWRs.

The once-through cooling system has no coolant circulation system and there is no water level during supercritical pressure operation. The depressurization behavior described above indicates that a decrease in the coolant inventory does not threaten the safety of the once-through cooling system as long as the core coolant flow rate is maintained. Inventory control is not necessary for the Super LWR and Super FR. The fundamental safety requirement of the Super LWR is maintaining the core coolant flow rate. Since the once-through cooling system has both coolant inlet and outlet, the core coolant flow rate is kept by "keeping the coolant supply from the cold-leg" and "keeping the coolant outlet open at the hot-leg" [54–64].

"Loss of feedwater flow" is the same as "loss of reactor coolant flow" for the once-through cooling Super LWR and Super FR. BWRs have a recirculation system and there is large coolant inventory in the RPV. PWRs have the secondary system as well as the primary system and there is a large coolant inventory in the steam generators. Therefore, the feedwater is more important for the Super LWR than for LWRs. "Feedwater flow," "feedwater system," and "feedwater pump" of the Super LWR are described as "main coolant flow," "main coolant system," and "reactor coolant pump (RCP)," respectively, in the safety analysis, to be distinguished from those of LWRs. The main coolant flow rate is equal to the core coolant flow rate and the main steam flow rate at the steady state due to once-through cooling system.

The safety principle of the Super LWR and Super FR is compared with those of PWRs and BWRs in Table 1.7. The main coolant flow rate and turbine inlet pressure are monitored and used for the emergency signal, instead of the "water level" of LWRs.

1.3.9.2 Plant and Safety Systems

The plant and safety systems of the Super LWR and Super FR are shown in Fig. 1.36 [56]. The safety system design is summarized in Sect. 6.3.2.

The relation between the levels of abnormalities and the safety system actuations are shown in Table 1.8 [54]. A decrease in the coolant supply is detected as low levels of the main coolant flow rate. The reactor scram, the AFS and the ADS/LPCI are actuated sequentially depending on the levels of abnormality. The reactor is scrammed at level 1 (90%) and then the AFS is actuated at level 2 (20%). Level 3 (6%) means that the decay heat cannot be removed at supercritical pressure, so the reactor is depressurized.

Table 1.7 Comparison of safety principles

	PWR	BWR	Super LWR, Super FR
Requirement	Primary coolant inventory	Coolant inventory in the reactor vessel	Coolant flow rate in the core
Monitored parameter	Water level in the pressurizer	Water level in the reactor vessel	Main coolant flow rate, turbine inlet pressure

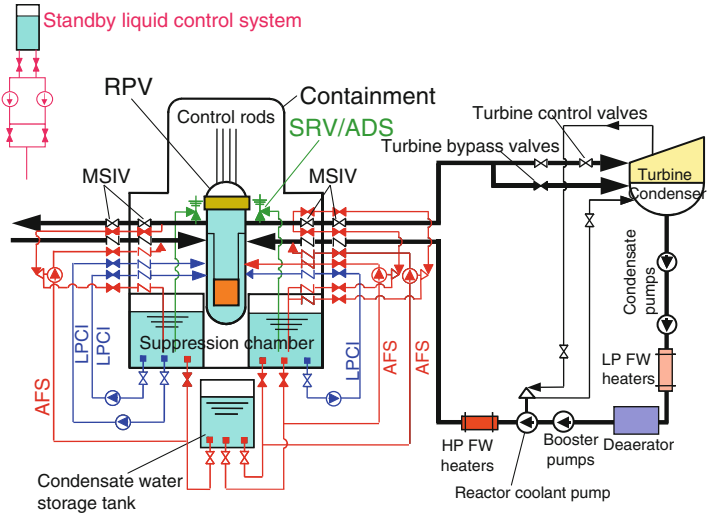

Fig. 1.36 Plant and safety systems of Super LWR and Super FR. (Taken from ref. [56] and used with permission from Korean Nuclear Society)

Table 1.8 Principle of safety system actuation

Flow rate low (feedwater or main steam)	
Level 1 (90%)[a]	Reactor scram
Level 2 (20%)[a]	AFS
Level 3 (6%)[a]	ADS/LPCI system
Pressure high	
Level 1 (26.0 MPa)	Reactor scram
Level 2 (26.2 MPa)	SRV
Pressure low	
Level 1 (24.0 MPa)	Reactor scram
Level 2 (23.5 MPa)	ADS/LPCI system

Taken from ref. [54] and used with permission from Atomic Energy Society of Japan
AFS auxiliary feedwater system, *ADS* automatic depressurization system, *LPCI* low pressure core injection system
[a]100% corresponds to normal operation

Closure of the coolant outlet is detected as pressure high levels. The reactor is scrammed at level 1 (26.0 MPa) and then the SRVs are actuated at level 2 (26.2 MPa). The ratio of the SRV set point and the normal operating pressure is smaller than that of an ABWR because the relative change of the core pressure is smaller in the Super LWR due to higher operating pressure of the latter.

Abnormal valve opening and pipe break are detected as pressure low levels. If the pressure decreases from supercritical to subcritical, dryout occurs on the fuel rod surface, which will lead to a rapid increase in the cladding temperature. Therefore, it is better to avoid keeping the core pressure near the critical pressure. In the present design, the ADS is actuated at level 2 (23.5 MPa), which is about 106% of the critical pressure (22.1 MPa). During rapid depressurization, an increase in the cladding temperature is prevented due to the large core flow rate even though dryout occurs.

Generally, the scram signal should be released before the emergency core cooling system (ECCS) signal. In consideration of this relationship, the low pressure scram set point, which is 24.0 MPa, is above the ADS/LPCI set point (one of the ECCS set points), which is 23.5 MPa.

1.3.9.3 Safety Criteria

Safety criteria need to be defined for the same abnormal transients and accidents as those of LWRs. Abnormal transients are defined as abnormal incidents that are expected to occur one or two times during the reactor service life. The requirements are the same as those of LWRs: no systematic fuel rod damage, no fuel pellet damage, and no pressure boundary damage. Abnormal incidents with expected frequency below 10^{-3} per year are further categorized as accidents as in LWRs. They are required not to result in excessive core damage.

Table 1.9 Principle of safety criteria for fuel rod integrity

Category	Requirement	Mechanical failure			Heat-up
		Buckling	Burst	PCMI	
Accident	No excessive damage			Enthalpy < Limit (RIA)	Oxidation<Limit MSCT<Limit
Transient	No systematic damage	ΔP on clad. <Limit	Plastic strain < Limit	Pellet temp.<Limit Plastic strain<Limit Enthalpy<Limit	

The principle of fuel rod integrity is summarized in Table 1.9. Four damage modes of the fuel cladding are expected at transients: (a) buckling collapse, (b) stress rupture, (c) PCMI, and (d) thermal damage [65].

The criterion for buckling collapse is simple: the pressure difference on the cladding does not exceed one-third of the buckling collapse pressure.

Removing the MDHFR criterion (analogous to the critical heat flux criterion of LWRs) and taking the MCST criterion were described in Sect. 1.3.2 and in ref. [66]. But the fuel rod integrity criteria for the stress rupture were further improved in two steps. The old criteria were derived from the mechanical strength requirement of the cladding based on ASME Boiler and Pressure Vessel Code Section III in which the requirement assumed an infinite period for the transients. The MCST criterion was set at 800°C for Ni-base alloy cladding and the fuel rods were designed to withstand that temperature [66].

But in reality, the period of transients is short. The improvement of fuel rod integrity assessment considering the period of transients was studied in Japanese liquid metal cooled fast breeder reactors (LMFBRs) R&D programs. Based on obtained results, it was proposed to raise the limit of the MCST from 830°C to over 900°C for future LMFBRs. It is possible to analyze the fuel rod integrity of the Super LWR and Super FR at transients using the FEMAXI-6 code. The improved criteria of fuel rod integrity for abnormal transients for Super LWRs were developed using the code [32]. The new criteria raised the limit of MCST to 850°C for stainless steel cladding. Experimental validation of the criteria remains for future study. Old and new criteria are compared in Table 1.10. The improved criteria for abnormal transients are further summarized in Table 1.11.

The criterion related to PCMI is that the plastic deformation of the cladding should be below 1.0%, which is the same as for LWRs. The relation between plastic deformation and damage of the candidate materials needs to be assessed by experiments.

The thermal damage criterion is limited by the cladding temperature. It is the same value derived from stress rupture. The criterion of MCST for accidents is 1,260°C for stainless steel cladding. It is the same value as the early USNRC criterion for LWRs using stainless steel cladding [67].

Table 1.10 Comparison of fuel rod integrity criteria for abnormal transients

Requirements	Old criteria	New criteria
No buckling collapse of cladding	Pressure difference $<1/3 \times$ collapse pressure	Pressure difference $<1/3 \times$ collapse pressure
No mechanical failure of cladding	ASME B&PV code III	No plastic strain
No melting of fuel pellet	Centerline temperature $<$ melting point	Centerline temperature $<$ melting point

Table 1.11 New criteria for fuel rod integrity for abnormal transients

	Old criteria	New criteria				
Maximum cladding surface temperature (°C)	800 (Ni-base alloy)	850 (Stainless steel)				
Maximum allowable power (%P_0)	none	Power rise rate [%P_0/s]	<0.1	0.1–1	1–10	>10
		Scram set point	120	124	136	182
Maximum system pressure (MPa)	28.9	28.9				

P_0 initial power

The initial conditions and criteria for MCST in abnormal transients and accidents are shown in Fig. 1.37. The maximum peak temperature at the steady state condition, 740°C, has changed with improvement of the core design method and data as already described in Sect. 1.3.4. But when 740°C is taken, the temperature difference between the limits, 110°C for abnormal transients and 520°C for accidents are the margins.

For reactivity insertion accidents (RIAs), the pellet enthalpy criterion of 230 cal/g UO_2 is taken. It is the same as for LWRs. For abnormal transients with reactivity insert over \$1, the criterion is set as 170 cal/g, again taken from that of LWRs. However, this criterion has not been applied to the safety analysis of the Super LWR and Super FR because no transient is followed by reactivity insertion over \$1. It should be considered in the future study whether the pellet enthalpy criterion for transients is necessary, as in LWRs, or not, as in sodium cooled reactors.

The concept of keeping pressure boundary integrity is the same as that of LWRs. The maximum allowable pressures are 28.9 MPa at a transient, which is 105% of the maximum pressure of normal operation, and 30.3 MPa at an accident, which is 110% of the maximum pressure of normal operation while they are 110% at a transient and 120% at an accident in LWRs. However, the Super LWR still has a sufficient margin to the criteria because its pressure change is milder than that of LWRs.

The criterion for anticipated transients without scream (ATWS) is the same as that of accidents. Experimental validation of the criteria remains for future study.

1.3.9.4 Safety Analysis at Supercritical Pressure

The abnormalities of the Super LWR and Super FR are considered with reference to those of LWRs (see Sect. 6.4). The initiating events for safety analysis are summarized in Table 1.12.

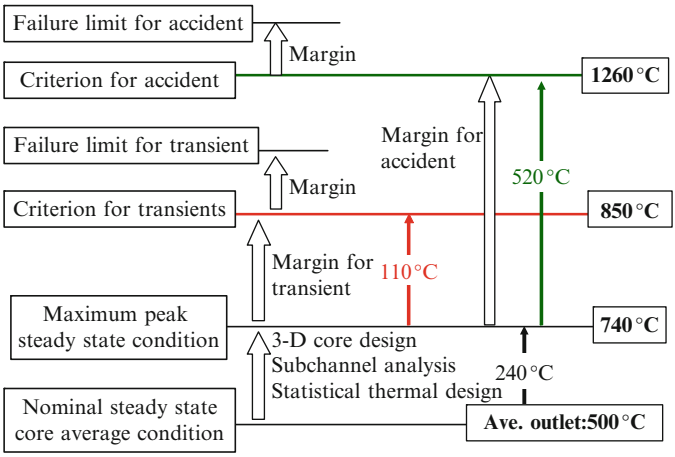

Fig. 1.37 Maximum cladding surface temperature criteria and margins for abnormal transients and accidents

Table 1.12 Abnormal events in safety analysis

Abnormal transients
Decrease in core coolant flow rate
Partial loss of reactor coolant flow
Loss of offsite power
Abnormality in reactor pressure
Loss of turbine load
Isolation of main steam line
Pressure control system failure
Abnormality in reactivity
Loss of feedwater heating
Inadvertent startup of AFS
Reactor coolant flow control system failure
Uncontrolled CR withdrawal at normal operation
Uncontrolled CR withdrawal at startup
Accidents
Decrease in core coolant flow rate
Total loss of reactor coolant flow
Reactor coolant pump seizure
Abnormality in reactivity
CR ejection at full power
CR ejection at hot standby
LOCA
Large LOCA
Small LOCA

The "reactor coolant flow abnormality" is important for the Super LWR because maintaining the core coolant flow rate is the fundamental safety requirement. It should be noted that there are two types of reactor coolant flow abnormalities with and without reactor scram before events; the former are abnormal transient types

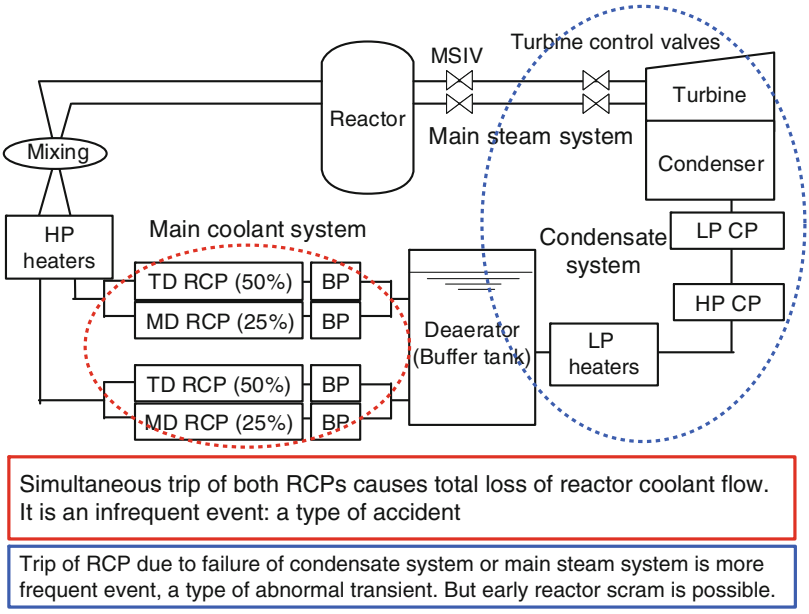

Fig. 1.38 Two types of "loss of flow" events

and the latter are accident types [55, 56, 64, 65]. This point is summarized in Fig. 1.38 and described in detail in Sect. 6.4.

The node-junction model of the safety analysis code at supercritical pressure is shown in Fig. 1.39. Mass, energy, and momentum conservation equations are solved. The heat transfer between fuel coolant channels and water rods is taken into account. The hot and average channels are analyzed. The Oka–Koshizuka heat transfer correlation is used for the analysis. It covers the flow and power conditions of the safety analysis. It gives smaller heat transfer coefficients at low mass flux condition compared with experiments and other existing correlations such as the Watts–Chou correlation and Bishop correlation. It predicts higher cladding temperature than other correlations. Location of the hottest cladding temperature tends to be at the high temperature "gas-like" coolant region above 500°C where the heat transfer coefficient should agree with the Dittus–Boelter correlation. The Oka–Koshizuka correlation agrees relatively well with the Dittus–Boelter correlation at this region compared with the other correlations.

The results of the "total loss of reactor coolant flow" accident are explained in Fig. 1.40. The heat conduction to the water rods increases and the water rods serve as a "heat sink". This heat conduction also thermally expands the water in the water rods and temporarily supplies water to the fuel channels. Thus, water rods serve as a "water source" also and enable the backup pumps (AFSs) to have a realistic delay time. The results of "loss of turbine load without turbine bypass" transient are shown in Fig. 1.41. This is a type of pressurization event and an important one for

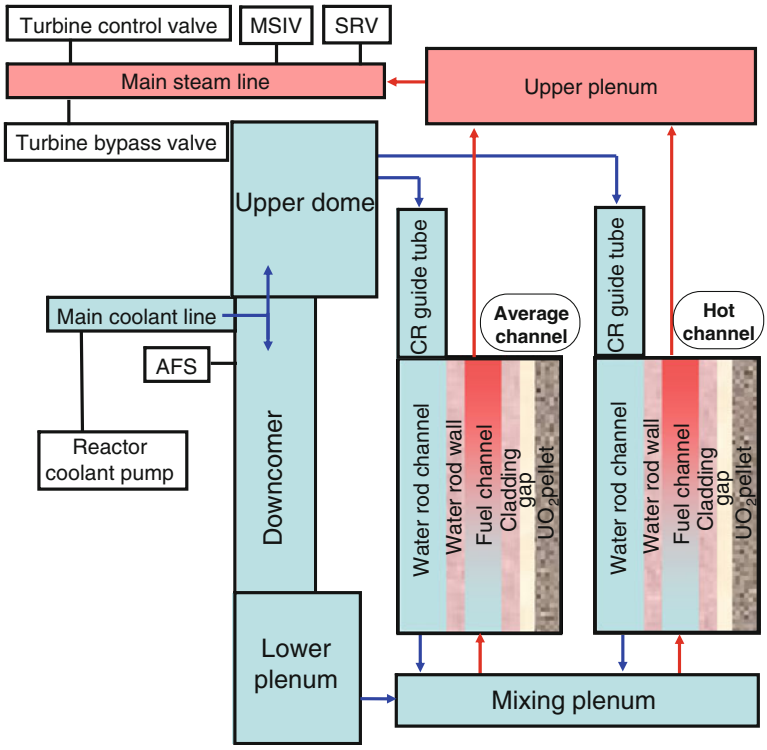

Fig. 1.39 Calculation model of SPRAT-DOWN for safety analyses

BWR safety design. But the power rise is mild for the Super LWR because of the smaller water density change than that of BWRs due to the high pressure. Flow stagnation occurs and increases density feedback. It also mitigates the power rise. The pressure change itself is also small at the supercritical pressure [65]. The abnormal transient and accident analyses are summarized in Sects. 6.7.1 and 6.7.2, respectively.

The anticipated transients without scram (ATWSs) of the Super LWR were analyzed to clarify its safety characteristics [68, 69]. An ATWS is defined as an abnormal transient followed by the failure of reactor scram. The results of "loss of offsite power" are shown in Fig. 1.42. An alternative action is not needed either to satisfy the safety criteria or to achieve a high temperature stable condition for all ATWS events. Initiating the automatic depressurization system is a good alternative action that induces a strong core coolant flow and inserts a negative reactivity. It provides an additional safety margin for the ATWS events. The Super LWR has excellent ATWS characteristics, providing a key reactor design advantage. The ATWS analyses are summarized in Sect. 6.7.4.

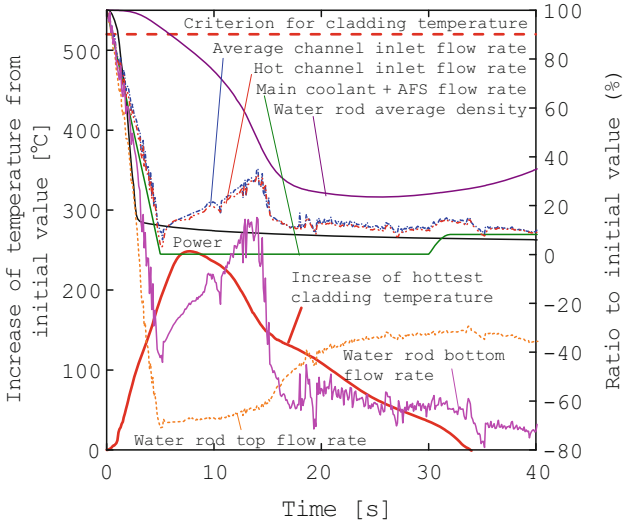

Fig. 1.40 Calculated results for "total loss of reactor coolant flow"

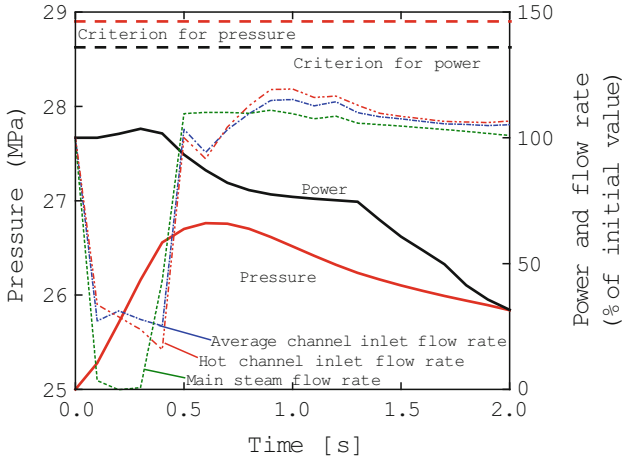

Fig. 1.41 Calculated results for "loss of turbine load without turbine bypass"

The change of cross flow within a subassembly may occur during transients. The MCST may change from the result of the single-channel calculation. A transient subchannel analysis code was developed and the safety analysis of a Super LWR was carried out [70]. The temperature rises from the steady state value are about 20°C at the abnormal transients and about 130°C at accidents. The maximum values still stay below the MCST criteria for transients and accidents. The development and application of the transient subchannel analysis code are summarized in Sect. 6.8.

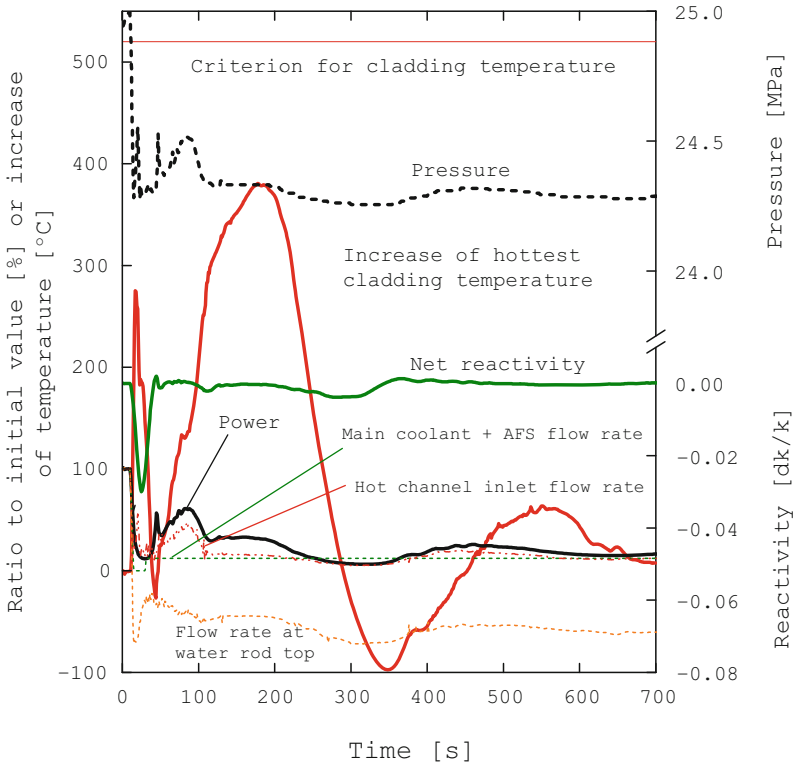

Fig. 1.42 Calculation results for "loss of offsite power" (ATWS) without alternative action

1.3.9.5 LOCA Analysis

Loss of coolant accidents (LOCAs) of the Super LWR and Super FR are treated as design basis accidents as in current LWRs. There are mainly two differences in the LOCA phenomena between the Super LWR/Super FR and LWRs. One is that a "double-ended break" does not occur in the Super LWR and Super FR. Figure 1.43 [71] compares blowdown phenomena among PWRs, BWRs and the Super LWR. Since PWRs and BWRs have circulation loops in the primary cooling system (i.e. the primary system of PWRs and the recirculation system of BWRs), two flow paths are generated on both sides of the break. In the Super LWR, only one break flow path is generated because the once-through cooling system has both the coolant inlet and outlet. It is a "single-ended break". Therefore, a 100% break is the largest break to be considered in the Super LWR LOCA analysis, while a 200% break should be considered in LWRs.

The reflooding phase of the Super LWR is similar to that of PWRs rather than that of BWRs. Figure 1.44 [71] compares the reflooding phenomena of PWRs and the Super LWR. When the Super LWR adopts the pressure suppression type

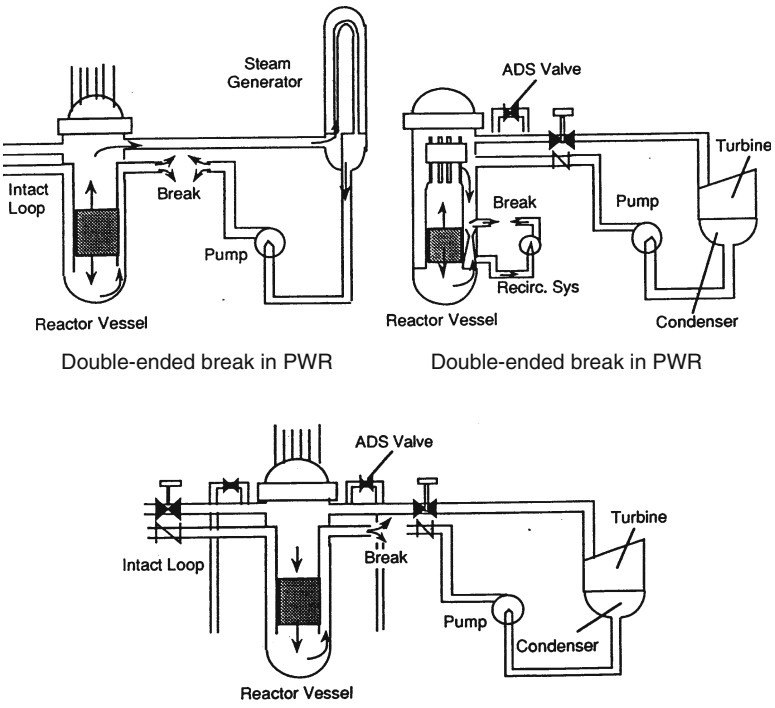

Fig. 1.43 Comparison of blowdown phenomena. (Taken from ref. [71] and used with permission from Atomic Energy Society of Japan)

containment as the BWRs, the steam generated in the core is released through the ADS lines to the suppression chamber while it is released through the steam generator and the break point to the dry type containment in PWRs. The submergence of the ADS line needs to be considered during reflooding. This is the second difference in LOCA phenomena. Whether the Super LWR and Super FR adopt the dry containment remains for future study. But the LOCA analyses have been performed with the pressure suppression containment [55, 56, 71–74].

The SCRELA code was developed for large LOCA analyses for the SCFR, an early version of the Super FR [72, 73]. The SPRAT-DOWN, including the downward flow water rod model for the Super LWR, was extended to the SPRAT-DPWN-DP code for the large LOCA analyses [71]. The critical flow at supercritical pressure is not known. Then, the correlation at the subcritical pressure has also been used in the supercritical pressure for the LOCA analyses since the duration of supercritical pressure is very short. Both codes were verified in comparison with the REFLA-TRAC code. The SPRAT-DOWN code was applied to the small LOCAs of the Super LWR because the system pressure stays in supercritical region at the small LOCAs [71].

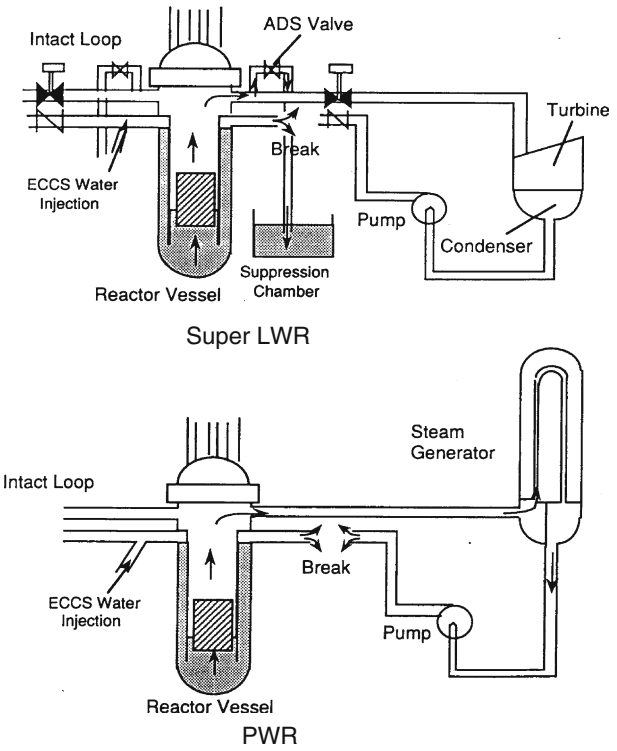

Fig. 1.44 Comparison of reflooding phenomena. (Taken from ref. [71] and used with permission from Atomic Energy Society of Japan)

Analysis results of 1–100% hot-leg/cold-leg breaks of the Super LWR are reported in ref. [71]. At the cold-leg large break, excessive core heat-up is mitigated by the ADS during blowdown because reactor depressurization induces core coolant flow. This is explained in Fig. 1.45. The coolant inventory in the top dome and the water rods is effectively used for core cooling. After blowdown, the core is slowly reflooded by the low pressure ECCS as in PWRs. The reflooding phase is influenced by submergence of ADS pipes in a suppression pool as seen in Fig. 1.46. The highest cladding temperature of the large LOCA is lower than the criterion (1,260°C) by about 430°C which appears during the reflooding phase. A small cold-leg break gives higher cladding temperatures than that of the large break because the ADS is not actuated in the analysis. The boundary of the large and small breaks that gives the highest cladding temperature is lower than the criterion by about 260°C. The analysis results of the cold-leg break small LOCAs are shown in Fig. 1.47. If the ADS actuation is assumed by the "drywell pressure high" signal, the cladding temperature is lower. The hot-leg break is less severe than the cold-leg break because it increases the core coolant flow rate and forced flooding is expected after blowdown.

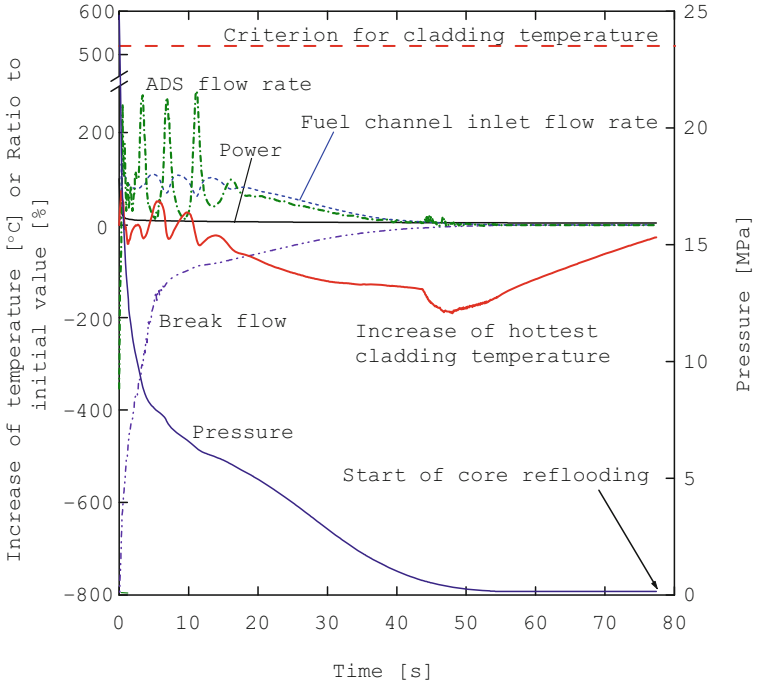

Fig. 1.45 Blowdown phase of 100% cold-leg break LOCA

The LOCA analyses are summarized in Sect. 6.7.3.

1.3.9.6 Summary of Safety Analysis

The results of safety analyses of the Super LWR are summarized in Fig. 1.48 [56]. The temperature rises of the fuel cladding of Super LWR are illustrated in comparison with the criteria and margins in Fig. 1.49. Safety characteristics of the Super LWR are summarized in Table 1.13.

1.3.9.7 Simplified Probabilistic Safety Assessment

No natural circulation coolant path exists in the once-through cycle reactor when the main feedwater pumps stop. The effect of the feature on core damage frequency was assessed by the simplified probabilistic safety assessment (PSA) method. Two analysis were performed; one was for the SCFR based on the early safety system design [73, 75]. In order to carry out the PSA of the SCFR, the potential significant events that can lead to severe core damage were identified as initiating events. Five initiating events, large LOCA, intermediate LOCA, two categories of small break

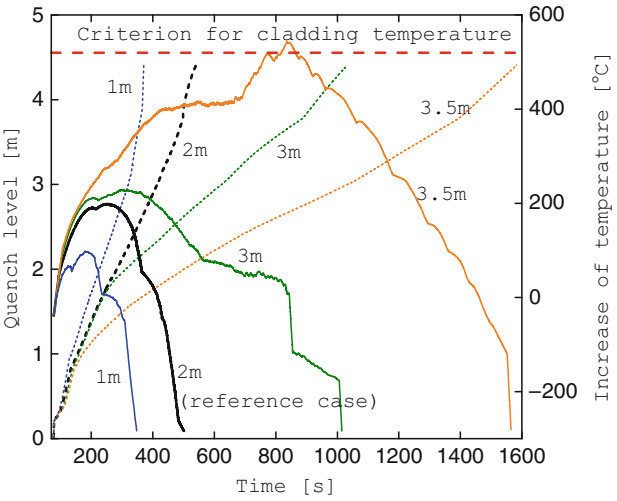

Fig. 1.46 Influence of submergence of quencher in suppression pool on reflooding phase of 100% cold-leg break LOCA

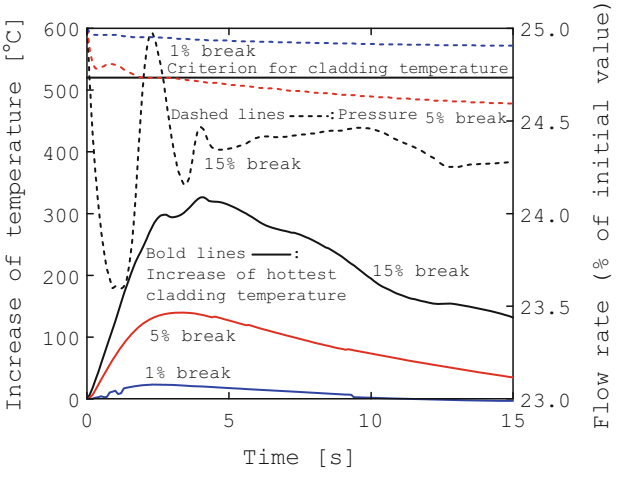

Fig. 1.47 Cold-leg small break LOCAs

LOCAs, and loss of offsite power (LOSP) were selected by considering SCFR characteristics and by acknowledging the results of NUREG 1150. Mitigation sequence for each initiating event was established with the required safety system. Event trees were constructed based on the mitigating sequences for each initiating event and referring to the current PSA results.

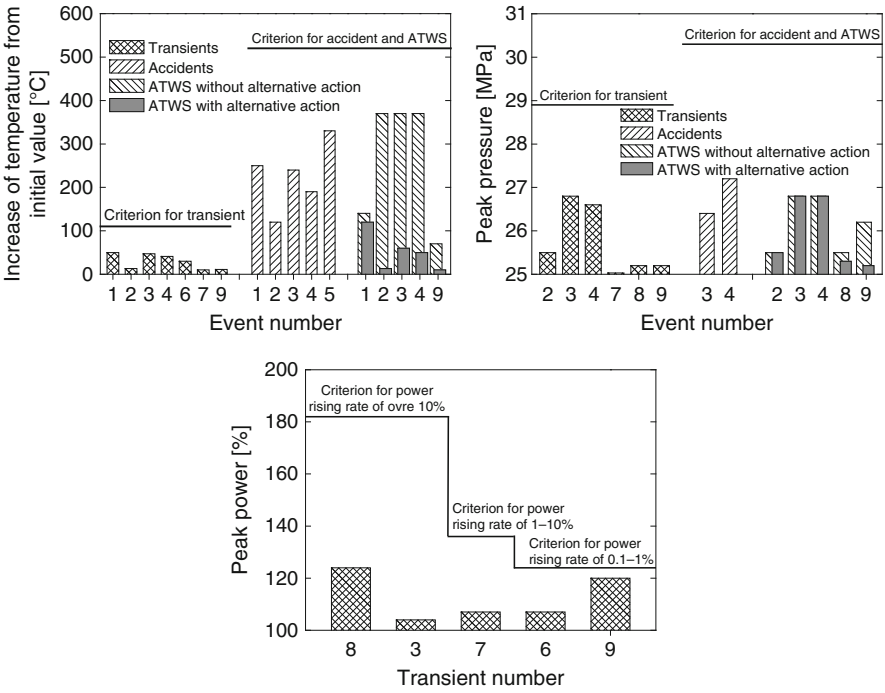

Fig. 1.48 Summary of safety analyses of the Super LWR. (Event numbers are taken from Table 1.12). (Taken from ref. [56] and used with permission from Korean Nuclear Society)

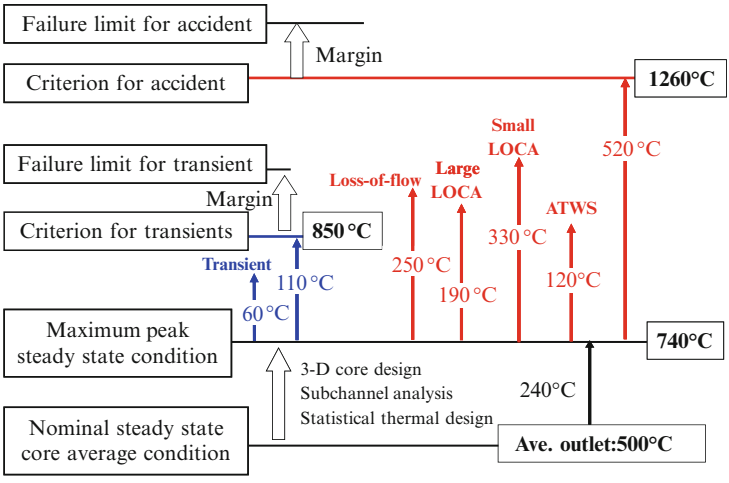

Fig. 1.49 Summary of temperature rises of the fuel cladding.

Table 1.13 Summary of safety characteristics of the Super LWR

Core cooling by depressurization
Top dome and water rods serve as an "in-vessel accumulator"
Loss of flow mitigated by water rods
Short period of high cladding temperature at transients
Mild behavior at transients, accidents and ATWS
Simple safety principle (keeping flow rate) due to once-through cooling cycle

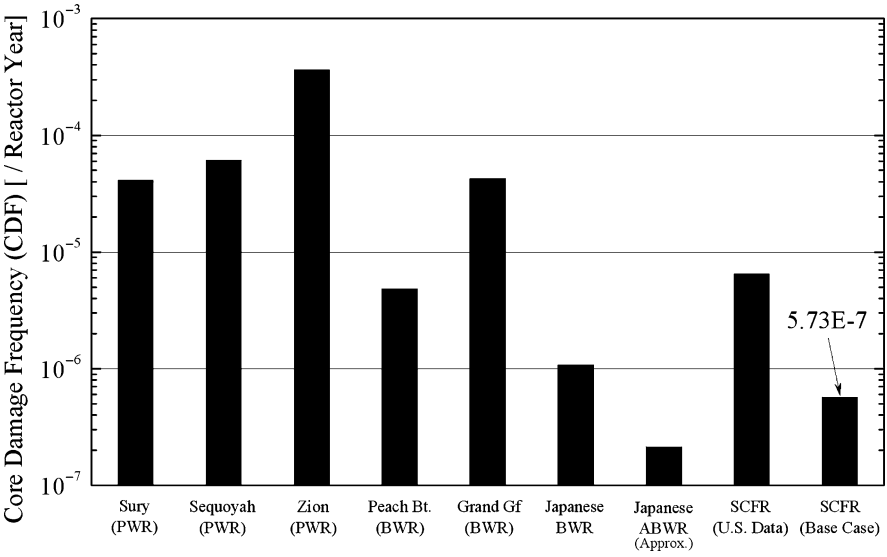

Fig. 1.50 Comparison of total core damage frequencies of SCFR (early design of the Super FR)

The total core damage frequency (CDF) of the SCFR was compared with the PSA results of current LWRs in Fig. 1.50. The estimated CDF is smaller than those of the US BWR plants considering the characteristics of the reactor system and referring to the Japanese PSA data. Accordingly, for the relative comparison between the two results, the case is calculated which imposes the same initiating event frequencies as in the US BWR plants. The estimated CDF of this case shows the similar trend to the results of US BWR plants. It is concluded that the CDF is not high. Although no natural circulation is established at total loss of feedwater flow in the once-through coolant system, the core damage frequency is maintained as the same level as the conventional Japanese BWR because of the diversity of feedwater systems in the direct cycle reactors.

The Super LWR was also studied using simplified PSA methodology in an event tree analysis. As shown in Fig. 1.51, it was found that the contribution of the large LOCA event was approximately 50% of the CDF. As shown in Fig. 1.52, it was found that the failures of coolant supply to the core and automatic depressurization caused most of the CDF. The PSA study on the Super LWR is summarized in Sect. 6.9.

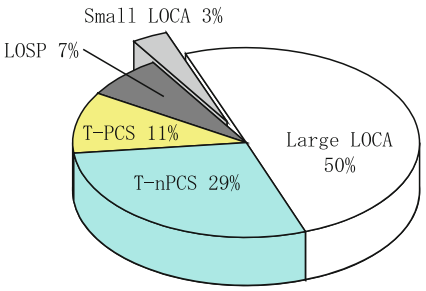

Fig. 1.51 Contributions of initiating events to total CDF in the Super LWR

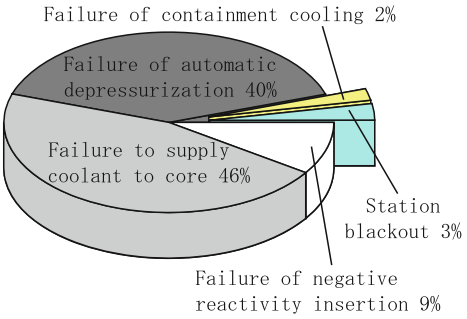

Fig. 1.52 Contributions of each function to total CDF in the Super LWR

1.3.10 Super FR

1.3.10.1 Fuel, Core and Plant System

Water cooled fast reactors require a tight fuel lattice. The once-through coolant cycle is compatible with the tight lattice core of water cooled fast reactors [76–78]. The increase in the core pressure drop due to the tight lattice does not cause problems with pumping power and stability because of the low coolant flow rate of the once-through cycle. Increasing orifice pressure drop for improving stability is also not a problem.

The plant system of the Super FR is the same as that of the Super LWR, a thermal reactor. Fast reactors do not need a moderator. Their power density is inevitably higher than that of thermal reactors. High power density is an advantage in economy. The Super FR has higher power density than the Super LWR. The Super LWR is expected to show better economy than LWRs due to the compactness, simplicity of the plant systems, and high thermal efficiency. Improving economy of the fast reactor over that of LWRs is an important goal of fast reactor development. The Super FR has good potential in this regard [79].

The supercritical pressure light water cooled fast reactors with MOX fuel have been studied at the University of Tokyo from the beginning (1989). But early designs adopted approximate two-dimensional core calculations and a linear

burn-up model. The core performances cannot be predicted accurately and cannot be used for the present Super FR design and analysis. Three-dimensional coupled neutronic and thermal-hydraulic calculations as made in the Super LWR core design are necessary for predicting the Super FR core performances accurately. The core design method of the Super FR is the same as that of the Super LWR. But a three-dimensional tri-z geometry was developed for the design [80–82]. A sub-channel analysis code for the Super FR was developed and used for evaluating the nominal MCST [83]. The principle of MOX fuel rod design of the Super FR is the same as that of UO_2 fuel of the Super LWR, but high Pu content needs to be accommodated. The fission gas release rate is high. The FEMAXI-6 code has been used for the design [84–87]. Care should be taken for meeting the requirement at both local and whole-core voiding in the core design. A core with negative void reactivities for both local and whole voiding conditions was designed [88, 89]. The core of the Super FR consists of hexagonal fuel assemblies with wrapper tubes (channel boxes). An example of core layout, seed and blanket assemblies are shown in Fig. 1.53. The zirconium hydride layer is placed in the blanket assembly for the negative coolant void reactivity. Examples of fuel and core characteristics are shown in Table 1.14 [87]. The two-pass flow scheme in the RPV is illustrated Fig. 1.54. The blanket fuel assemblies are cooled by downward flow to increase the average reactor outlet temperature. Part of the seed assemblies can also be cooled by downward flow.

Supercritical water is single-phase fluid. A CFD code is useful for predicting the behavior [90–92]. The radial distribution of cladding temperature was evaluated by a CFD code [93, 94]. Cladding temperatures, especially their circumferential

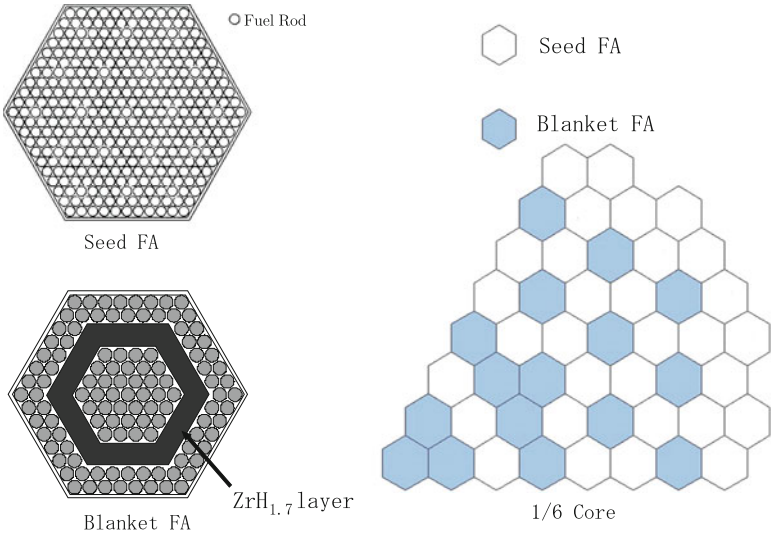

Fig. 1.53 Example of seed and blanket fuel assemblies and core layout

Table 1.14 Examples of fuel and core design characteristics of Super FR

Fuel rod diameter (mm)	5.5
P/D	1.19
Gap clearance (mm)	1.045
Cladding thickness (mm)	0.4
Pellet cladding gap (mm)	0.03
Heated length (cm)	200
Assembly pitch (cm)	11.561
Number of rods in a seed assembly (total/fuel/CR tube)	271/252/19
Core thermal power (MWt)	1,602
Equivalent diameter (cm)	186
Number of seed assemblies	162
Number of blanket assemblies	73
Coolant outlet temperature (°C)	504.6
MCST calculated by subchannel analysis (°C)	628.5
Average power density (W/cm^3)	294.8
Coolant void reactivity (%Δk/k) at BOEC/EOEC	−0.839/−1.712

Taken from ref. [87] and used with permission from Atomic Energy Society of Japan

distribution, are difficult to measure accurately by experiments because of the narrow spacing between the fuel rods. The radical temperature distribution of a uniform channel is approximately 12°C, when heat conduction of fuel cladding is considered as seen in Fig. 1.55 [93]. It is also seen from the figure that the temperature difference between inner and outer claddings is approximately 24°C. The MCST criterion is converted to that of the maximum cladding centerline temperature by adding 12°C for the evaluation of cladding stress. The temperature of supercritical "steam" is sensitive to the enthalpy change. The pressure drop increases when heating is in the narrow channel. This reduces the coolant flow in the channel and increases the temperature. The effect was analyzed in detail by the CFD code for unsymmetrical geometric and heating conditions. Adjusting the spacing between the fuel rods and unheated surface toward the heated perimeters is effective for making the temperature distribution uniform [93, 94].

A large-scale CFD calculation is useful for the design of the Super FR and Super LWR. For example, the ACE-3D code for supercritical water calculation was developed for analysis of the 37-fuel rod bundle geometry. Validation of the code with 7-rod bundle experiments can be expected to reduce future R&D work on fuel assemblies. The flow characterization within the RPV will also be made by CFD calculation.

The neutron spectrum of the Super FR is compared with those of LWRs and the sodium cooled fast reactor in Fig. 1.56. The blanket assemblies of the Super FR are equipped with zirconium hydride layer for the negative coolant void reactivity. The spectrum near the layer is similar to that of LWRs. Both fast and thermal neutron spectra are available in the Super FR. Availability of both will be suitable for the transmutation of long-lived fission products as well as minor actinides [95, 96]. The improved core design for the high power density was reported [87].

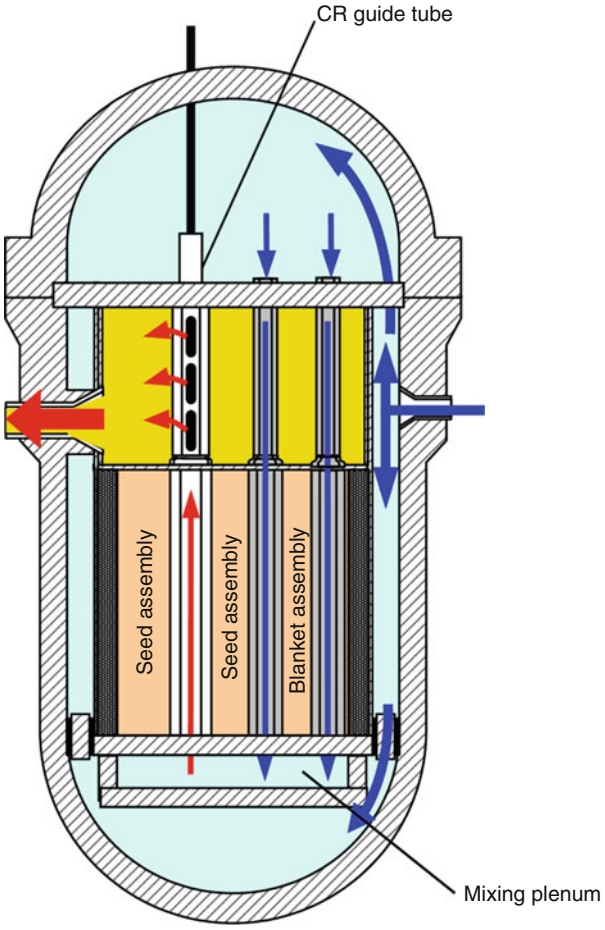

Fig. 1.54 Two-pass flow scheme with downward flow in blanket assemblies and part of the seed assemblies

The plant and safety systems of the Super FR are the same as that of the Super LWR. The safety and stability analyses of the Super FR have been reported [97–100]. Improvement of the plant control system was studied for the Super FR. The power to flow rate ratio was taken for the control parameter of the feedwater pumps in order to suppress a fluctuation of the main steam temperature. This is the same as in supercritical FPPs. It showed better convergence than taking only the feedwater flow rate as the control parameter [101].

A cut-away view of the RPV is shown in Fig. 1.57 [102]. The outlet nozzles are exposed to the high temperature outlet coolant. The structural considerations were made on the reactor vessel and internals. A seal pipe is provided at the main steam nozzle as seen in the Fig. 1.57 [102].

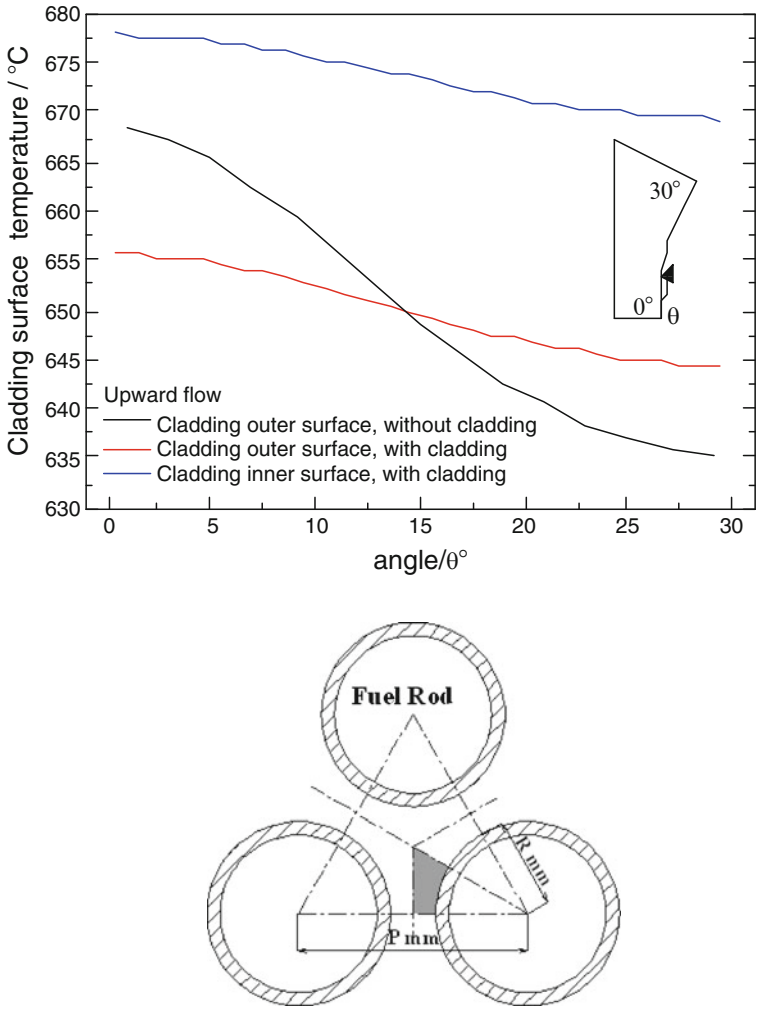

Fig. 1.55 Examples of radial temperature distributions on fuel cladding surface. (Taken from ref. [93] and used with permission from Atomic Energy Society of Japan)

1.3.10.2 Zirconium Hydride Layer Concept for Negative Void Reactivity

The reactivity increases at the LOCA in large-sized fast reactors due to the neutron spectrum hardening. In the design of water cooled fast reactors, negative reactivity addition is necessary for inherent decrease of reactor power at the LOCA. Increasing the leakage by flattening the core shape is not suitable for the Super FR because that would make the RPV wall thick. Softening the spectrum of the core by using graphite is the alternative, but it is not effective for water cooled fast reactors.

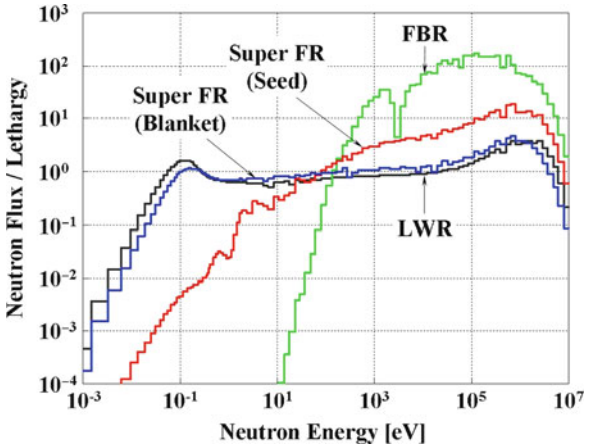

Fig. 1.56 Comparison of neutron spectra of the Super FR, a LWR and a sodium cooled fast breeder reactor

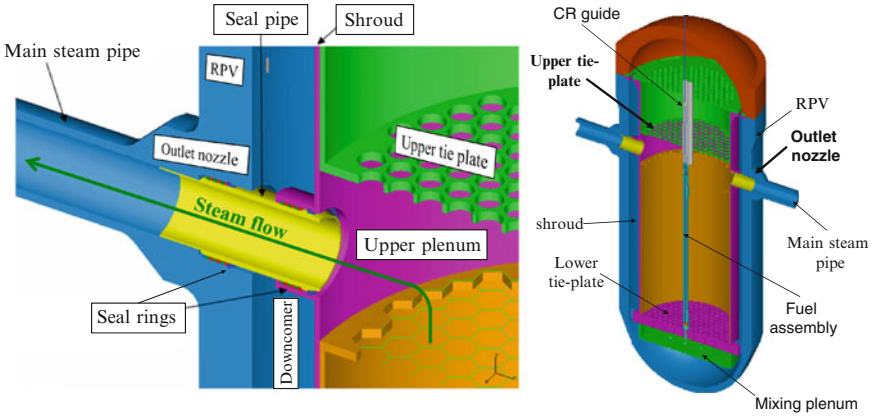

Fig. 1.57 Example of in-core structure of Super FR. (Taken from ref. [102] and used with permission from Atomic Energy Society of Japan)

Placing a thin zirconium hydride layer between the seed and blanket fuel assemblies was found effective in changing the reactivity with steam density in the study of a steam cooled fast reactor [103, 104]. The typical geometry and calculation result are shown in Figs. 1.58 and 1.59, respectively. The effectiveness was explained in the subsequent studies [105, 106]. The mechanism is described in Sect. 7.3. The fast neutrons are generated in the seed assemblies. They are moderated by the thin zirconium hydride layer between the seed and blanket. The layer is installed in the blanket assemblies in the present Super FR design. The moderated neutrons are effectively absorbed in the blanket fuel by the capture of U-238. The

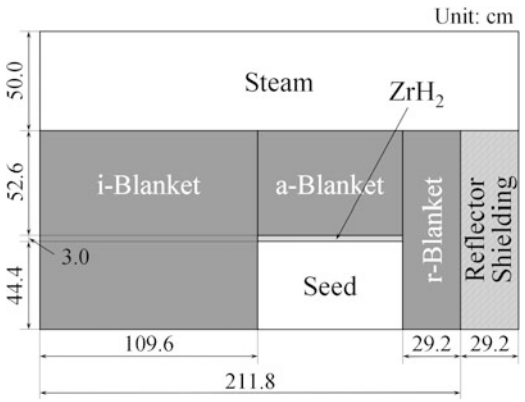

Fig. 1.58 Original zirconium hydride layer concept of indirect cycle supercritical steam cooled fast reactor in two-dimensional core calculation model

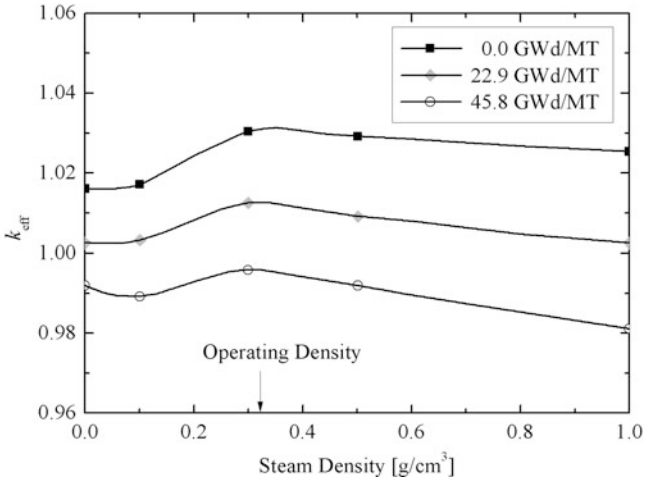

Fig. 1.59 Change of effective multiplication factor with steam density for the indirect cycle supercritical steam cooled fast reactor

whole-core neutron balance becomes negative due to the effective absorption of moderated neutrons. Without placing the zirconium hydride layer, the fast neutrons from the seed fuel assemblies cause fast fissions in the blanket fuel. This gives rise to the positive reactivity at voiding.

The mechanism of achieving negative reactivity is not whole-core spectrum softening by the moderator, but moderation through the zirconium hydride layer and absorption in the blanket. The breeding capability is not deteriorated much because the neutron spectrum of the remaining part of the core does not change much.

The zirconium hydride layer concept is suitable for the Super FR, because the core shape stays normal, and is not flattened. The thickness of the RPV stays within

the fabrication capability. The thickness will be comparable with that of the PWR RPV, when high tensile strength steel is used. Such steel has already been developed for a large-sized PWR.

It should be pointed out that making the effective multiplication factor the maximum at the operating steam density (Fig. 1.59) is not desirable. The reactivity coefficient becomes positive during the startup from the flooded core. The effective multiplication factor should be increased when the core is flooded.

But getting an operating steam density of 0.3 g/cm^3 (Fig. 1.59) requires supercritical pressure. This was the start of Super FR and Super LWR studies at the University of Tokyo. The plant system of the supercritical steam cooled fast reactor was an indirect cycle at first [104], but the advantage of the once-through cycle was soon recognized and a report on this was made in 1992 [2, 107].

1.3.11 Computer Codes and Database

The scope of studies and computer codes are summarized in Table 1.15. SRAC is a neutronic core calculation code developed by Japan Atomic Energy Agency (JAEA) [21]. FEMAXI-6 is a light water reactor fuel analysis code also developed by JAEA [31]. All other codes in the table were developed mostly by graduate students at the University of Tokyo during their thesis studies. Some codes did not have names.

One-dimensional burn-up and two-dimensional R-Z core calculation procedures for the fast reactor are found in refs. [108, 109]. The LOCA analysis code, SCRELA was described in ref. [110]. The procedure for a simplified PSA is also described there. The single channel thermal-hydraulic calculation code SPROD, the two-dimensional coupled core calculation scheme of the thermal spectrum reactor with water rods and transient and accident analysis code at supercritical-pressure, SPRAT are described in ref. [111].

Table 1.15 Scope of studies and computer codes

Fuel and core
Single channel thermal hydraulics (SPROD), 3D coupled core neutronic/thermal-hydraulic (SRAC-SPROD), Coupled subchannel analysis, Statistical thermal design method, Fuel rod behavior (FEMAXI-6), Data base of heat transfer coefficients of supercritical water (Oka–Koshizuka correlation)
Plant system; Plant heat balance and thermal efficiency
Plant control
Safety; Transient and accident analysis at supercritical-and subcritrical pressure (SPRAT-F, SPRAT-DOWN), ATWS analysis (SPRAT-DOWN), LOCA analysis (SCRELA,SPRAT-DOWN-DP), Time-dependent subchannel analysis
Start-up (sliding pressure and constant pressure)
Stability (TH and core stabilities at supercritical and subcritical-pressure)
Probabilistic safety assessment

Analysis of the heat transfer deterioration mechanism by numerical simulation using the k–ε turbulence model is in ref. [112]. Transient and accident analysis code for fast reactors, SPRAT-F, and calculation of the Oka–Koshizuka heat transfer correlation for the safety analysis at supercritical pressure are described in ref. [113].

Plant heat balance and the thermal efficiency calculation are in ref. [114]. This reference also includes the two-dimensional coupled core calculation procedure for the thermal reactor.

The plant dynamics code for the analysis of plant control and startup thermal considerations are described in ref. [115]. The subchannel analysis code and the analysis are found in refs. [116, 117]. Thermal-hydraulic and coupled stability calculations at supercritical and at subcritical pressure as well as startup considerations are described in ref. [118].

Three-dimensional, coupled core calculation scheme using SRAC, ASMBURN, COREBN, and the JENDL3.3 nuclear data of JAEA and SPROD and the core design method are described in ref. [119]. It also includes fuel rod design and rationalization of fuel integrity criteria during transients at high temperature using FEMAXI-6. Three dimensional coupled core design calculation of the Super FR is described in ref. [120]. The statistical thermal design procedure is described in refs. [26, 27].

Safety analysis of the Super LWR is described in ref. [121]. The SPRAT-DOWN code for the analysis of downward flowing water rods and the SPRAT-DOWN-DP code for depressurization in an LOCA were prepared. The LOCA analysis of the Super LWR was performed in combination with SPRAT-DOWN-DP and the reflooding module of SCRELA. ATWS analysis is also described in ref. [121]. The momentum equation is included in the SPRAT-DOWN code from the ATWS analysis. The design of the two-pass core of the Super LWR and the safety analysis at subcritical pressure during startup are described in ref. [122].

An improved core design procedure of the Super LWR that coupled the subchannel analysis with three-dimensional coupled core calculations is described in ref. [28]. The time-dependent subchannel analysis code for safety analysis of the Super LWR is described in ref. [123].

Watts–Chou correlation was employed as the heat transfer correlation for the core design of the Super LWR and Super FR, because of the accuracy and applicability to both upward and downward flow cooling. For safety analysis, the Oka–Koshizuka correlation is used. CFD analysis of the effect of grid spacers on heat transfer correlation is found in ref. [124].

1.4 Past Concepts of High Temperature Water and Steam Cooled Reactors

Reviews of high temperature water and steam cooled fast reactor concepts from the 1950s to the mid 1990s are described in Appendix B grouped as: supercritical pressure water cooled reactors; nuclear super heaters; and steam cooled fast reactors.

A steam cooled fast reactor is defined as one in which the core inlet coolant is "steam", not water. Blowers are required for steam cooled reactors instead of reactor coolant pumps. The pumping power of blowers is huge. Some supercritical pressure water cooled reactors have adopted pressure tubes instead of the RPV and have separate moderator and coolant. Indirect cycle reactors with a RPV are also found.

What is the closest to the Super LWR and Super FR is the high pressure FBR of B&W (Fig. B.22 in Appendix B) operating at 3,700 psia (25.52 MPa). It adopts a RPV, but the inlet temperature of the reactor coolant is 750°F (399°C). This is above the pseudo-critical temperature and so it is a type of steam cooled reactors. In addition to the required blowers to drive the large volume of steam as coolant and the large pumping power consumption in steam cooled reactors, a large fraction of the reactor outlet coolant is consumed for heating the feedwater up to "steam". This is also a disadvantage.

No detailed calculations and analyses have been given in the reports on the past concepts, including their safety systems and safety analysis.

The Super LWR and Super FR are new concepts based on the experiences with LWRs and fast reactors as well as supercritical FPPs. The concepts have been developed with full numerical analyses.

1.5 Research and Development

1.5.1 Japan

The conceptual design study made at the University of Tokyo for the Super LWR and Super FR was described in Sect. 1.3. The early designs carried other names such as SCLWR, SCLWR-H, SCFR, SCFR-H, SCFBR-H, SWFR etc. Publications are found on the home page [125].

Heat transfer experiments and material research studies have been carried out at Kyushu University, JAEA, the University of Tokyo and elsewhere. Comparison of heat transfer coefficients predicted by different correlations is shown in Fig. 1.60. Accuracy above 500°C is important for the calculation of MCST. Calculated MCSTs with different correlations are compared in Table 1.16 [122]. The largest difference is 44°C. Current heat transfer correlations were developed based on experiments using smooth circular tubes. Experiments on fuel bundle geometry are necessary. The effect of grid spacers on the heat transfer correlation should be included in the prediction of MCST. The correlation of downward flow is necessary for the design. Downward flow is adopted in the low temperature region below the pseudo-critical temperature.

Dryout or boiling transition may occur during the sliding-pressure startup of the once-through reactor as seen in Fig. 1.21 [43, 44]. Ribbed tubes and spiral tapes have been used for the supercritical boilers to improve the critical heat flux. The

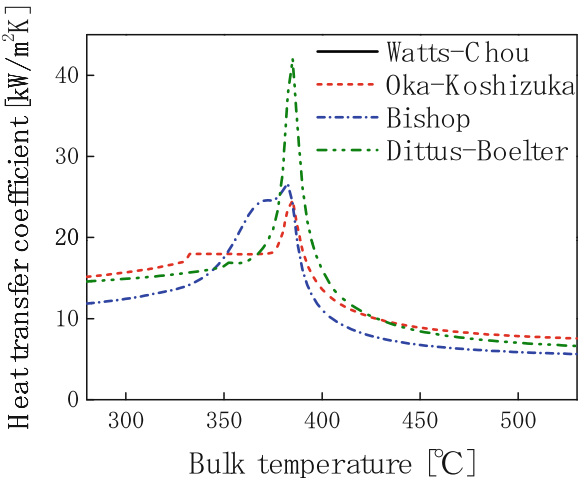

Fig. 1.60 Comparison of heat transfer correlations

Table 1.16 Maximum cladding surface temperatures predictions by different heat transfer correlations (in °C)

	BOEC	MOEC	EOEC
Watts–Chou	637	638	647
Oka–Koshizuka	604	606	603
Bishop	627	629	635
Dittus–Boelter	617	618	616

Taken from ref. [122]

photo of one ribbed tube, a so-called rifled tube is seen in Fig. 1.61. Critical heat flux may also be increased by use of the grid spacers.

There are no correlations of critical flow in supercritical fluid. The condensation of supercritical steam in water also needs to be tested by experiments. A list of thermal-hydraulic experiments done by researchers of Kyushu University using HCFC22 as surrogate fluid is given in Fig. 1.62. Single-tube and 7-rod bundle tests were done. A photo of the test loop installed at Kyushu University along with the test sections is seen in Fig. 1.63 [126]. Single-tube and 7-rod bundle heat transfer testing were carried out at JAEA using supercritical water as working fluid [127, 128].

Experiments on some austenitic stainless steels as cladding materials were performed at JAEA and the University of Tokyo. Creep rapture strength of austenitic stainless steel PNC316 and PNC1520 that had been developed for the sodium cooled fast reactor and that of PNC316 are shown in Fig. 1.64 [119] as well as the result of fuel rod analysis. The upper part of the fuel rod is exposed to high temperatures and general corrosion is important at them. Stress

Fig. 1.61 Rifled tube of a supercritical boiler

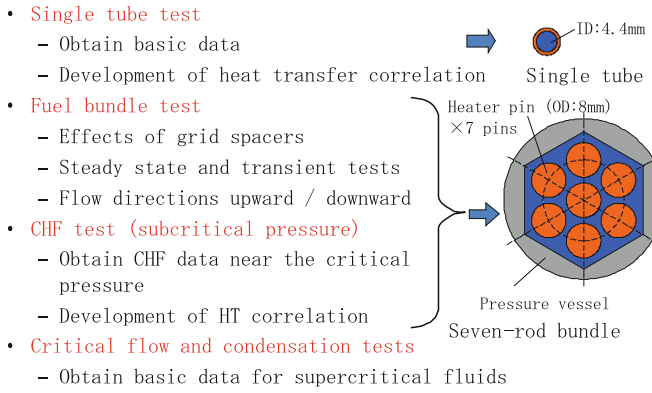

Fig. 1.62 Thermal-hydraulic experiments done by researchers of Kyushu University

corrosion cracking needs to be tested at low temperature. The cladding material development should be made in close collaboration with considerations on water chemistry. The difference from LWRs is that all the reactor coolant goes to the turbine and is purified after condensation. The Super LWR and Super FR are like the supercritical FPPs.

The temperature difference between the moderator in the water rods and the coolant in the fuel channels is large, approximately 250°C. Without thermal insulator, thermal stress exceeds the tensile strength of typical stainless steel as shown in Fig. 1.65 [122]. Yittria-stabilized zirconia was developed for the thermal insulator [129].

Supercritical water exhibits unique properties. Supercritical water chemistry and dissolution of corrosion products in supercritical water have been studied [130–132].

Researchers and engineers in the Japanese nuclear industry have also been studying reactor plants, thermal hydraulics of supercritical fluid and materials [133–138].

The symposium on supercritical water cooled reactors started in 2000. The first and second ones were held at the University of Tokyo in November 2000 and September 2003. The third one was held at Shanghai Jiao Tong University, China in March 2007. The fourth one was held is Heidelberg, Germany in March 2009. The proceedings were published.

Test loop

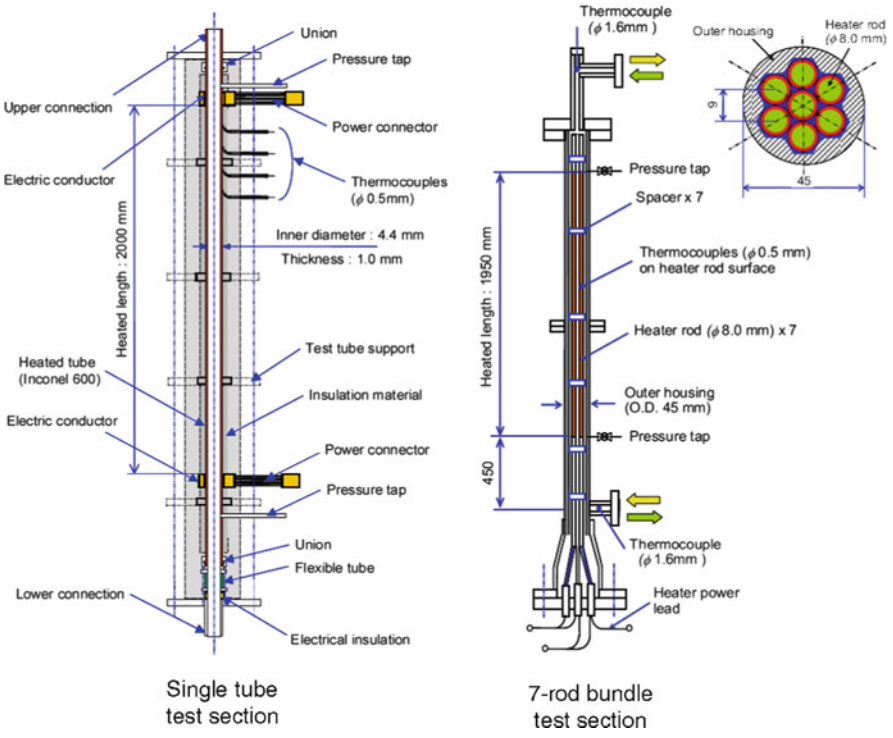

Fig. 1.63 Thermal-hydraulic test loop installed at Kyusyu University. (Taken from ref. [126] and used with permission from Atomic Energy Society of Japan)

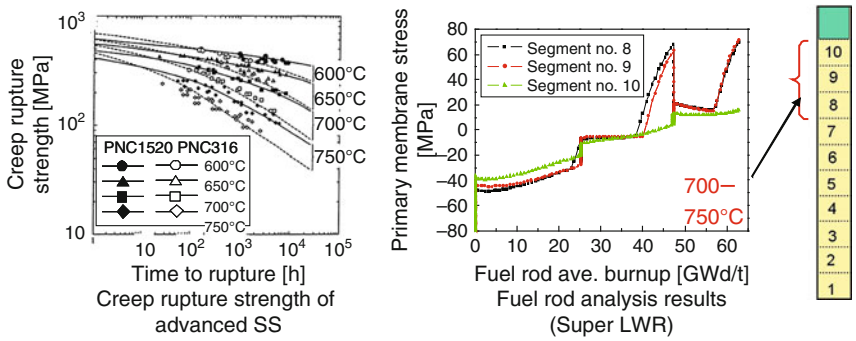

Fig. 1.64 Creep rupture strength of austenitic stainless steel and primary membrane stress on a fuel rod cladding. (Taken from ref. [119])

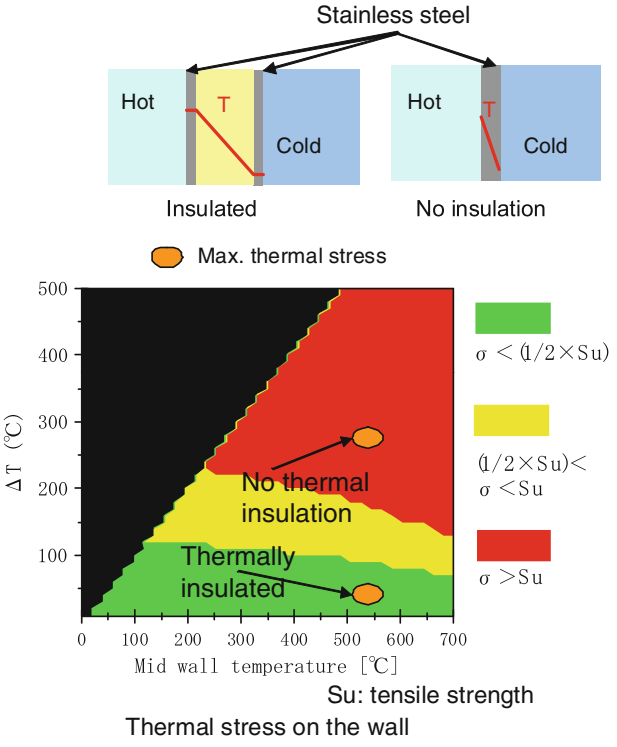

Fig. 1.65 Thermal stresses with and without thermal insulator layer. (Taken from ref. [122])

1.5.2 Europe

Research and development of the supercritical water cooled reactor are being done in Europe as the High Performance Light Water Reactor (HPLWR) with funding by the European Union. The first phase work for the HPLWR was conducted in 2000–2002. Forschungs Zentrum Karlsruhe (FZK) was the coordinator. The University of Tokyo was invited to participate and its design was taken as the reference. The results of the first phase were reported in refs. [139–142]. The second phase started in September 2006 again with FZK as the coordinator. Design and integration, core design, safety, materials, and heat transfer are being studied by ten European partners [143–145]. The HPLWR activities are found in the FZK homepage [146].

1.5.3 GIF and SCWR

The Generation Four International Forum (GIF) was started in 2002. The supercritical water cooled reactor (SCWR) was taken as one of the six generation 4 reactors. Canada serves as the lead country. The activities are seen in the GIF home page [147]. Canadian researchers are also carrying out studies of a pressure tube type SCWR [148–151].

1.5.4 Korea, China, US, Russia and IAEA

SCWR research in Korea has been mainly promoted by the Korea Atomic Energy Research Institute (KAERI) and Korea Electric Power Research Institute (KEPRI) [152–156]. Funding for research and development of the SCWR was begun in 2007 in China. Eight organizations take part in it. Shanghai Jiao Tong University is the lead organization [157]. R&D, conceptual design, and construction of an experimental SCWR (ESCWR) was announced in 2009. In the US, SCWR had also been researched in the early 2000s [158–160]. Russian research has a long history and many experiences have been obtained with supercritical FPPs. There are thermal-hydraulic test loops at IPPE in Obninsk. A workshop on supercritical water cooled reactors was held at NIKIET in Moscow in October 2008. The Coordinated Research Program (CPP) on heat transfer of supercritical fluid has been organized by the International Atomic Energy Agency (IAEA) [161].

Glossary

ABWR	advanced boiling water reactor
ADS	automatic depressurization system
ATWS	anticipated transients without scream

BOP	balance of plant
CAD	computer aided design
CDF	core damage frequency
CFD	computational fluid dynamics
CPP	Coordinated Research Program
CR	control rod
CV	containment vessel
ECCS	emergency core cooling system
FPP	fossil-fuel fired power plant
FR	fast reactor
FZK	Forschungs Zentrum Karlsruhe
GIF	Generation Four International Forum
HPLWR	High Performance Light Water Reactor
IAEA	International Atomic Energy Agency
JAEA	Japan Atomic Energy Agency
KAERI	Korea Atomic Energy Research Institute
KEPRI	Korea Electric Power Research Institute
LLLP	low leakage fuel loading pattern
LMFBR	liquid metal cooled fast breeder reactors
LOCA	loss of coolant accidents
LOSP	loss of offsite power
LPCI	low pressure core injection system
LWR	light water reactor
MCST	maximum cladding surface temperature
MDHFR	minimum deteriorated heat flux ratio
MLHGR	maximum linear heat generation rate
PCMI	pellet cladding mechanical interaction
PID	proportional, integral and differential
PSA	probabilistic safety assessment
RCP	reactor coolant pump
RPV	reactor pressure vessel
SCLWR	supercritical pressure light water cooled reactor
SCWR	supercritical water cooled reactor

References

1. J. M. Utterback, Mastering the Dynamics of Innovation, Harvard Business School Press, Boston MA, USA (1994)
2. Y. Oka, S. Koshizuka and T. Yamasaki, "Direct Cycle Light Water Reactor Operating at Supercritical Pressure," *Journal of Nuclear Science and Technology*, Vol. 29(6), 585–588 (1992)
3. Y. Oka and S. Koshizuka, "Concept and Design of a Supercritical-Pressure, Direct-Cycle Light Water Reactor," *Nuclear Technology*, Vol. 103, 295–302 (1993)
4. Y. Oka, S. Koshizuka, T. Jevremovic and Y. Okano, "Systems Design of Direct-Cycle, Supercritical-Water-Cooled Reactors," *Transactions of ENC'94, International Nuclear Congress*, Vol. 2, 473–477 (1994)

5. Y. Oka, S. Koshizuka, T. Jevremovic and Y. Okano, "Systems Design of Direct-Cycle Supercritical-Water-Cooled Fast Reactors," *Nuclear Technology*, Vol. 109, 1–10 (1995)
6. Y. Oka, S. Koshizuka, T. Jevremovic, Y. Ohno and K. Kitoh, "Direct-Cycle Supercritical-Pressure, Light-Water-Cooled Reactors for Improving Economy and Plutonium Utilization," *Proc. Global95, International Conference on Evaluation of Emerging Nuclear Fuel Cycle Systems*, Versailles, France, September 11–14, 1995, 930–937 (1995)
7. Y. Oka and S. Koshizuka, "General Features of Direct-Cycle, Supercritical-Pressure, Light-Water-Cooled Reactors," *Proc. ICONE-4*, New Orleans, LA, April, March 10–14, 1996, Vol. 2, 191–198 (1996)
8. Y. Okano, S. Koshizuka and Y. Oka, "Core Design of a Direct-Cycle, Supercritical-pressure, Light Water Reactor with Double Tube Water Rods," *Journal of Nuclear Science and Technology*, Vol. 33, 365–373 (1996)
9. K. Yamagata, K. Nishikawa, S. Hasegawa, T. Fujii and S. Yoshida, "Forced Convective Heat Transfer to Supercritical Water Flowing in Tubes," *International Journal of Heat and Mass Transfer*, Vol. 15, 2575 (1972)
10. S. Koshizuka, N. Takano and Y. Oka, "Numerical Analysis of Deterioration Phenomena in Heat Transfer to Supercritical Water," *International Journal of Heat and Mass Transfer*, Vol. 38, 3077–3084 (1995)
11. K. Kitoh, S. Koshizuka and Y. Oka, "Improvement of Transient Criteria of a Supercritical Water Cooled Reactor Based on Numerical Simulation," *Proc. ICONE-5*, Nice, France, May 26–30, 1997, ICONE5-2341 (1997)
12. K. Dobashi, A. Kimura, Y. Oka and S. Koshizuka, "Conceptual Design of a High Temperature Power Reactor Cooled and Moderated by Supercritical Light Water," *Annals of Nuclear Energy*, Vol. 25(8), 487–505 (1998)
13. T. Mukohara, S. Koshizuka and Y. Oka, "Core Design of a High-Temperature Fast Reactor Cooled by Supercritical Light Water," *Proc. ICONE-6*, San Diego, CA, May 10–15, 1998, ICONE-6229 (1998)
14. Y. Okano, S. Koshizuka and Y. Oka, "Design of Water Rod Cores of a Direct Cycle, Super-Critical-Pressure Light Water Reactor," *Annals of Nuclear Energy*, Vol. 21, 601–611 (1994)
15. Y. Okano, S. Koshizuka and Y. Oka, "Core Design of a Direct-Cycle, Supercritical-Pressure, Light Water Reactor with Double Tube Water Rods," *Journal of Nuclear Science and Technology*, Vol. 33, 365–373 (1996)
16. Y. Okano, S. Koshizuka and Y. Oka, "Direct-Cycle, Supercritical-Pressure, Light-Water-Cooled Thermal Spectrum Reactor with Double Tube Water Rods," *Proc. PHYSOR 96*, Vol. 2, 11–20 (1996)
17. K. Dobashi, Y. Oka and S. Koshizuka, "Core and Plant Design of the Power Reactor Cooled and Moderated by Supercritical Light Water with Single Tube Water Rods," *Annals of Nuclear Energy*, Vol. 24(16), 1281–1300 (1997)
18. A. Yamaji, Y. Oka and S. Koshizuka, "Core Design of a High Temperature Reactor Cooled and Moderated by Supercritical Light Water," *Proc. GENES4/ANP2003*, Kyoto, Japan, September 15–19, 2003, Paper 1041 (2003)
19. A. Yamaji, Y. Oka and S. Koshizuka "Three-dimensional Core Design of SCLWR-H with Neutronics and Thermal-Hydraulic Coupling," *Proc. Global2003*, New Orleans, November 16–20, 2003, 1763–1771 (2003)
20. A. Yamaji, Y. Oka and S. Koshizuka, "Three-dimensional Core Design of High Temperature Supercritical-Pressure Light Water Reactor with Neutronic and Thermal-Hydraulic Coupling," *Journal of Nuclear Science and Technology*, Vol. 42(1), 8–19 (2005)
21. K. Okumura, K. Kaneko and K. Tsuchihashi, "SRAC95; General Purpose Neutronics Code System," JAERI-Data/Code 96-015, Japan Atomic Energy Research Institute (JAERI) (1996) (in Japanese)
22. A. Yamaji, K. Kamei, Y. Oka and S. Koshizuka, "Improved Core Design of High Temperature Supercritical-Pressure Light Water Reactor," *Proc. ICAPP'04*, Pittsburgh, PA, June 13–17, 2004, Paper 4331 (2004)

23. A. Yamaji, K. Kamai, Y. Oka and S. Koshizuka, "Improved Core Design of the High Temperature Supercritical-Pressure Light Water Reactor," *Annals of Nuclear Energy*, Vol. 32, 651–670 (2005)
24. K. Kamei, A. Yamaji, Y. Ishiwatari, Y. Oka and J. Liu, "Fuel and Core Design of Super Light Water Reactor with Low Leakage Fuel Loading Pattern," *Journal of Nuclear Science and Technology*, Vol. 43(2), 129–139 (2006)
25. A. Yamaji, T. Tanabe, Y. Oka, J. Yang, J. Liu, Y. Ishiwatari and S. Koshizuka, "Evaluation of the Nominal Peak Cladding Surface Temperature of the Super LWR with Subchannel Analyses," *Proc. Global 2005*, Tsukuba, Japan, October 9–13, 2005, Paper 556, (2005)
26. J. Yang, Y. Oka, J. Liu, Y. Ishiwatari and A. Yamaji, "Development on Statistical Thermal Design Procedure for Super LWR," *Proc. Global 2005*, Tsukuba, Japan, October 9–13, 2005 Paper 555 (2005)
27. J. Yang, Y. Oka, J. Liu, Y. Ishiwatari and A. Yamaji, "Development of Statistical Thermal Design Procedure to Engineering Uncertainty of Super LWR," *Journal of Nuclear Science and Technology*, Vol. 43(1), 32–42 (2006)
28. M. Kadowaki, "Rationalization of Core Design Method and Improved Core Design of Super LWR," Master's thesis, University of Tokyo (2009) (in Japanese)
29. Y. Ishiwatari, I. Hongo, Y. Oka, et al., "Numerical Analysis of Heat Transfer Enhancement by Grid Spacers in Supercritical Water," *Proc. NURETH-13*, Kanazawa, Japan, September 27–October 2, 2009, N13P1436 (2009)
30. A. Yamaji, Y. Oka and S. Koshizuka, "Fuel Design of High Temperature Reactors Cooled and Moderated by Supercritical Light Water," *Proc. GENES4/ANP2003*, Kyoto, Japan, September 15–19, 2003, Paper 1040 (2003)
31. M. Suzuki and H. Saitou, "Light Water Reactor Fuel Analysis Code FEMAXI-6 (Ver.1); Detailed Structure and User's Manual," Department of Reactor Safety Research, Nuclear Safety Research Center, Tokai Research Establishment, Japan Atomic Energy Research Institute (JAERI)
32. A. Yamaji, Y. Oka, Y. Ishiwatari, J. Liu and S. Koshizuka, "Rationalization of the Fuel Integrity and Transient Criteria for the Super LWR," *Proc. ICAPP'05*, Seoul, Korea, May 15–19, 2005, Paper 5538 (2005)
33. A. Yamaji, Y. Oka, Y. Ishiwatari, J. Liu, S. Koshizuka and M. Suzuki, "Principle of Rationalizing the Criteria for Abnormal Transients of the Super LWR with Fuel Rod Analyses," *Annals of Nuclear Energy*, Vol. 33(11–12), 984–993 (2006)
34. A. Yamaji, Y. Oka, J. Yang, J. Liu, Y. Ishiwatari and S. Koshizuka, "Design and Integrity Analyses of the Super LWR Fuel Rod", *Proc. Global 2005*, Tsukuba, Japan, October 9–13, 2005 Paper 556 (2005)
35. K. Kamei, A. Yamaji, Y. Ishiwatari, J. Liu and Y. Oka, "Fuel and Core Design of Super LWR with Stainless Steel cladding," *Proc. ICAPP'05*, Seoul, Korea, May 15–19, 2005, Paper 5428 (2005)
36. T. Nakatsuka, Y. Oka and S. Koshizuka, "Control of a Fast Reactor Cooled by Supercritical Light Water," *Nuclear Technology*, Vol. 121, 81–92 (1998)
37. T. Nakatsuka, Y. Oka and S. Koshizuka, "Plant Control of a Fast Breeder Reactor Cooled by Supercritical Light Water," *Proc. 1997 International Meeting on Advanced Reactors Safety (ARS '97)*, Orlando, FL, June 1–5 1997, 1165–1172 (1997)
38. T. Nakatsuka, Y. Oka and S. Koshizuka, "Plant Control of the Fast Reactor Cooled by Supercritical Light Water", *Proc. ICONE-6*, San Diego, CA, May 10–15, 1998, ICONE-6224 (1998)
39. Y. Ishiwatari, Y. Oka and S. Koshizuka, "Control of a High Temperature Supercritical Pressure Light Water Cooled and Moderated Reactor with Water Rods," *Journal of Nuclear Science and Technology*, Vol. 40(5), 298–306 (2003)

40. Y. Ishiwatari, C. Peng, T. Sawada, S. Ikejiri and Y. Oka, "Design and Improvement of Plant Control System for a Super Fast Reactor," *Proc. ICAPP'09*, Tokyo, Japan, May 10–14 2009, Paper 9261 (2009)
41. T. Nakatsuka, Y. Oka and S. Koshizuka, "Startup Thermal Considerations for Supercritical-Pressure Light Water-Cooled Reactors," *Nuclear Technology*, Vol. 134(3), 221–230 (2001)
42. T. Nakatsuka, Y. Oka and S. Koshizuka, "Start-up of Supersritical-pressure Light Wtater Cooled Reactors," *Proc. ICONE-8*, Baltimore, MD., April 2–6, 2000, ICONE-8304 (2000)
43. T. T. Yi, Y. Ishiwatari, S. Koshizuka and Y. Oka, "Startup Thermal Analysis of a High-Temperature Supercritical-Pressure Light Water Reactor," *Journal of Nuclear Science and Technology*, Vol. 41(8), 790–801 (2004)
44. T. T. Yi, Y. Ishiwatari, J. Liu, S. Koshizuka and Y. Oka, "Thermal and Stability Considerations of Super LWR during Sliding Pressure Startup," *Journal of Nuclear Science and Technology*, Vol. 42(6), 537–548 (2005)
45. T. T. Yi, Y. Ishiwatari, S. Koshizuka and Y. Oka, "Startup of a High-Temperature Reactor Cooled and Moderated by Supercritical-Pressure Light Water", *Proc. GENES4/ANP2003*, Kyoto, Japan, September 15–19, 2003, Paper 1036 (2003)
46. S. Yamada, Y. Ishiwatari, S. Ikejiri, et al., "Design and Analysis of Procedures for System Pressurization and Line-Switching to One-through Mode in Plant Startup of SCWR," *Proc. NURETH-13*, Kanazawa, Japan, September 27–October 2, 2009, N13P1435 (2009)
47. S. Ji, H. Shirahama, S. Koshizuka and Y. Oka, "Stability Analysis of Supercritical-Pressure Light Water-Cooled Reactor in Constant Pressure Operation," *Proc. ICONE-9*, Nice, France, April 8–12, 2001, ICONE-9306 (2001)
48. Tin Tin Yi, S. Koshizuka and Y. Oka, "Linear Stability Analysis of a High-temperature Supercritical-pressure Light Water Reactor", *Proc. Global 2003*, New Orleans, LA, November 16–20, 2003, 1781–1790 (2003)
49. T. T. Yi, S. Koshizuka and Y. Oka, "A Linear Stability Analysis of Supercritical Water Reactors, (I) Thermal-Hydraulic Stability," *Journal of Nuclear Science and Technology*, Vol. 41(12), 1166–1175 (2004)
50. T. T. Yi, S. Koshizuka, Y. Oka, "A Linear Stability Analysis of Supercritical Water Reactors, (II) Coupled Neutronic Thermal-Hydraulic Stability," *Journal of Nuclear Science and Technology*, Vol. 41(12), 1176–1186 (2004)
51. J. Cai, Y. Ishiwatari, S. Ikejiri and Y. Oka, "Thermal and Stability Considerations for a Supercritical Water-Cooled Fast Reactor with Downward-Flow Channels During Power-Raising Phase of Plant Startup," *Nuclear Engineering and Design*, Vol. 239, 665–679 (2009)
52. A. Hotta, et al., "BWR Regional Instability Analysis by TRAC0BF1-ENTRÉE-I: Application to Density-wave Oscillation," *Nuclear Technology*, Vol. 135(1), 1–6 (2001)
53. A. Hotta, et al., "BWR Regional Instability Analysis by TRAC0BF1-ENTRÉE-II: Application to Righals Unit-1 Stability Test," *Nuclear Technology*, Vol. 135(1), 17–38 (2001)
54. Y. Ishiwatari, Y. Oka, S. Koshizuka, A. Yamaji and J. Liu, "Safety of Super LWR, (I) Safety System Design," *Journal of Nuclear Science and Technology*, Vol. 42(11), 927–934 (2005)
55. Y. Ishiwatari, Y. Oka, S. Koshizuka and J. Liu, "Safety Characteristics of the Super LWR Design Concept," *Proc. ICAPP'07, Nice*, France, May 13–18, 2007, Paper 7309 (2007)
56. Y. Ishiwatari, Y. Oka and S. Koshizuka, "Safety of the Super LWR," *Nuclear Engineering and Technology*, Vol. 39(4), 257–272 (2007)
57. Y. Okano, S. Koshizuka, et al., "Flow Induced Transient Analysis of a Supercritical Pressure, Light-Water-Cooled Fast Breeder Reactor," *Proc. 3 rd JSME/ASME Joint International Conf. on Nuclear Engineering*, Kyoto, Japan, April 23–27, 1995, 891–895 (1995)
58. K. Kitoh, S. Koshizuka and Y. Oka, "Control Rod, Pressure and Flow-Induced Accident and Transient Analyses of a Direct-Cycle, Supercritical Pressure, Light-Water-Cooled Fast Breeder Reactor," *Proc. ICONE-4*, New Orleans, LA, April, March 10–14, 1996, Vol. 2, 537–545 (1996)

59. Y. Okano, S. Koshizuka and Y. Oka, "Flow and Pressure-Induced Transient Analysis of the Supercritical-Pressure, Light-Water-Cooled and Moderated Reactor," *Proc. ICONE-4*, New Orleans, LA, April, March 10–14, 1996, Vol. 1, 771–780 (1996)
60. Y. Okano, S. Koshizuka, K. Kitoh and Y. Oka, "Flow-Induced Accident and Transient Analyses of a Direct-Cycle, Light-Water Cooled, Fast Breeder Reactor Operating at Supercritical Pressure," *Journal of Nuclear Science and Technology*, Vol. 33(4), 307–315 (1996)
61. K. Kitoh, S. Koshizuka and Y. Oka, "Pressure and Flow-Induced Accident and Transient Analysis of a Direct-Cycle, Supercritical-Pressure, Light-Water-Cooled Fast Reactor," *Nuclear Technology*, Vol. 123, 233–244 (1998)
62. Y. Ishiwatari, Y. Oka and S. Koshizuka, "Safety Analysis of a High Temperature Supercritical Pressure Light Water Cooled and Moderated Reactor," *Proc. ICAPP*, Hollywood, FL, June 9–13, 2002, Paper 1045 (2002)
63. Y. Ishiwatari, Y. Oka and S. Koshizuka, "Safety Analysis of High Temperature Reactor Cooled and Moderated by Supercritical Water," *Proc. GENES4/ANP2003*, Kyoto, Japan, September 15–19, 2003, Paper 1059 (2003)
64. Y. Ishiwatari, Y. Oka and S. Koshizuka, "Safety Design Principle of Supercritical Water Cooled Reactors," *Proc. ICAPP'04*, Pittsburg, PA, June 13–17, 2004, Paper 4319 (2004)
65. Y. Ishiwatari, Y. Oka, S. Koshizuka, A. Yamaji and J. Liu, "Safety of Super LWR, (II) Safety Analysis at Supercritical Pressure," *Journal of Nuclear Science and Technology*, Vol. 42 (11), 935–948 (2005)
66. K. Kitoh, S. Koshizuka and Y. Oka, "Refinement of Transient Criteria and Safety Analysis for a High-Temperature Reactor Cooled by Supercritical Water," *Nuclear Technology*, Vol. 135, 252–264 (2001)
67. F. D. Coffman, Jr., LOCA Temperature Criterion for Stainless Steel Clad Fuel, NUREG-0065, (1976)
68. Y. Ishiwatari, Y. Oka, S. Koshizuka and J. Liu, "ATWS Characteristics of Super LWR With/Without Alternative Action," *Journal of Nuclear Science and Technology*, Vol. 44(4), 572–580 (2007)
69. Y. Ishiwatari, Y. Oka and S. Koshizuka, "ATWS Analysis of Supercritical Pressure Light Water Cooled Reactor," *Proc. Global 2003*, New Orleans, LA, November 16–20, 2003, 2335–2341 (2003)
70. K. Yoshimura, Y. Ishiwatari, et al., "Development of Transient Subchannel Analysis Code of Super LWR and Application to Flow Decreasing Events," *Proc. NURETH-13*, Kanazawa, Japan, September17–October 2, 2009, N13P1434 (2009)
71. Y. Ishiwatari, Y. Oka, S. Koshizuka and J. Liu, "LOCA Analysis of Super LWR," *Journal of Nuclear Science and Technology*, Vol. 43(3), 231–241 (2006)
72. J.H. Lee, S. Koshizuka and Y. Oka, "Development of a LOCA Analysis Code for the Supercritical-Pressure Light Water Cooled Reactors," *Annals of Nuclear Energy*, Vol. 25 (16), 1341–1361 (1998)
73. J.H. Lee, "LOCA Analysis and Safety System Consideration for the Supercritical-Water Cooled Reactor," Doctoral Thesis, the University of Tokyo (1996)
74. Y. Ishiwatari, Y. Oka and S. Koshizuka, "LOCA Analysis of High Temperature Reactor Cooled and Moderated by Supercritical Water," *Proc. GENES4/ANP2003*, Kyoto, Japan, September 15–19, 2003, Paper 1060 (2003)
75. J.H. Lee, Y. Oka and S. Koshizuka, "Safety System Consideration of a Supercritical-Water Cooled Fast Breeder Reactor with Simplified PSA," *Reliability Engineering & System Safety*, Vol. 64, 327–338 (1999)
76. Y. Oka and S. Koshizuka "Supercritical-Pressure, Once-Through Cycle Light Water Cooled Reactor Concept," *Journal of Nuclear Science and Technology*, Vol. 38(12), 1081–1089 (2001)

77. Y. Oka and S. Koshizuka "Once-Through Cycle, Supercritical-Pressure Light Water Cooled Reactor Concept," *Proc. Global 2001*, Paris, France, September 9–13, 2001, FP-172 (2001)
78. Y. Oka, S. Koshizuka, Y. Ishiwatari and A. Yamaji "Elements of Design Consideration of Once-Through Cycle, Supercritical-Pressure Light Water Cooled Reactor," Proc. ICAPP, Hollywood, FL, June 9–13, 2002, Paper 1005 (2002)
79. Y. Oka, Y. Ishiwatari, et al., "Research Program of a Super Fast Reactor," *Proc. ICAPP'06*, Reno, NV, June 4–8, 2006, Paper 6353 (2006)
80. J. Yoo, Y. Ishiwatari, Y. Oka and J. Liu, "Composite Core Design of High Power Density Supercritical Water Cooled Fast Reactor," *Proc. Global 2005*, Tsukuba, Japan, October 9–13, 2005, Paper 248 (2005)
81. J. Yoo, Y. Ishiwatari, Y. Oka and J. Liu, "Conceptual Design of Compact Supercritical Water-cooled Fast Reactor with Thermal Hydraulic Coupling," *Annals of Nuclear Energy*, Vol. 33(11–12), 945–956 (2006)
82. J. Yoo, Y. Oka, J. Yang and J. Liu, "Static Thermal Design Analyses of Supercritical Water-Cooled Fast Reactor," *Proc. ICAPP'06*, Reno, NV, June 4–8, 2006, Paper 6224 (2006)
83. J. Yoo, Y. Ishiwatari, Y. Oka and J. Liu, "Subchannel Analysis of Supercritical Light Water-Cooled Fast Reactor Fuel Assembly," *Nuclear Engineering and Design*, Vol. 237, 1096–1105 (2007)
84. L. Cao, Y. Oka, Y. Ishiwatari and Z. Shang, "Fuel, Core Design and Subchannel Analysis of a Super Fast Reactor," *Journal of Nuclear Science and Technology*, Vol. 45(2), 138–148 (2008)
85. J. Yoo, Y. Oka, Y. Ishiwatari and J. Liu, "Thermo-Mechanical Analysis of Supercritical Pressure Light Water-Cooled Fast Reactor Fuel Rod by FEMAXI-6 Code", *Annals of Nuclear Energy*, Vol. 33(17), 1379–1390 (2006)
86. H. Ju, L. Cao, Y. Ishiwatari, Y. Oka and S. Ikejiri, "Research and Development of a Super Fast Reactor (3) Fuel Rod Analyses under Normal Operating Condition," *Proc. 16PBNC*, Aomori, Japan, October 13–18, 2008, P16P1292 (2008)
87. H. Ju, L. Cao, et al., "Core Design and Fuel Rod Analyses of a Super Fast Reactor with High Power Density," *Proc. ICAPP'09*, Tokyo, Japan, May 10–14, 2009, Paper 9264 (2009)
88. L. Cao, H. Ju, Y. Ishiwatari, et al., "Research and Development of a Super Fast Reactor (2) Core Design Improvement on Local Void Reactivity," *Proc. 16th PBNC*, Aomori, Japan, October 13–18, 2008, P16P1291 (2008)
89. L. Cao, Y. Oka, Y. Ishiwatari and S. Ikejiri, "Three-Dimensional Core Analysis on a Super Fast Reactor with Negative Local Void Reactivity," *Nuclear Engineering and Design*, Vol. 239, 408–417 (2009)
90. X. Cheng, E. Laurien and Y.H. Yang, "CFD Analysis of Heat Transfer in Supercritical Water in Different Flow Channels," *Proc. Global 2005*, Tsukuba, Japan, October 9–13, 2005, Paper 369 (205)
91. J. Yang, Y. Oka, Y. Ishiwatari, J. Liu and J. Yoo, "Numerical Study on Heat Transfer in Supercritical Pressure Water in Tight Fuel Rod Channels," *Proc. ICAPP'06*, Reno, NV, June 4–8 2006, Paper 6334 (2006)
92. J. Yang, Y. Oka, Y. Ishiwatari, J. Liu and J. Yoo, "Numerical Investigation of Heat Transfer in Upward Flows of Supercritical Water in Circular Tubes and Tight Fuel Rod Bundles," *Nuclear Engineering and Design*, Vol. 237, 420–430 (2007)
93. J. Gou, Y. Ishiwatari, Y. Oka, M. Yamakawa and S. Ikejiri, "Research and Development of Super Fast Reactor (5) Thermal Hydraulic Analysis of Tight-laiice Subchannels," *Proc. 16th PBNC*, Aomori, Japan, October 13–18, 2008, P16P1294 (2008)
94. J. Gou, Y. Ishiwatari, Y. Oka, M. Yamakawa, "CFD Analyses in Tight-Lattice Subchannels and Seven-Rods Bundle Geometries of a Super Fast Reactor," *Proc. ICAPP09*, Tokyo, Japan, May 10–15, 2009, Paper 9262 (2009)

95. L. Cao, H. Lu, Y. Ishiwatari, Y. Oka and S. Ikejiri, "Research and Development of a Super Fast Reactor (4) Transmutation Analyses of Minor Actinides and Transuranium Elements," *Proc. 16th PBNC*, Aomori, Japan, October 13–18, 2008, P16P1293 (2008)
96. H. Lu, Y. Ishiwatari, C. Han, Y. Oka, S. Ikejiri, "Evaluation of Transmutation Performance of Long-Lived Fission Products with a Super Fast Reactor," *Proc. ICAPP09*, Tokyo, Japan, May 10–15, 2009, Paper 9263 (2009)
97. S. Ikejiri, Y. Guo, Y. Ishiwatari, Y. Oka and T. Sawada, "Research and Development of a Super Fast Reactor (6) Analyses of Abnormal Transients," *Proc. 16th PBNC*, Aomori, Japan, October 13–18, 2008, P16P1295 (2008)
98. S. Ikejiri, Y. Ishiwatari, Y. Oka, "Loss of Coolant Accident Analysis of a Supercritical-Pressure Water-Cooled Fast Reactor with Downward Flow Channels," *Proc. ICAPP09*, Tokyo, Japan, May 10–15, 2009, Paper 9257 (2009)
99. J. Cai, Y. Ishiwatari, S. Ikejiri and Y. Oka, "Thermal and Stability Considerations for a Supercritical Water-cooled Fast Reactor During Power-Raising Phase of Plant Startup," *Proc. ICAPP09*, Tokyo, Japan, May 10–15, 2009, Paper 9265 (2009)
100. J. Cai, Y. Ishiwatari, S. Ikejiri and Y. Oka, "Thermal and Stability Considerations for a Supercritical Water-Cooled Fast Reactor with Downward-Flow Channels During Power-Raising Phase of Plant Startup," *Nuclear Engineering and Design*, Vol. 239, 665–679 (2009)
101. Y. Ishiwatari, C. Peng, T. Sawada, S. Ikejiri and Y. Oka, "Design and Improvement of Plant Control System for a Super Fast Reactor," *Proc. ICAPP09*, Tokyo, Japan, May 10–15, 2009, Paper 9261 (2009)
102. Y. Ishiwatari, M. Yamakawa, Y. Oka and S. Ikejiri, "Research and Development of a Super Fast Reactor (1) Overview and High-Temperature Structural Design," *Proc. 16th PBNC*, Aomori, Japan, October 13–18, 2008, P16P1290 (2008)
103. K. Kataoka and Y. Oka, "Neutronic Feasibility of Supercritical Steam Cooled Fast Breeder Reactor," *Journal of Nuclear Science and Technology*, Vol. 28, 585–58 (1991)
104. Y. Oka and K. Kataoka "Conceptual Design of a Fast Breeder Reactor Cooled by Supercritical Steam," *Annals of Nuclear Energy*, Vol. 19, 243–247 (1992)
105. Y. Oka, T. Jevremovic and S. Koshizuka, "Negative Void Reactivity in Large FBRs with a Hydrogeneous Moderator," *Transactions of American Nuclear Society*, Vol. 68, Part A, 301–303 (1993)
106. Y. Oka and T. Jevremovic, "Negative Void Reactivity in Large Fast Breeder Reactors with Hydrogeneous Moderator Layer," *Annals of Nuclear Energy*, Vol. 23, 1105–1115 (1996)
107. Y. Oka and S. Koshizuka, "Conceptual Design of a Supercritical-Pressure Direct-Cycle Light Water Reactor," *Proc. ANP'92*, Tokyo, Japan, October 25–29, 1992, Vol. 1, Session 4.1, 1–7 (1992)
108. K. Kataoka, "A Supercritical Steam Cooled Fast Breeder Reactor," Doctoral thesis, the University of Tokyo (1990) (in Japanese)
109. T. Jeveremovic, "Conceptual Design of Fast Breeder Reactors Cooled by Supercritical Steam," Doctoral thesis, the University of Tokyo (1993)
110. J.H. Lee, "LOCA Analysis and Safety System Consideration for the Supercritical-Water Cooled Reactor," Doctoral thesis, the University of Tokyo (1996)
111. Y. Okano, "Systems Design of Direct-Cycle Supercritical-Water-Cooled Fast Reactors," Doctoral thesis, the University of Tokyo (1997) (in Japanese)
112. N. Takano, "A Numerical Investigation of Heat Transfer Deterioration Mechanism at Supercritical Water Cooling," Master's thesis, the University of Tokyo (1994) (in Japanese)
113. K. Kitoh, "Safety Analysis of a Supercritical Water Cooled Reactor," Doctoral thesis, the University of Tokyo (1997) (in Japanese)
114. K. Dobashi, "Conceptual Design of Supercritical-pressure Light Water Cooled and Moderated Reactor," Doctoral thesis, the University of Tokyo (1998) (in Japanese)
115. T. Nakatsuka, "Control and Startup of Supercritical Pressure Light Water Cooled Reactor," Doctoral thesis, the University of Tokyo (1998) (in Japanese)

116. T. Mukohara, "Design of Supercritical-Pressure Light Water Cooled Fast Reactor and the Subchannel Analysis," Doctoral thesis, the University of Tokyo, (2001) (in Japanese)
117. Y. Tanabe, "Subchannel Analysis of Super LWR," Master's thesis, the University of Tokyo, (2005) (in Japanese)
118. T. T. Yi, "Startup and Stability of a High-Temperature Supercritical-Pressure Light Water Reactor," Doctoral thesis, the University of Tokyo (2004)
119. A. Yamaji, "Core and Fuel Design of Super LWR," Doctoral thesis, the University of Tokyo (2005) (in Japanese)
120. J. Yoo, "Three-dimensional Core Design of Large Scale Supercritical Light Water Cooled Fast Reactor", Doctoral thesis, the University of Tokyo (2006) (in Japanese)
121. Y. Ishiwatari, "Safety of Super LWR", Doctoral thesis, the University of Tokyo (2006) (in Japanese)
122. K. Kamei, "Core Design of Super LWR and the Safety Analysis at Subcritical-Pressure", Master's thesis, the University of Tokyo (2006) (in Japanese)
123. K. Yoshimura, "Development of a Transient Subchannel analysis code and safety analysis for the Super LWR," Graduate thesis, the University of Tokyo (2009) (in Japanese)
124. I. Hongo, "Numerical Analysis of Heat Transfer Enhancement by Grid Spacers on High Temperature Supercritical Fluid", Master's thesis, the University of Tokyo (2009) (in Japanese)
125. http://www.nuclear.jp/~rohonbu/lab/paper/paper.htm, //www.f.waseda.jp/okay/UTpaper/paper.htm
126. H. Mori, M. Ohno, et al., "Research and Development of a Super Fast Reactor (7) Heat Transfer to a Supercritical Pressure Fluid Flowing in a Sub-bundle Channel," *Proc. 16th PBNC*, Aomori, Japan, October 13–18, 2008, P16P1297 (2008)
127. K. Ezato, M. Akiba, et al., "Research and Development of a Super Fast Reactor (8) Heat Transfer Experiments Around a Simulated Fuel Rod with Supercritical Pressure Water," *Proc. 16th PBNC*, Aomori, Japan, October 13–18, 2008, P16P1240 (2008)
128. K. Ezato, Y. Seki, et al., "Heat Transfer in a Seven-Rod Test Bundle with Supercritical Pressure Water (1) Experiments," *Proc ICAPP'09,* Tokyo, Japan, May 10–14, 2009 Paper 9464 (2009)
129. K. Sasaki, T. Kubo, et al., "Research and Development of a Super Fast Reactor (10) Fabrication and Characterization of Durable Thermal Shielding Material," *Proc. 16th PBNC*, Aomori, Japan, Oct. 13–18, 2008, P16P1427 (2008)
130. Z. Han, Y. Katsumura, et al., "Effect of Temperature On the Absorption Spectra of the Solvated Electron in 1-Propanol and 2-Propanol: Pulse Radiolysis and Laser Photolysis Studies at Temperatures Up to Supercritical Condition," *Radiation Physics and Chemistry*, Vol. 77, 409–415 (2008)
131. Z. Han and Y. Muroya, "Research and Development of a Super Fast Reactor (11) An Approach to Evaluate the Elution Characteristic of Stainless Materials in Subcritical and Supercritical Water," *Proc. 16th PBNC*, Aomori, Japan, October 13–18, 2008, P16P1315 (2008)
132. Z. Han and Y. Muroya, "Development of a New Method to Study Elution Properties of Stainless Materials in Subcritical and Supercritical Water," *Proc. 4th Int. Symp. on SCWR*, Heidelberg, Germany, March 8–11, 2009, Paper No. 75 (2009)
133. S. Tanaka, Y. Shirai, et al., "Plant Concept of Supercritical Pressure Light Water Reactor," *Proc. ICONE-5*, Nice, France, May 26–30, 1997, ICONE-5-2346 (1997)
134. S. Shiga, K. Moriya, Y. Oka, S. Yoshida, H. Takahashi, "Progress of Development Project of Supercritical Water Cooled Power Reactor, 2003," *Proc. ICAPP'03*, Cordoba, Spain, May 4–7, 2003, Paper 3258 (2003)
135. A. Shioiri, K. Moriya, et al., "Development of Supercritical-Water Cooled Power Reactor Conducted by a Japanese Joint Team," *Proc. GENES4/ANP2003*, Kyoto, Japan, September 15–19, 2003, Paper 1121 (2003)
136. Y. Oka and K. Yamada, "Research and Development of High Temperature Light Water Cooled Reactor Operating at Supercritical-Pressure in Japan," *Proc. ICAPP'04*, Pittsburgh, PA, June 13–17, 2004, Paper 4233 (2004)

137. K. Yamada, S. Sakurai, et al., "Recent Activities and Future Plan of Thermal-Spectrum SCWR Development in Japan," *Proc. 3 rd Int. Symp. on SCWR*, Shanghai, China, March 12–15, 2007, Paper No. SCWR2007-P054 (2007)
138. Y. Ishiwatari, Y. Oka and K. Yamada, "Japanese R&D Projects on Pressure-Vessel Type SCWR," *Proc. 4th Int. Symp. on SCWR*, Heidelberg, Germany, March 8–11, 2009, Paper No. 73 (2009)
139. G. Heusener, U. Muller, T. Schulenberg and D. Square, "A European Development Program for a High Performance Light Water Reactor (HPLWR)," *Proc. 1st Int. Symp. on Supercritical Water-cooled Reactors*, Tokyo, Japan, November 6–9, 2000, Paper 102 (2000)
140. D. Squarer, D. Bittermann, et al., "Overview of the HPLWR Project and Future Direction," *Proc. ICAPP'03*, Cordoba, Spain, May 4–7, 2003, Paper 3137 (2003)
141. D. Squarer, T. Schulenberg, et al., "High Performance Light Water Reactor," *Nuclear Engineering and Design*, Vol. 221, 167–180 (2003)
142. J. Starflinger, N. Aksan, et al., "Roadmap for Supercritical Water-Cooled Reactor R&D in Europe," *Proc. GLOBAL 2003*, New Orleans, LA, November 16–20, 2003, 1137–1142 (2003)
143. J. Starflinger, T. Schulenberg, et al., "European Research Activities within the Project: High Performance Light Water Reactor Phase 2," *Proc. ICAPP'07*, Nice, France, May 13–18, 2007, Paper 7416 (2007)
144. T. Schulenberg and J. Starflinger, "European Research Project on the High Performance Light Water Reactor," *Proc. 4th Int. Symp. on SCWR*, Heidelberg, Germany, March 8–11, 2009, Paper No. 54 (2009)
145. J. Starflinger, T. Schulenberg, et al., "Results of the Mid-Term Assessment of the High Performance Light Water Reactor 2 Project," *Proc. ICAPP'09*, Tokyo, Japan, May 10–14, 2009, Paper 9268 (2009)
146. //www.iket.fzk.de/hplwr/
147. //www.gen-4.org/Technology/systems/scwr.htm
148. D. Brady, D. Duttey, et al., "Generation IV Reactor Development in Canada," *Proc. 3 rd Int. Symp. on SCWR*, Shanghai, China, March 12–15, 2007, SCR2007-P057 (2007)
149. D. Boyle, D. Brady, et al., "Canada's Generation IV National Program – Overview," *Proc. 4th Int. Symp. on SCWR*, Heidelberg, Germany, March 8–11, 2009, Paper No. 74 (2009)
150. C.K. Chow and H.F. Khartabil, "Conceptual Fuel Channel Designs for CANDU-SCWR," *Nuclear Engineering and Technology*, Vol. 40(2), 139–146 (2008)
151. H.F. Khartabil, "Review and Status of the Gen-IV CANDU-SCWR Passive Moderator Core Cooling System," *Proc. ICONE-16*, Orlando, FL, May 11–15, 2008, ICONE16-48741 (2008)
152. Y.Y. Bae, K.M. Bae, et al., "R&D on a Supercritical Pressure Water Cooled Reactor in Korea," *Proc. ICAPP'06*, Reno, NV, June 4–8, 2006, Paper 6022 (2006)
153. Y.Y. Bae, K.M. Bae, et al., "SCWR Research in Korea," *Proc. 3 rd Int. Symp. on SCWR*, Shanghai, China, March 12–15, 2007, SCR2007-P006 (2007)
154. Y.Y. Bae, G. Jang, et al., "Research Activities on a Supercritical Pressure Water Reactor in Korea," *Nuclear Engineering and Technology*, Vol. 39(4), 273–286 (2007)
155. Y.Y. Bae, H.Y. Kim, et al., "Update on the SCWR Research in Korea," *Proc. 4th Int. Symp. on SCWR*, Heidelberg, Germany, March 8–11, 2009, Paper No. 52 (2009)
156. S.Y. Hong, K. Lee, et al., "Interim Results of SCWR Development Feasibility Study in Korea," *Proc. 4th Int. Symp. on SCWR*, Heidelberg, Germany, March 8–11, 2009, Paper No. 50 (2009)
157. X. Cheng, "R&D Activities on SCWR in China," *Proc. 4th Int. Symp. on SCWR*, Heidelberg, Germany, March 8–11, 2009, Paper No. 53 (2009)
158. J. Buongiorno, "The Supercritical Water Cooled Reactor: Ongoing Research and Development in the U.S.," *Proc. ICAPP'04*, Pittsburgh, PA, June 13–17, 2004, Paper 4229 (2004)

159. S.M. Modro, "The Supercritical Water Cooled Reactor Research and Development in the U.S.," *Proc. ICAPP'05*, Seoul, Korea, May 15–19, 2005, Paper 5694 (2005)
160. J. Buongiorno and P. Macdonald, "Supercritical Water Reactor (SCWR), Progress Report for the FY03 Generation-IV R&D Activities for the Development of the SCWR in the U.S.," INEEL/EXT03-03-01210, Idaho National Engineering and Environmental Laboratory (2003)
161. S. León and N. Aksan, "IAEA Coordinated Research Programme on Heat Transfer Behavior and Thermo-Hydraulics Code Testing for Super Critical Water Cooled Reactors," *Proc. ICAPP'09*, Tokyo, Japan, May 10–14, 2009, Paper 9482 (2009)